

MOLECULAR ASSEMBLY OF POLYCYANOARENES WITH SILVER SALTS
AND SYNTHESIS OF POLYCYCLIC AROMATIC HYDROCARBONS

A DISSERTATION IN
Chemistry
and
Pharmaceutical Sciences

Presented to the Faculty of the University
of Missouri-Kansas City in partial fulfillment of
the requirements for the degree

DOCTOR OF PHILOSOPHY

by
GERARDO B. MÁRQUEZ
B.Sc. Central University of Venezuela, 1993

Kansas City, Missouri
2012

© 2012
GERARDO B. MÁRQUEZ
ALL RIGHTS RESERVED

MOLECULAR ASSEMBLY OF POLYCYANORENES WITH SILVER SALTS AND
SYNTHESIS OF POLYCYCLIC AROMATIC HYDROCARBONS

Gerardo Batalla Márquez, Candidate for the Doctor of Philosophy Degree

University of Missouri-Kansas City, 2012

ABSTRACT

This dissertation encompasses the investigation of two distinct subjects. In the first part, which is in the area of molecular self-assembly, the complexation of organonitrile aryl compounds with three different types of silver (I) salts is examined in the solid state. The assembly of 1-(2,2-dicyanovinyl)naphthalene with silver hexafluoroantimonate resulted in a cationic 3D network. Complexation of 4-(2,2-dicyanovinyl)biphenyl with silver tetrafluoroborate and hexafluoroantimonate from benzene generated two similar structures. While the former displays a cationic 3D network, the latter is defined by cationic 2D sheets. Complexation of 9-(2,2-dicyanovinyl)anthracene with silver hexafluoroantimonate from toluene afforded a cationic 2D ribbon, and from benzene, it yielded cationic 2D sheets. These complexes contained solvent bonded to their structures. However, the hexafluoroantimonate ion is nonbonding.

The crystal association of 1,4-bis(cyanovinyl)benzene with silver triflate from benzene yielded neutral 2D sheets whose imperfect-rectangular macrocyclic arrangements are interconnected on both sides by bridges of benzene. On the other hand, the assembly of 1,3-bis(cyanovinyl)benzene with silver triflate from benzene afforded a neutral 3D network formed by two interconnected rings. Solvent and triflate counterions are bonded in both complexes.

In the second part of this dissertation, the focus was on the synthesis of four linear PAHs containing a perylene center formed by the connection of two substituted fluoranthene units. Our synthetic approach included the elaboration of fluoranthene building blocks (monomers), followed by the coupling of the monomers resulting in dimers, and finally, ring closure of those dimers, which form the target structures. All of the stages were monitored by mass spectrometry, ^1H NMR, and ^{13}C NMR spectroscopy. Out of four dimers, only one successfully underwent ring closure. The UV/Vis absorption and fluorescence spectra for the only obtained target compound evaluated in chloroform showed absorption bands at 318, 352, 518, 558, and 606 nm and emission bands at 615 and 667 nm. The fluorescence quantum yield at 558 nm was $\phi_{\text{F}} = 0.21$, and at 606 nm was $\phi_{\text{F}} = 0.4$. Since the differentiation between the targets relies on the substitution pattern, these results suggest that changes in the fluoranthene moiety render changes in the reactivity through the coupling reaction.

This abstract of 347 words is approved as to form and content.

APPROVAL PAGE

The faculty listed below, appointed by the Dean of the College of Arts and Sciences have examined a dissertation titled “Molecular Assembly of Polycyanoarenes with Silver Salts and Synthesis of Polycyclic Aromatic Hydrocarbons,” presented by Gerardo B. Márquez, candidate for the Doctoral of Philosophy degree, and certify that in their opinion it is worthy of acceptance.

Supervisory Committee

Kathleen V. Kilway, Ph.D., Committee Chair
Department of Chemistry

Charles J. Wurrey, Ph.D.
Department of Chemistry

Ekaterina Kadnikova, Ph.D.
Department of Chemistry

Simon Friedman, Ph.D.
Department of Pharmaceutical Sciences

William G. Gutheil, Ph.D.
Department of Pharmaceutical Sciences

CONTENTS

ABSTRACT	iii
LIST OF ILLUSTRATIONS.....	viii
TABLES	xiii
ACKNOWLEDGEMENTS.....	xiv

Chapter

1. Introduction and literature review	1
Factors that affect self-assembly	8
Objectives and synthetic approaches	26
Results and discussion	30
Summary	51
Conclusions.....	54
Experimental section	55
2. Introduction and literature review	59
From planar to highly twisted PAHs	62
Methods used for the building of PAHs	69
Perylene structures	77
Objectives and synthetic approaches	80
Results and discussion	85
Conclusions.....	104

Experimental section	109
REFERENCES	127
VITA.....	139

ILLUSTRATIONS

Figures	Page
1. Examples of linkers	3
2. Examples of connectors	4
3. Coordination geometry of polymer 3	6
4. Pictorial representation cyclic structures	7
5. Nanoscopic 3D molecule	9
6. Structure of tetradentate ligands	10
7. View of the pentacoordinate complex 9	10
8. The coordination environment of Ag(I) in complex 12	12
9. Thermal ellipsoid plot of the cationic unit ⁷⁺	15
10. Thermal ellipsoid plot of the cationic unit ⁹⁺	16
11. Plot of two [Ag(py) ₂] ⁺ fragments (from structure 23 or 24)	18
12. Pictorial representation of silver (I) environment of complex 25	19
13. Possible conformations of 3,3'-pytz (31)	21
14. Pictorial representation of the zigzag chain exhibited by $\{[\text{Cd}(\mu\text{-}3,3'\text{-pytz})(\text{NO}_3)_2(\text{MeOH})_2]\}_\infty$ (32)	23
15. Pictorial representation of the ladder exhibited by complexes $\{[\text{Cd}_2(\mu\text{-}3,3'\text{-pytz})_3(\text{NO}_3)_4(\text{EtOH})]\}_\infty$ (33), $\{[\text{Cd}_2(\mu\text{-}3,3'\text{-pytz})_3(\text{NO}_3)_4(\text{CH}_2\text{Cl}_2)]_\infty$ (34), and $\{[\text{Zn}_2(\mu\text{-}3,3'\text{-pytz})_3(\text{NO}_3)_4](\text{CH}_2\text{Cl}_2)_2\}_\infty$ (37)	23

16. Pictorial representation of $\{[\text{Zn}_2(3,3'\text{-pytz})_2(\text{NO}_3)_4(\text{MeOH})_2(\mu\text{-}3,3'\text{-pytz})]\}_\infty$ (35) and $\{[\text{Zn}_2(3,3'\text{-pytz})_2(\text{NO}_3)_4(\text{EtOH})_2(\mu\text{-}3,3'\text{-pytz})]\}_\infty$ (36)	24
17. Structures of the ligands 38-41	25
18. Structures of the ligands 42-47	28
19. ORTEP representation of complex 48 showing the coordination geometry	34
20. A complementary view of complex 48	34
21. ORTEP representation of complex 49 showing the coordination geometry	37
22. Representation of the cyclic unit observed in complex 49	37
23. ORTEP representation showing the coordination geometry of complex 50	40
24. ORTEP representation of a dimer of complex 50	40
25. ORTEP representation showing the coordination environment of complex 51	43
26. ORTEP representation showing the orientation of the solvent in complex 51	43
27. ORTEP representation showing the coordination geometry of complex 52	45
28. Representation of the cyclic unit observed in complex 52	45
29. ORTEP representation showing the coordination geometry of complex 53	47
30. ORTEP representation showing a macrocyclic unit of 53	47
31. ORTEP representation showing the coordination geometry of complex 54	50
32. ORTEP representation showing the two ring units in structure 54	50
33. Examples of alternant PAHs.....	60
34. Examples of nonalternant PAHs.....	61
35. Schematic representation of helicity for [6]helicene (58)	63
36. Pictorial representation of carbon allotropes	65

37. Chemical structure of fullerene derivative 73	66
38. Molecular representations of dyes 74a-74c	68
39. Second-generation Grubbs catalyst	71
40. Chemical structures of peryleneimide chromophores	78
41. Target molecules 106-109	82
42. Structure of twisted compound 60	90
43. Compound 106 under regular light and under UV-Vis light.....	101
44. UV/Vis absorption and fluorescence spectra of 106 in chloroform	102

ILLUSTRATIONS

Scheme	Page
1. Synthesis of Ni(II) macrocyclic complex	5
2. Synthesis of complex 12	12
3. Synthesis of bipyridine complex	13
4. Synthesis of Ni(II) complexes 21-22	15
5. Synthesis of the ligands 42-47	27
6. Synthesis of complexes 48-54	30
7. Diels-Alder cycloaddition of maleic anhydride to perylene (61)	70
8. Examples of PAHs obtained through RCM	71
9. The proposed pathway in FVP	72
10. Three dicyclopentapyrenes obtained using FVP	74
11. Synthesis of an “Arrowlike” PAH	75
12. Synthesis of benzo[s]picene	77
13. Synthesis of 5,10,15,20-tetraphenylbenzo[5,6]indeno[1,2,3- <i>cd</i>] benzo[5,6]indeno[1,2,3- <i>lm</i>]perylene (103)	79
14. Synthesis of 1,2,3,4,9,10,11,12-octaphenyldiindeno [1,2,3- <i>cd</i> :1',2',3'- <i>lm</i>]perylene (105)	80
15. Retrosynthetic analysis of perylene molecules	84
16. Construction of amino acid 118	85
17. Construction of amino acid 119	86

18. Construction of amino acids 120 and 121	88
19. Synthesis of phenylcyclopentadienone 122	89
20. Synthetic pathway through the fluoranthenes.....	91
21. Synthesis of the dimers	92
22. Synthetic route through 1,2,7,8-tetrahydrodicyclopenta[<i>cd,lm</i>]perylene (141)	95
23. An alternative route to the synthesis of the dimers.....	97
24. Ring closure of the dimers	99
25. Proposed route A for future investigation	106
26. Proposed route B for future investigation.....	108

TABLES

Table	Page
1. Cu(II)/benzoate/4,4'-bipyridine complexes	14
2. Selected data for cobalt succinates products	20
3. Complexation of Cd(II) and Zn(II) with 3,3'-pytz.....	22
4. Crystal data for ligands 42 , 43 , 45 , and 46	29
5. Crystal data for compounds 48-51	31
6. Crystal data for compounds 52-54	32
7. Selected bond lengths (Å) and angles (deg.) for C ₂₈ H ₁₆ AgF ₆ N ₂ Sb (48)	33
8. Selected bond lengths (Å) and angles (deg.) for C ₁₆ H ₁₀ AgBF ₄ N ₂ (49)	36
9. Selected bond lengths (Å) and angles (deg.) for C ₂₂ H ₁₆ AgF ₆ N ₂ Sb (50)	39
10. Selected bond lengths (Å) and angles (deg.) for C ₃₂ H ₂₆ AgF ₆ N ₂ Sb (51)	42
11. Selected bond lengths (Å) and angles (deg.) for C ₂₄ H ₁₆ AgF ₆ N ₂ Sb (52)	44
12. Selected bond lengths (Å) and angles (deg.) for C ₂₂ H ₁₂ Ag ₂ F ₆ N ₄ O ₆ S ₂ (53)	46
13. Selected bond lengths (Å) and angles (deg.) for C ₃₈ H ₁₈ Ag ₄ F ₁₂ N ₈ O ₁₂ S ₄ (54)	49
14. Summary of topological features of the cyanovinylarene-silver(I) complexes.....	53
15. Results for the coupling of monomers 114-117 under different conditions	93
16. The different conditions employed to obtain products 106-109 from dimers 110-113	99
17. UV data of compounds 64 , 105 , 144 , 145 , 103 , 98 , 99 , and 106	103

ACKNOWLEDGEMENTS

I would like to express my truthful gratitude to my adviser Dr. Kilway for giving me the opportunity to be part of her group. During my years under her supervision, I learned important research skills, and most important I learned the necessary abilities that help to consolidate a good work environment.

I would also like to recognize my committee members Dr. Wurrey, Dr. Kadnikova, Dr. Gutheil, and Dr. Friedman for committing their valuable time reviewing my dissertation.

My sincere appreciation to my coworkers Robert Clevenger, Bradley Miller, Rachel Weiler, and Gregory Giese for their support, and for keeping a good attitude regardless of the situation.

I have to recognize the tremendous help that I received from Dr. Ho (X-ray spectroscopy), Dr. Pascal (X-ray spectroscopy and mass spectrometry), Dr. Peng (UV/Vis absorption and fluorescence spectroscopy), and Dr. King (mass spectrometry). In addition, I should mention Dr. Barron (interpretation of the X-ray data and help with visualization using the Mercury program), and Dr. Van Horn (Mercury program and EndNote programs).

Finally, I am extremely grateful to all of the past undergraduate students that were part of this research: John VanScoy, Deanna Travis, Linda Silva, Katie Kincaid –Longhauser, Adam Brummett, and Jessica Townsend.

Dedicated to my parents, Keith as well as those who have suffered abuse.

CHAPTER 1

MOLECULAR ASSEMBLY OF POLYCYANOARENES WITH SILVER SALTS

INTRODUCTION AND LITERATURE REVIEW

One of my research topics is embedded in the area of molecular self-assembly. This term has been defined by Lawrence¹ as those systems that use noncovalent interactions to form a highly organized structure.² A broader definition would include the formation of supramolecular structure *via* covalent forces (e.g., metal-ligand bonds), noncovalent forces (e.g., hydrogen bonds) or various combinations of the two forces. In the solid state, the latter definition is more properly called molecular architecture or inorganic crystal engineering (ICE). The importance of crystal engineering is condensed in this sentence by Desiraju:³ “if one can predict and control crystal structure of molecules, then one can in principle control the properties of the resulting solids too”. In other words, this statement opens the door for designing novel materials with desirable properties,^{4,5} which include electrical conductivity,⁶ catalytic activity,⁷ photoluminescence,⁸ molecular recognition,⁹ and molecular adsorption.¹⁰

Through the years, the number of terminologies describing certain types of ICE has increased.¹¹ For instance, discrete motifs like metal–organic polygons and polyhedra are referred to as MOPs and metal-organic containers are called MOCs. On the other hand, polymeric materials like coordination polymers utilize the acronym CPs or MOFs for metal–organic frameworks. These terminologies express a specific quality or property of the structure but the concept behind them is essentially the same for all.

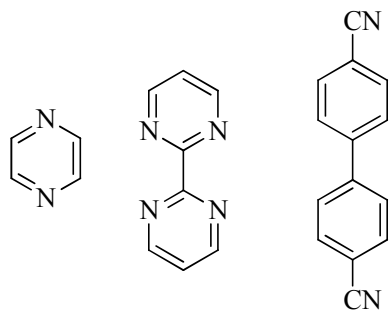
In ICE, the metal ions are referred to frequently as “connectors” and ligands are referred as to “linkers”. The combination of these two units creates a much stronger interaction than the

typical hydrogen bonds and van der Waals interactions, which are observed in living systems. Transition–metal ions are the most common connectors, which have coordination numbers from two to seven. Therefore, several geometries are possible: linear, T– or Y–shaped, tetrahedral, square planar, square pyramidal, trigonal pyramidal, trigonal bipyramidal, octahedral, trigonal prismatic, or pentagonal bipyramidal. In addition, these metals can be used as metal-complex connectors, which mean that certain sites on the metal are chelated or are part of a ring. In this way, the metal-complex connectors can control angles and limit the number of coordination sites. On the other hand, different kinds of linkers (building units) have been employed. The most prevalent linkers comprise nitrogen-containing heteroaromatic compounds (six– and five–membered rings), nitrile-substituted aromatic compounds, and carboxylate aromatic molecules. A list of linkers and connectors are depicted in Figures 1 and 2, respectively.^{12,13}

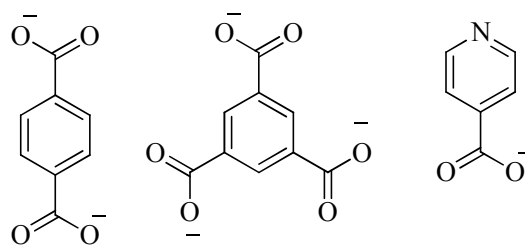
(a) Inorganic ligands

Halides (F, Cl, Br, and I), Cyanometallate ($[M(CN)_x]^{n-}$), CN^- , SCN^-

(b) Neutral organic ligands



(c) Anionic organic ligands



(d) Cationic organic ligands

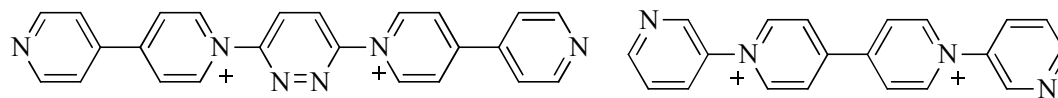


Figure 1. Examples of linkers.

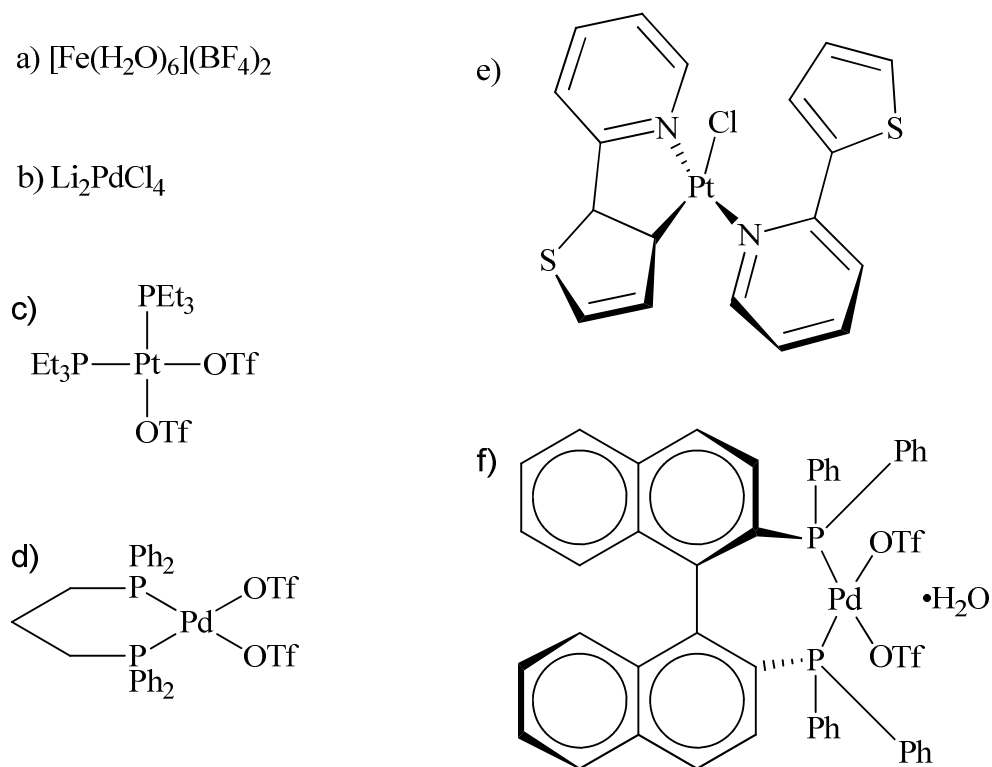
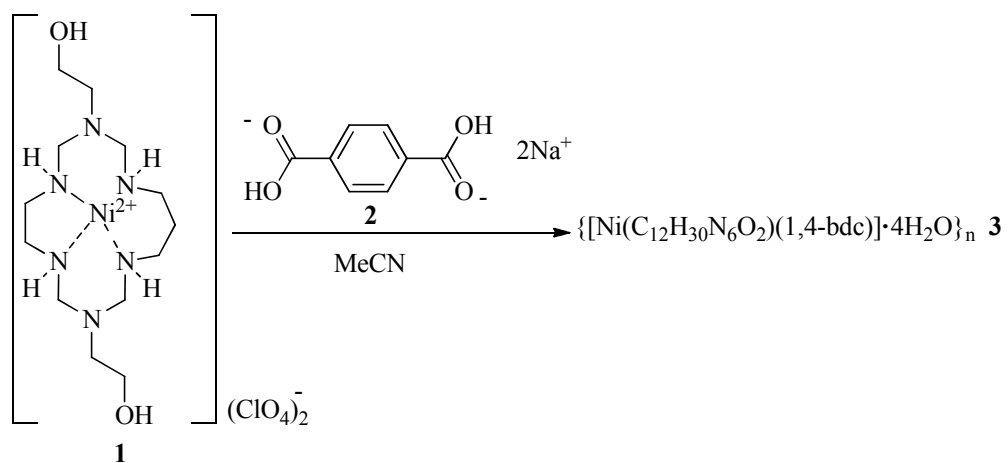


Figure 2. Examples of connectors.

An example that illustrates the concept of metal–complex connectors and linkers is found in the synthesis of a 3D network using a Ni(II) macrocyclic complex (connector) (**1**) and a disodium terephthalate (**2**) (linker) (Scheme 1). Ni(II) in the resulting polymer $\{[\text{Ni}(\text{C}_{12}\text{H}_{30}\text{N}_6\text{O}_2)(1,4\text{-bdc})]\cdot 4\text{H}_2\text{O}\}_n$ (**3**) ($\text{C}_{12}\text{H}_{30}\text{N}_6\text{O}_2$ = macrocyclic ligand and bdc = benzenedicarboxylate) shows a distorted octahedral coordination geometry. Each terephthalate anion binds two metal ions forming a linear one dimensional (1D) coordinating polymer (Figure 3). The 3D network is a consequence of the hydrogen bonding interactions between the chains.¹⁴



Scheme 1. Synthesis of a Ni(II) macrocyclic complex.

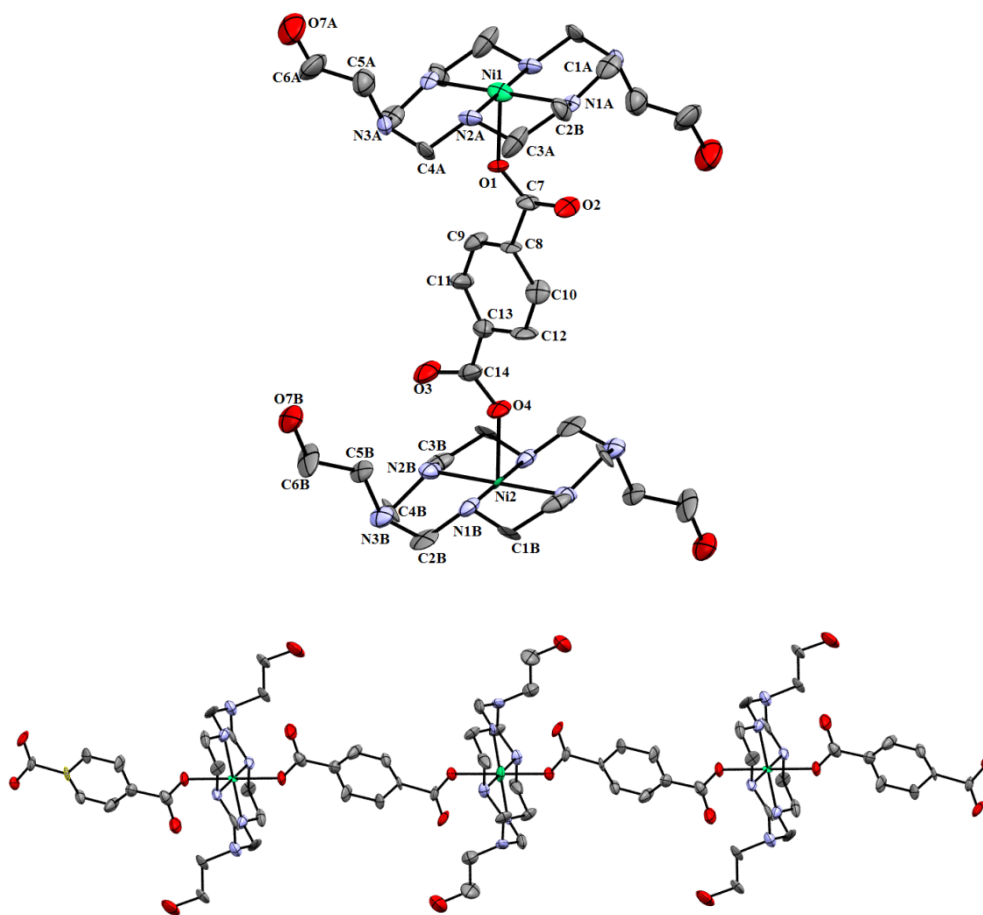


Figure 3. (a) ORTEP representation showing the coordination geometry of polymer **3**. (b) View of the 1D coordination polymer **3**.

An approach that offers an organized way to design discrete molecular polygons and polyhedra (MOPs) is known as a “Molecular Library Model strategy”.¹⁵ The aforementioned method developed by Fujita and then schematized by Stang^{16,17} consists of the assembly of any cyclic structure from predominantly transition metals and rigid building blocks (organic ligands). Two subunits are defined in this design: linear rodlike (L) units that contain two opposing reactive sites and angular units (A) with angles from 0° to 180°. However, the design of 3D structures requires that at least one of the angular subunits include three reactive sites.

The final shape of a structure would depend on the selected subunits. For instance, the combination of three linear ditopic subunits (L^2_3) and three angular ones (A^2_3) with a 60° bending angle form a planar molecular triangle. A molecular square can be constructed from the combination of four linear ditopic units (L^2_4) and four angular ones (A^2_4) which have 90° bending angles. Molecular hexagons require six linear ditopic units (L^2_6) and six angular ones (A^2_6) with a 120° bending angle. The assembly of molecular tetrahedrons requires six linear ditopic units (L^2_6) and four angular tritopic units (A^3_4) with a 60° bending angle. Finally, molecular cubes can be constructed using twelve linear ditopic units (L^2_{12}) and eight 90° angular tritopic units (A^3_8). Some of these structures can be built from many other combinations. The previously discussed structures are depicted below (Figure 4) (superscript denotes topicity, and subscript denotes the number of subunits).

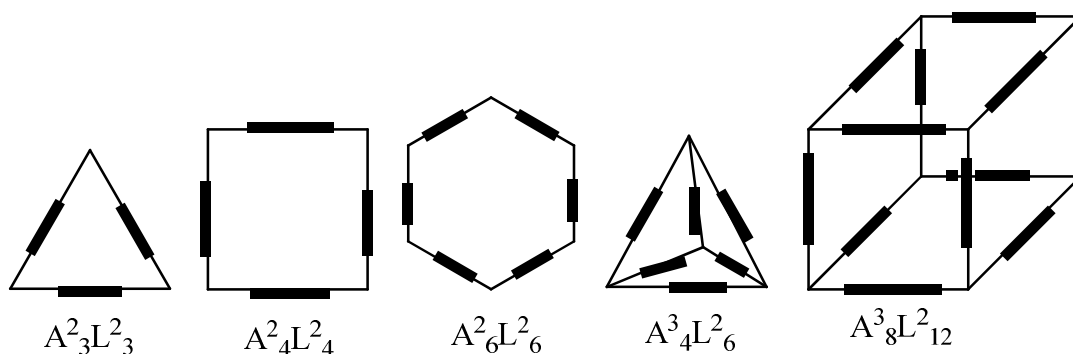


Figure 4. Pictorial representation of cyclic structures.

Factors that affect self-assembly

Self-assembly and, explicitly, crystal engineering of coordination complexes depend on many factors. The control of one factor is not difficult but control of more than one makes it almost impossible to predict the resulting structures. These factors may comprise the chemical structure of the ligand, the coordination geometry of the metal, pH value of the solution, counterion, non-covalent interactions (e.g., M–M or M– π attractions), temperature, and solvent.¹⁸

Ligand

The structure of the ligand is important and can have more than one function. Ligands have been frequently chosen with particular characteristics that can reflect a useful property in the final design of a network. They may exhibit multiple shapes and binding sites, and their structures can be rigid or flexible. In this context, soft bases like N-heteroaromatics have been successfully paired with d^{10} transition metals, e.g., Ni, Pd, or Pt (soft acids). For instance, the synthesis of 3D structures using four tritopic organic ligands with six metal ions (Pd or Pt) afforded “container compounds” with dimensions ranging from ~2–5 nm in diameter.¹⁹ A specific example of a “container” was formed from the assembly of (ethylenediamine)palladium (II) dinitrate (**4**) with 2,4,6-tris(4'-pyridyl)-1,3,5-triazene (**5**) (Figure 5). The resulting cage **6** can encapsulate four molecules of adamantyl carboxylate ions, as determined by X-ray crystallographic analysis.

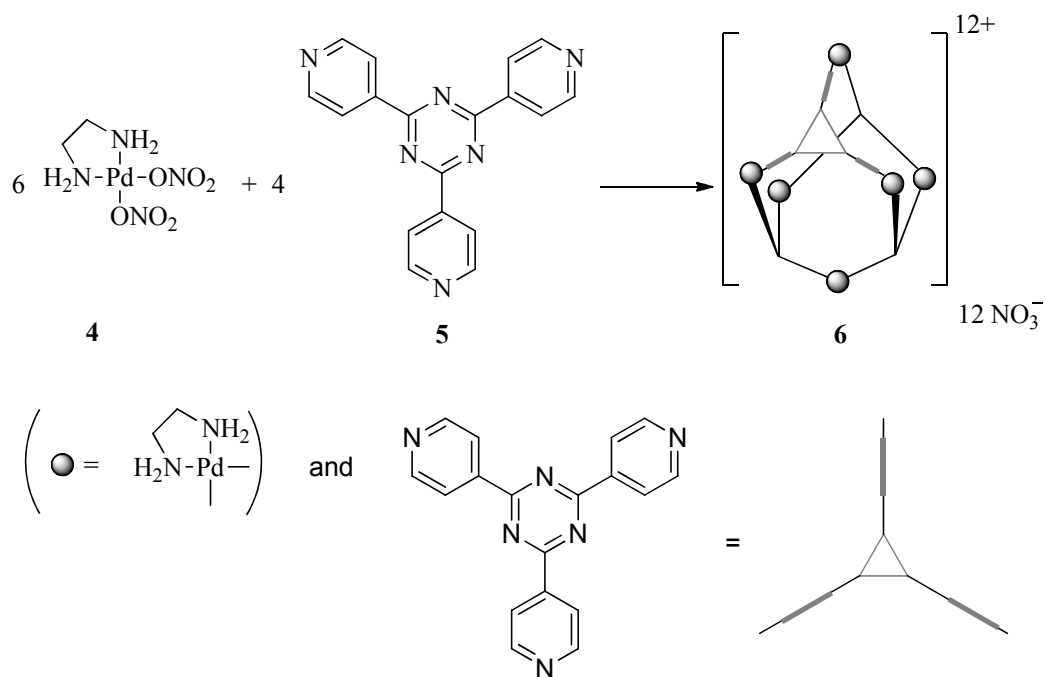


Figure 5. Nanoscopic 3D molecule.

In another investigation, the assembly of tetradentate ligands, 4,4'-bipyridazine (4,4'-*bpdz*) (**7**) and pyridazino[4,5-*d*]pyridazine (*pp*) (**8**) (Figure 6), with silver (I) afforded unusual 3D coordination frameworks²⁰ that included rare high five-fold AgN_5 and six-fold AgN_6 assemblies. Specifically, ligand **8** was treated with $\text{AgClO}_4 \cdot \text{H}_2\text{O}$ to afford the complex, $\text{Ag}_4(\text{pp})_5(\text{ClO}_4)_4$ (**9**), which exhibits a pentacoordinate geometry (Figure 7).

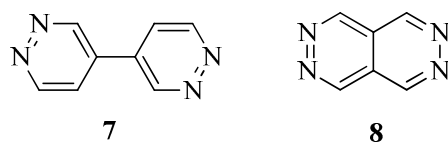


Figure 6. Structure of tetradentate ligands.

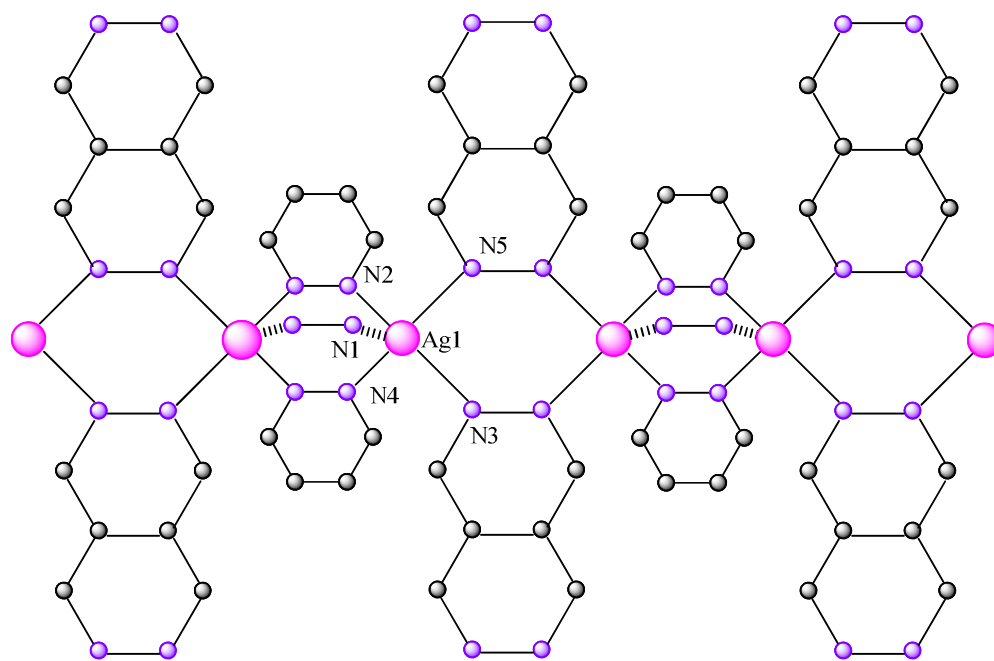
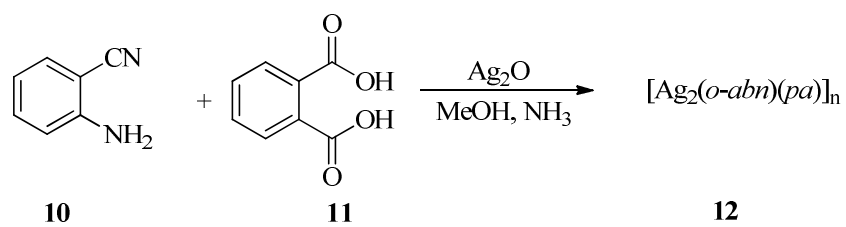


Figure 7. View of the pentacoordinate complex 9 showing the alternation of double and triple pyridazine bridges.

Coordination number of the metal

The coordination number and the resulting geometry of a metal are extremely important in the design of networks because these parameters aid in the prediction of the structure in the solid state. This was a valid motivation that propelled Moore et al.²¹ to elaborate a coordination table of the *d*-block elements using information from the Cambridge Structural Database (CSD). The resulting table provides information about the tendency of *d* elements to adopt specific geometries. For instance, silver (I) normally displays coordination numbers of 2, 3, and 4, with 3 and 4 being the most predominant in the database for polymeric silver complexes. The observed geometries are linear, bent, trigonal planar, T-shaped, pyramidal, tetrahedral, trigonal pyramidal, and square planar.²² Since 1995, a quick survey of the CSD for arrangements containing silver (I) salts and organonitrile ligands was performed. The search resulted in over 700 structures with silver (I) showing an expanded range of coordination numbers from two to eight but once again clearly favoring coordination numbers 3 and 4.²³⁻²⁵ For instance, *o*-aminobenzonitrile, *o*-abn, (**10**), was combined with phthalic acid, paH₂ (**11**) and Ag₂O under basic conditions to afford the complex, [Ag₂(*o*-abn)(pa)]_n (**12**) (Scheme 2). Silver in this complex exhibits two different environments, one is four-coordinated tetrahedral, and the other is five-coordinated square pyramidal (Figure 8).



Scheme 2. Synthesis of complex **12**.

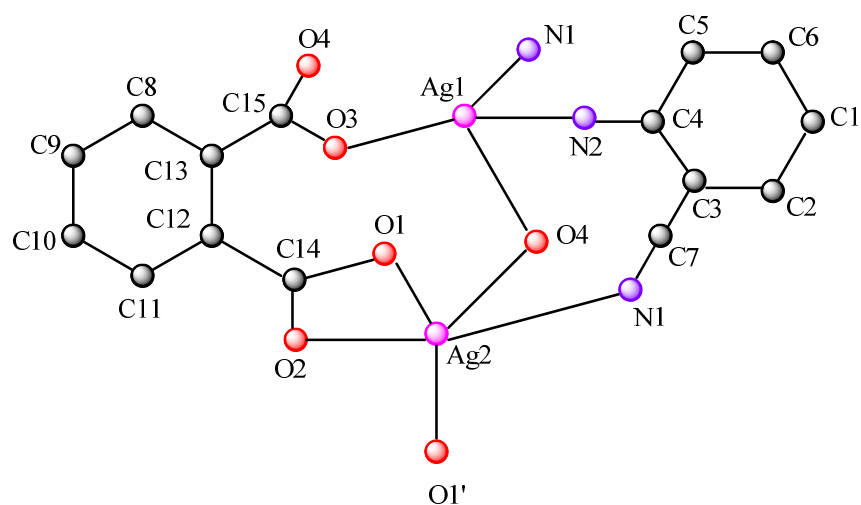
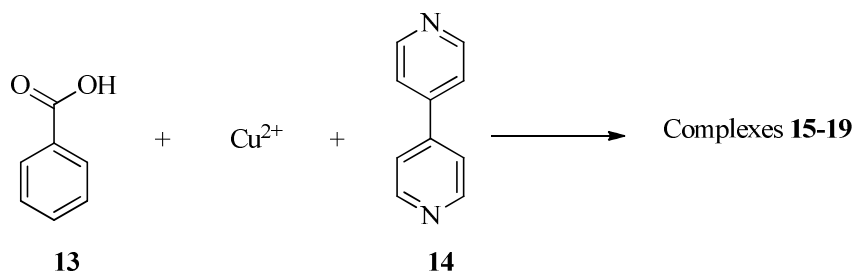


Figure 8. The coordination environment of Ag(I) in complex **12**.

pH effect

The pH value of the reaction is influential in the assembly of some molecular conglomerates. As stated by Zheng,¹⁸ the degree of deprotonation can affect the mode by which ligands binds, and the ligand-to-metal proportion in the products. In addition, pH can induce *in situ* formation of ligands that result in structures different from the initial ones. An example of the pH effect on supramolecular structures is found in the synthetic approach that used benzoic acid (**13**) and 4,4'-bipyridine (**14**) as a ligands, and Cu(II) as the metal counterpart (Scheme 3). The pH was varied from 5.5 to 8.0, and five different complexes were obtained (Table 1). At pH = 5.5, a zero-dimensional (0D) discrete structure (**15**) was obtained. The reaction at pH 6.0 afforded two dimeric complexes (**16**) and (**17**). A neutral pH favored a one-dimensional structure (**18**) while a two-dimensional structure (**19**) was obtained at pH = 8. The distinctions on these structures were attributed to the degree of deprotonation of benzoic acid.²⁶



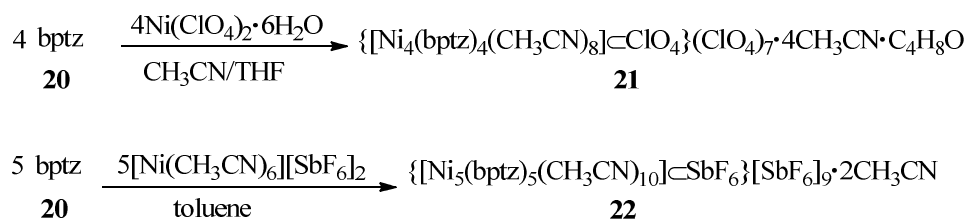
Scheme 3. Synthesis of bipyridine complexes.

Table 1. Cu(II)/benzoate/4,4'-bipyridine complexes.

pH	Dimensionality	Resulting structures
5.5	0D, mononuclear	[Cu(H ₂ O)(benzoate) ₂ (4,4'-bipy) ₂](benzoic acid) ₂ ·(4,4'-bipy) (15)
6	0D, dinuclear	[Cu ₂ (H ₂ O) ₂ (benzoate) ₄ (4,4'-bipy) ₃](H ₂ O) ₉ (16)
6	0D, dinuclear	[Cu ₂ (benzoate) ₄ (4,4'-bipy) ₃] (17)
7.5	1D, chain	[Cu ₃ (H ₂ O) ₄ (benzoate) ₆ (4,4'-bipy) _{4,5}]·(4,4'-bipy)·(H ₂ O) ₅ (18)
8	2D, layer	[Cu ₃ (OH) ₂ (H ₂ O) ₂ (benzoate) ₄ (4,4'-bipy) ₂] (19)

Counterion

The impact of counterions on structure formation can be associated in some way with the size and shape of the anions.^{27,28} For instance, the complexation of 3,6-bis(2-pyridyl)-1,2,4,5-tetrazine (bptz) (**20**) with transition metal salts (M(II) = Ni, Zn, Mn, Fe, and Cu) afforded molecular squares when using the metal salts containing the relative small anions ClO₄⁻ and BF₄⁻. On the other hand, the use of metal salts containing the larger SbF₆⁻ anion favored the formation of a molecular pentagon.²⁹ Specifically, the reaction of bptz **20** with Ni(ClO₄)₂·H₂O in acetonitrile yielded a square complex **21**, while the combination of **20** and [Ni(CH₃CN)₆][SbF₆]₂ in toluene afforded pentagon complex **22** (Scheme 4).



Scheme 4. Synthesis of Ni(II) complexes **21** and **22**.

Compound **21** is formed from four pairs of Ni(II) ions situated at the vertices of a square and each ligand bridges two Ni(II) centers. The diagonal average distance between the metals is 9.676 Å, and the average distance between each Ni(II) is 6.847 Å. A perchlorate ion is encapsulated in the cavity. The Ni(II) environment is approximately octahedral, having four positions occupied by two ligands (bptz) and two attached by two acetonitrile molecules (Figure 9).

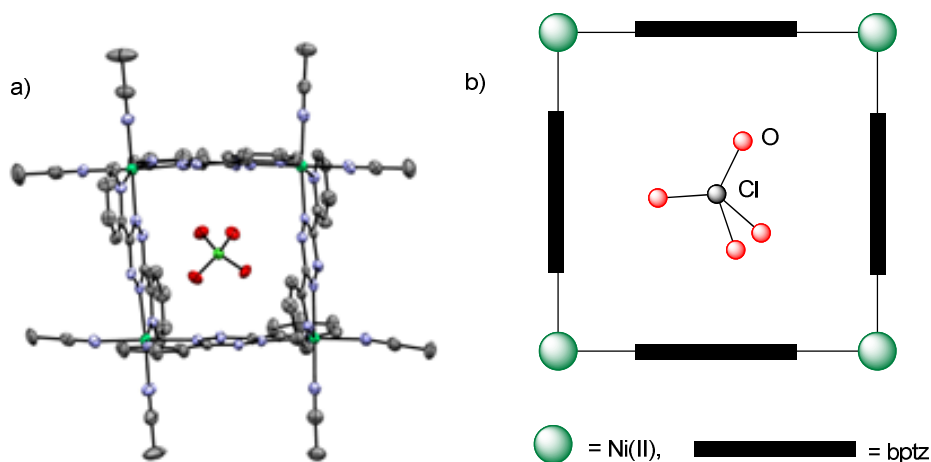


Figure 9. a) Thermal ellipsoid plot of the cationic unit $\{[\text{Ni}_4(\text{bptz})_4(\text{CH}_3\text{CN})_8]\text{ClO}_4\}^{7+}$ in **21**·4CH₃CN·C₄H₈O. b) pictorial representation of the cationic unit in which the average distance Ni^{II}···Ni separation is 6.847 Å

On the other hand, complex **22** is formed by five pairs of Ni(II) metals positioned at the vertices of a pentagon and five ligands (bptz) acting as connectors between the metal centers. This six-coordinated complex is composed of two ligands occupying four sites with the two remaining sites being attached by acetonitrile molecules. The void is occupied by one SbF_6^- ion. The Ni...Ni...Ni vertex angles ($107.8\text{--}108.2^\circ$) are in the range of an ideal pentagon (Figure 10).

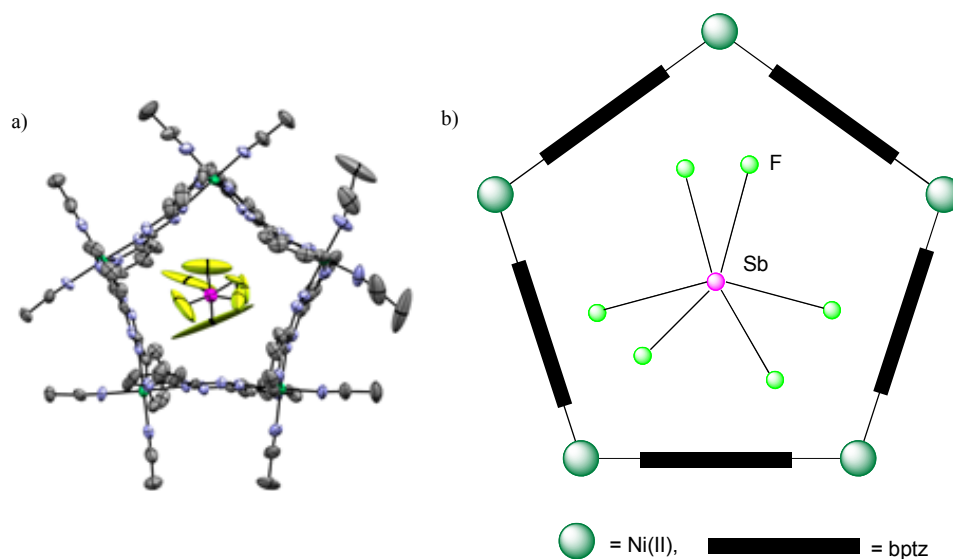


Figure 10. a) Thermal ellipsoid plot of the cationic unit $\{[\text{Ni}_5(\text{bptz})_5(\text{CH}_3\text{CN})_{10}]\text{SbF}_6\}^{9+}$ in **22**·2 CH_3CN . b) Pictorial representation of the cationic unit. The five Ni...Ni...Ni vertex angles ($107.83\text{--}108.19^\circ$) are close to those values in an ideal pentagon.

Non-covalent interactions

There are other interactions, which can contribute to the overall dimensionality of molecular networks. The formation of polymeric structures, oligomers, infinite chains, or infinite two-dimensional sheets can be directed by closed-shell d^{10} - d^{10} attractions (metallophilic interactions).³⁰ The most commonly observed are Au^1 - Au^1 (aurophilic) interactions, whose strengths (29–46 kJ/mol) are comparable to hydrogen bond interactions.³¹ On the other hand, Ag^1 - Ag^1 (argentophilic) interactions, which possess lesser strength than the former, can influence the shape of a network and expand the dimensionality. For instance, the assembly of pyridine with silver (I) perchlorate and silver (I) tetrafluoroborate yielded isomorphous structures $\text{C}_{10}\text{H}_{10}\text{AgN}_2^+\cdot\text{ClO}_4^-$ (**23**) and $\text{C}_{10}\text{H}_{10}\text{AgN}_2^+\cdot\text{BF}_4^-$ (**24**) (Figure 11). These two 1:2 silver (I) pyridine adducts showed strong argentophilic interactions between $[\text{Ag}(\text{py})_2]^+$ ions, forming pairs of $[\text{Ag}(\text{py})_2]_2^{2+}$. The $\text{Ag}\cdots\text{Ag}$ contact distances are both approximately 3.00 Å. These distances are shorter than the sum of van der Waals radii of the two Ag atoms, which is 3.44 Å,³² but longer than the Ag–Ag distance in metallic silver, which is 2.88 Å.^{33,34} Therefore, these $[\text{Ag}(\text{py})_2]_2^{2+}$ pairs are expected to generate strong bonding interactions between them.³⁵

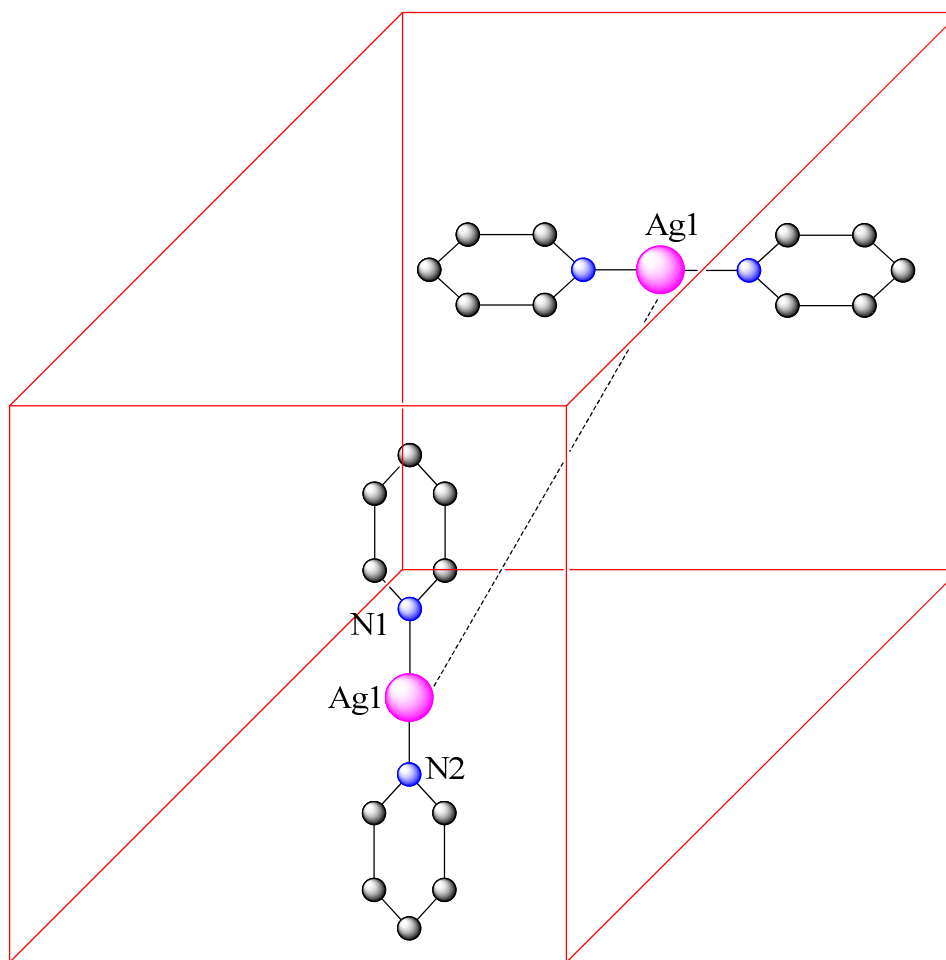


Figure 11. Plot of two $[\text{Ag}(\text{py})_2]^+$ fragments (from structure **23** or **24**) showing the close contact to each other. Counterions (ClO_4^- or BF_4^-) and hydrogens were omitted for clarity.

$\text{M}-\pi$ interactions are common between transition metal cations and unsaturated organic molecules. A study of the association of silver (I) with aromatic hydrocarbons (benzene, toluene, *o*-xylene, *m*-xylene, *p*-xylene, naphthalene, biphenyl, diphenylmethane, and phenanthrene) has demonstrated that the more extended conjugated electronic systems exhibit stronger $\text{Ag}(\text{I})-\pi$ interactions.³⁶ An example of an $\text{M}-\pi$ interaction is observed in the monomeric structure of $[\text{Ag}(\text{C}_{26}\text{H}_{18})(\text{ClO}_4)(\text{C}_6\text{H}_6)_2]$ (**25**) (Figure 12). The complex is

coordinated by two benzene molecules, one oxygen atom from the perchlorate ion, and one carbon-carbon π interaction from η^2 -diphenylanthracene, defining a pseudotetrahedral structure. The silver-ligand π interactions have Ag-C6 and Ag-C7 distances of 2.68 (1) and 2.57 (1) Å, respectively. On the other hand, the silver-benzene π interactions have Ag-C29, Ag-C30, and Ag-C34 distances of 2.62, 2.49, and 2.57 Å, respectively.³⁷

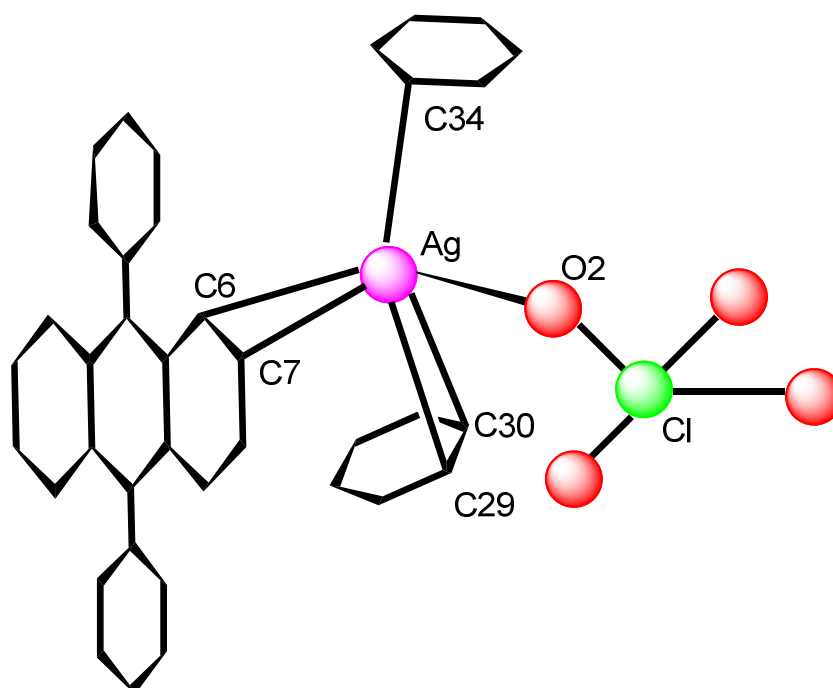


Figure 12. Pictorial representation of silver (I) environment of complex **25** keeping the same numerical labels show in the original structure.³⁷

Temperature

The temperature in the synthesis of organometallic complexes can have noticeable effects in the final topology of a structure.³⁸ This premise is illustrated in the synthesis of five cobalt succinates from identical starting materials at different temperatures. Starting from cobalt hydroxide, succinic acid, and water in a 1:1:28 ratio, the resulting products were characterized by powder X-ray diffraction. Under moderately basic conditions employed in this experiment, Co(II) has a strong preference for octahedral geometry, therefore, the loss of water molecules must be balanced with an increase of more cobalt atoms coordinated to the carboxylate ions. Therefore, an increase of dimensionality is observed, resulting in 1D chains up to 100 °C, 2D sheets at 150 °C, and 3D materials at 190 °C and above. In addition, the density of the network and the number of Co(II) atoms per 1000 Å³ reveals a noticeable increase. Products **26**, **27**, **28**, **29**, and **30** along with some selected data are given in Table 2.³⁹

Table 2. Selected data for cobalt succinate products.³⁹

T °C	Phase	H ₂ O/Co ²⁺ ^a	Density g/cm ³	Co ²⁺ /10 ³ Å ³	Dimensionality ^b
60	Co(H ₂ O) ₄ (C ₄ H ₄ O ₄) ₂ (26)	4(4)	1.945	4.74	1(0)
100	Co(H ₂ O) ₂ (C ₄ H ₄ O ₄) ₂ (27)	2(2)	1.926	5.5	1(0)
150	Co ₄ (H ₂ O) ₂ (OH) ₂ (C ₄ H ₄ O ₄) ₃ ·2H ₂ O (28)	1(1/2)	2.085	7.28	2(2)
190	Co ₆ (OH) ₂ (C ₄ H ₄ O ₄) ₅ ·2H ₂ O (29)	1/3(0)	2.197	8.05	3(2)
250	Co ₅ (OH) ₂ (C ₄ H ₄ O ₄) ₄ (30)	0(0)	2.337	8.88	3(2)

^aThe first number describes the total water content, and the second the total water attached to cobalt centers.

^bThe first number describes the total dimensionality, and the second one gives the M–O–M dimensionality.

Solvent

The role of the solvent in the crystal engineering of networks is diverse. For instance, it can be directly coordinated to the metal or it can influence the nucleation step in the crystallization process,⁴⁰ which ultimately defines the final composition of the structure. The effect of the solvent in the formation of inorganic coordination polymers has been examined by Schröder⁴¹ using 3,6-bis(pyridin-3-yl)-1,2,4,5-tetrazine, (3,3'-pytz) (**31**) as a building block ligand (this compound has two alternative conformations, *transoid* and *cisoid*, Figure 13) and the metal ions Cd(II) and Zn(II). Along with the ligand, the anion (NO₃)⁻ was fixed. Three different solvent mixtures were used: MeOH/CH₂Cl₂, EtOH/CH₂Cl₂, and ⁱPrOH/CH₂Cl₂.

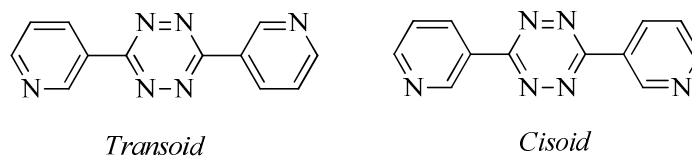


Figure 13. Possible conformations of 3,3'-pytz (**31**).

The structures were characterized by single crystal X-ray diffraction methods. The resulting coordination polymers revealed that their formation motif was governed by the choice of the solvent. All Cd(II) complexes were seven-coordinate, forming distorted pentagonal bipyramidal structures, while all Zn(II) complexes were six-coordinate, resulting in distorted octahedral motifs. In addition, the *transoid* conformation of 3,3'-pytz was the only one

observed in these complexes. The reaction of $\text{Cd}(\text{NO}_3)_2 \cdot 4\text{H}_2\text{O}$ and 3,3'-pytz **31** in $\text{MeOH}/\text{CH}_2\text{Cl}_2$ resulted in the zigzag chain polymer motif **32**, while the substitution of MeOH with EtOH or $i\text{PrOH}$ afforded noninterpenetrated ladder structures **33** and **34**. On the other hand, the complexation of $\text{Zn}(\text{NO}_3)_2 \cdot 6\text{H}_2\text{O}$ and 3,3'-pytz **31** in $\text{MeOH}/\text{CH}_2\text{Cl}_2$ or $\text{EtOH}/\text{CH}_2\text{Cl}_2$ solution afforded alternating single- and double-bridged species in structures **35** and **36**. Finally, the reaction in $i\text{PrOH}/\text{CH}_2\text{Cl}_2$ resulted in non-interpenetrated ladder complex **37** (Table 3 and Figures 14–16).

Table 3. Complexation of Cd(II) and Zn(II) with 3,3'-pytz.

Solvent	Compound
$\text{MeOH}/\text{CH}_2\text{Cl}_2$	$\{[\text{Cd}(\mu\text{-}3,3'\text{-pytz})(\text{NO}_3)_2(\text{MeOH})_2]\}_\infty$ (32)
$\text{EtOH}/\text{CH}_2\text{Cl}_2$	$\{[\text{Cd}_2(\mu\text{-}3,3'\text{-pytz})_3(\text{NO}_3)_4(\text{EtOH})]\}_\infty$ (33)
$i\text{PrOH}/\text{CH}_2\text{Cl}_2$	$\{[\text{Cd}_2(\mu\text{-}3,3'\text{-pytz})_3(\text{NO}_3)_4(\text{CH}_2\text{Cl}_2)]_\infty$ (34)
$\text{MeOH}/\text{CH}_2\text{Cl}_2$	$\{[\text{Zn}_2(3,3'\text{-pytz})_2(\text{NO}_3)_4(\text{MeOH})_2(\mu\text{-}3,3'\text{-pytz})]\}_\infty$ (35)
$\text{EtOH}/\text{CH}_2\text{Cl}_2$	$\{[\text{Zn}_2(3,3'\text{-pytz})_2(\text{NO}_3)_4(\text{EtOH})_2(\mu\text{-}3,3'\text{-pytz})]\}_\infty$ (36)
$i\text{PrOH}/\text{CH}_2\text{Cl}_2$	$\{[\text{Zn}_2(\mu\text{-}3,3'\text{-pytz})_3(\text{NO}_3)_4](\text{CH}_2\text{Cl}_2)_2\}_\infty$ (37)

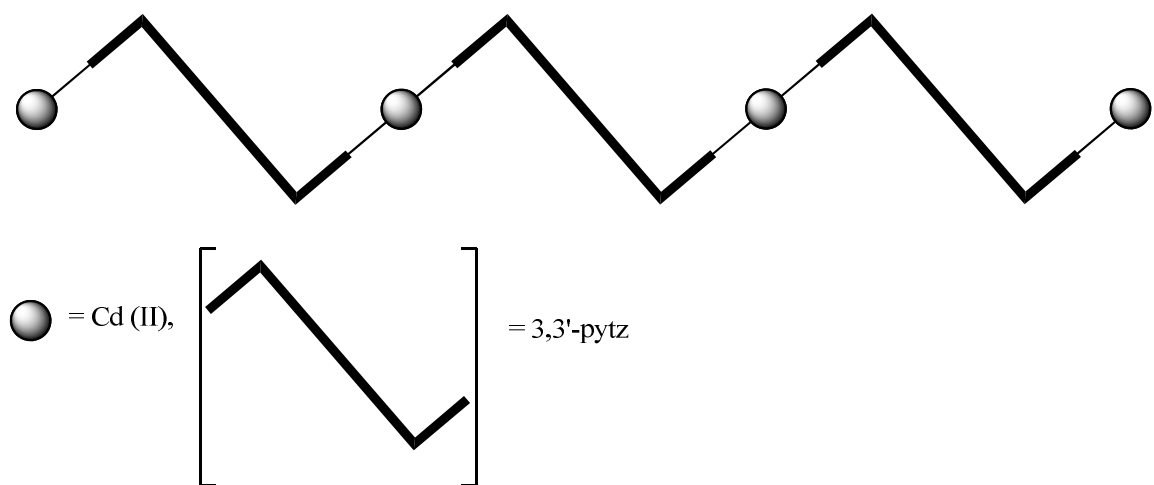


Figure 14. Pictorial representation of the zigzag chain exhibited by $\{[\text{Cd}(\mu\text{-}3,3'\text{-pytz})(\text{NO}_3)_2(\text{MeOH})_2]\}_\infty$ (**32**).

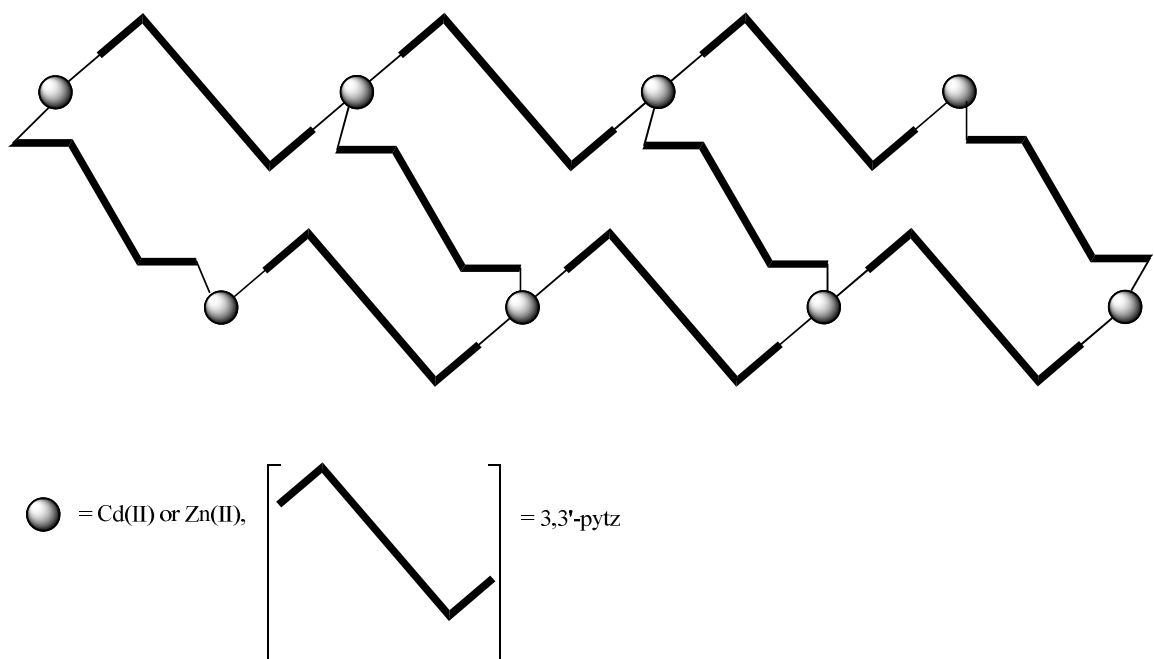


Figure 15. Pictorial representation of the ladder exhibited by complexes $\{[\text{Cd}_2(\mu\text{-}3,3'\text{-pytz})_3(\text{NO}_3)_4(\text{EtOH})]\}_\infty$ (**33**), $\{[\text{Cd}_2(\mu\text{-}3,3'\text{-pytz})_3(\text{NO}_3)_4(\text{CH}_2\text{Cl}_2)]\}_\infty$ (**34**), and $\{[\text{Zn}_2(\mu\text{-}3,3'\text{-pytz})_3(\text{NO}_3)_4](\text{CH}_2\text{Cl}_2)_2\}_\infty$ (**37**).

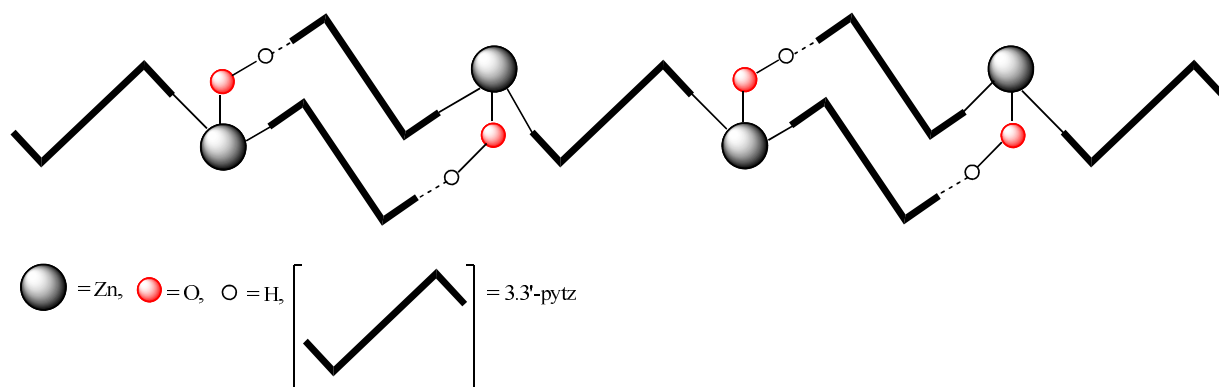


Figure 16. Pictorial representation of $\{[\text{Zn}_2(3,3'\text{-pytz})_2(\text{NO}_3)_4(\text{MeOH})_2(\mu\text{-}3,3'\text{-pytz})]\}_\infty$ (**35**) and $\{[\text{Zn}_2(3,3'\text{-pytz})_2(\text{NO}_3)_4(\text{EtOH})_2(\mu\text{-}3,3'\text{-pytz})]\}_\infty$ (**36**) showing how hydrogen-bonding interactions contribute to form single- and double-bridged species structures.

In the previous paragraphs, the concept of crystal engineering was introduced along with its fascinating chemistry that proclaims: “Ideally, the crystal to be designed has a specific function...”⁴² The sole notion of being able to design structures with predetermined properties has appealed to many devoted scientists who work in ICE of the solid state. This premise impelled our group to jump into this research area with the goal of contributing to this subject. Therefore, we started a methodical study of the complexation of organonitrile compounds with transition metal ions containing silver (I). The expectations were to gain useful information about the composition of silver–ligand complex in the solid state, which in turn may reveal important trends in the design of useful structures.

Polynitrile compounds, which were chosen as the building blocks, represented a good option because they are easily accessible through well-known synthetic procedures. In addition, there is vast information obtained in the previous study conducted by Moore using these polycyano building blocks.^{43,44} Furthermore, as it was shown before when discussing the coordination number of the metal many assemblies of silver with N-aromatic ligands have been reported due to their interesting structures.

Our first study in this area addressed the molecular assembly of the flexible and sterically hindered 1,3,5-tris(cyanomethyl) and 1,4-bis(cyanomethyl) arenes **38-41** (Figure 17) with silver triflate.⁴⁵

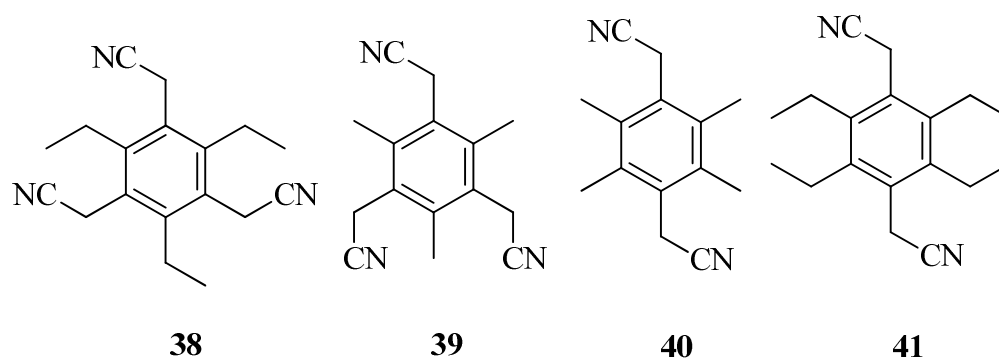


Figure 17. Structure of the ligands **38-41**.

The complexation of 1,3,5-tris(cyanomethyl)-2,4,6-triethylbenzene (**38**) with the silver salt from benzene produced a layered structure with distorted square pyramidal silver sites. The

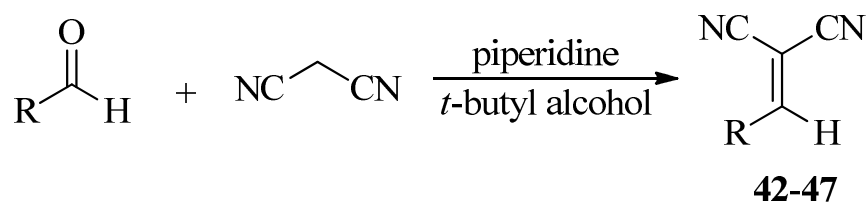
assembly of 1,3,5-tris(cyanomethyl)-2,4,6-trimethylbenzene (**39**) was found to depend on the solvent of crystallization. Crystallization from benzene or toluene resulted in a porous, channel-containing, solvated structure, while the structure resulting from the crystallization from acetone comprised a network solid with the absence of solvent. The structure obtained for silver triflate with 1,4-bis(cyanomethyl)-2,3,5,6-tetramethylbenzene (**40**) from benzene and 1,4-bis(cyanomethyl)-2,3,5,6-tetraethylbenzene (**41**) from toluene generated sheet-like network solids where the counterions were coordinated to the silver. For all the previously described complexes, the presence of methyl or methylene substituents in the benzene ring imposed a three-dimensional restriction. Consequently, cyanomethyl groups were forced to be out of the plane, which in turn reduced the available conformations of the ligands and drove the resulting structures.

Objectives and synthetic approaches

In this study, we want to extend our previous investigation by exploring the consequences of changing the length of the π system and the number of chelation sites on resulting silver (I) complexes in the solid state. Our primary goal is to collect enough information concerning the capability of nitrile ligands to accommodate silver ions, and determine the preferred coordination geometry adopted in a spatial arrangement. Indeed, we want to acquire information about how systematic changes in nitrile ligands affect metal coordination geometries at the primary structural level, and the formation of molecular networks and conglomerates at the secondary and tertiary levels. Our choice for silver salts was based upon their solubility in organic solvents, and their ability to coordinate. Three different types of

silver salts resulted in X-ray quality crystals. These isolated complexes contain triflate, which has been found to poorly coordinate traditional metal ions,⁴⁶ tetrafluoroborate and hexafluoroantimonate both of which have noncoordinating character.^{47,48}

The ligands (**42-47**) were easily accessible in a one-step synthesis using a Knoevenagel condensation reaction between the appropriate aromatic aldehyde and malononitrile as a depicted below (Scheme 5).⁴⁹



42 R = Ph, 84%

43 R = 1-C₁₀H₇, 71%

44 R = 4-PhC₆H₄, 57%

45 R = 9-C₁₄H₉*

46 R = 4-HOCC₆H₄, 34%

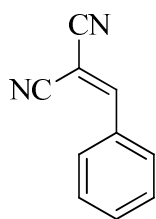
47 R = 3-HOCC₆H₄, 57%

Scheme 5. Synthesis of the ligands (*compound **45** was synthesized by a collaborator following the same scheme outlined above and his purity was confirmed by melting point, proton and carbon NMR spectroscopy).

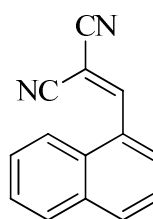
These synthesized ligands contain the two characteristics that would be surveyed in this chapter: π length and topicity. The first group, composed of compounds **42-45**, provides ditopic ligands where the length of the π system has been varied. On the other hand, the assembly

dependence on topicity is examined through the complexation of tetratopic compounds **46** and **47** with silver salts (Figure 18).

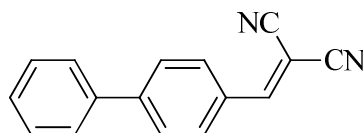
Ditopic ligands



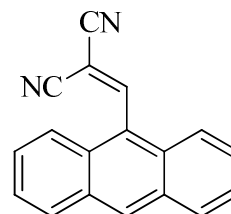
2,2-Dicyanovinylbenzene (**42**)



1-(2,2-Dicyanovinyl)naphthalene (**43**)

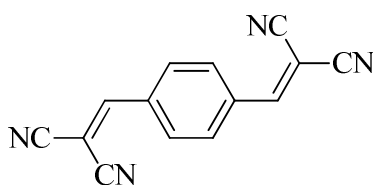


4-(2,2-Dicyanovinyl)biphenyl (**44**)

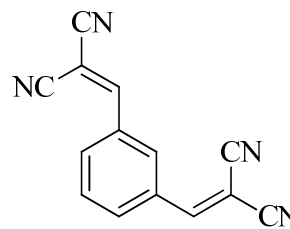


9-(2,2-Dicyanovinyl)anthracene (**45**)

Tetratopic ligands



1,4-Bis(2,2-dicyanovinyl)benzene (**46**)



1,3-Bis(2,2-dicyanovinyl)benzene (**47**)

Figure 18. Structures of the ligands.

Selected crystal data and torsion angles for ligands **42**,⁵⁰ **43**,⁵¹ **45**,⁵² and **46**⁵³ have been collected from the literature and are listed in Table 4. The torsion angles are the angles between the $C_{ar}-C_{ar}$ and the $C_{\pi}-C_{\pi}$ of the ligands and are listed to compare the resulting dihedral angle upon complexation with silver.

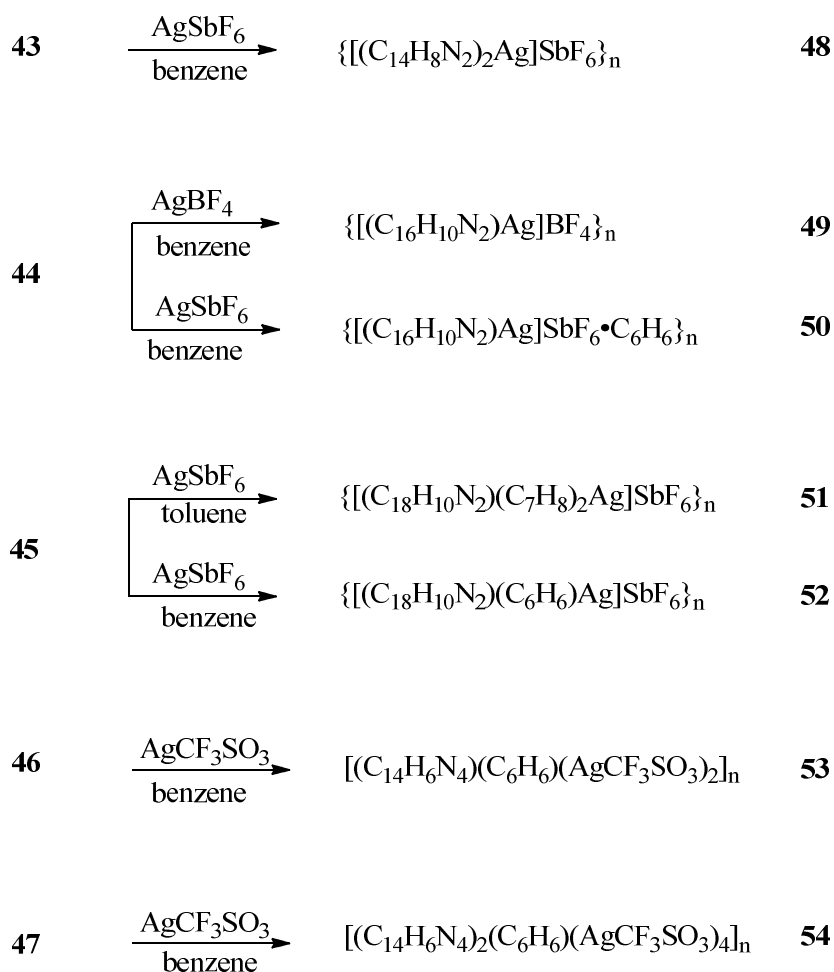
Table 4. Crystal data for ligands **42**, **43**, **45**, and **46**.

Compound	(42)	(43)
Formula	C ₁₀ H ₆ N ₂	C ₁₄ H ₈ N ₂
Space group	<i>P2₁/n</i>	<i>P2₁/n</i>
Cell lengths <i>a, b, c</i> (Å)	9.368(6), 3.916(3), 22.015(15)	3.8272(10), 15.784(4), 17.226(4)
Cell b angle (deg.)	93.58(2)	91.22(2)
Cell volume (Å ³)	806.0(9)	1040.3(4)
<i>Z</i>	4	4
<i>R(F)</i> (obs)	0.0585	0.0573
Selected torsion angles	C(2) (C1) C(7) C(8) -10.1(4) C(6) C(1) C(7) C(8) -171.5(2)	C(2) C(1) C(11) C(12) -38.3(3) C(10) C(1) C(11) C(12) 144.1(2)
Compound	(45)	(46)
Formula	C ₁₈ H ₁₀ N ₂	C ₁₄ H ₆ N ₄
Space group	<i>P2₁/n</i>	<i>P2₁/n</i>
Cell lengths <i>a, b, c</i> (Å)	32.461(7), 4.1267(8), 20.067(4)	6.957(2), 8.621(3), 10.717(4)
Cell b angle (deg.)	107.58(3)	114.45(2)
Cell volume	2562.6(9)	585.1(4)
<i>Z</i>	8	2
<i>R(F)</i> (obs)	0.0677	0.06
Selected torsion angles	C(11)-C(9)-C(15)-C(16) 50.2(4) C(14)-C(9)-C(15)-C(16) -134.1(3) C(11)-C(9)-C(15)-C(16) 50.2(4), -48.9 (4) C(14)-C(9)-C(15)-C(16) -134.1(3), 135.3(3)	C(2)-C(1)-C(4)-C(5) -165.6(2) C(3)-C(1)-C(4)-C(5) -13.8(2)

For convenience, the original atom labels have been modified in order to match with the experimental ones.

Results and discussion

With the exception of ligand **42**, all of the other ligands were successfully complexed with one or two silver (I) salts (Scheme 6). The complete crystallographic information for complexes **48-54** is listed in Tables 5 and 6.



Scheme 6. Synthesis of the complexes.

Table 5. Crystal data for compounds **48-51**.

Compound	48	49	50	51
Formula	C ₂₈ H ₁₆ AgF ₆ N ₄ Sb	C ₁₆ H ₁₀ AgBF ₄ N ₂	C ₂₂ H ₁₆ AgF ₆ N ₂ Sb	C ₃₂ H ₂₆ Ag F ₆ N ₂ Sb
Fw	752.07	424.94	651.99	782.17
Crystal system	Tetragonal	Orthorhombic	Monoclinic	Monoclinic
Space group	<i>P</i> 4 ₃ 2 ₁ 2	<i>P</i> 2 ₁ 2 ₁ 2 ₁	<i>P</i> 2 ₁ / <i>c</i>	<i>P</i> 2 ₁ / <i>c</i>
<i>a</i> , Å	13.8573(2)	7.0244 (2)	15.4531(3)	19.1214(17)
<i>b</i> , Å	13.8573(2)	13.8705 (4)	18.4968(4)	7.9306(5)
<i>c</i> , Å	14.2195(1)	15.5315 (4)	15.3355(3)	19.4367(18)
α , deg.	90	90	90	90
β , deg .	90	90	93.8205(8)	96.445(3)
γ , deg .	90	90	90	90
<i>V</i> , Å ³	2730.50(8)	1513.26(7)	2730.50(6)	2928.8(4)
<i>Z</i>	4	4	8	4
ρ (calcd.), g cm ⁻³	1.829	1.865	1.98	1.774
crystal size	0.08 x 0.14 x 0.16	0.21 x 0.15 x 0.15	0.12 x 0.13 x 0.17	0.01 x 0.03 x 0.14
<i>T</i> , K	200 (2)	200 (2)	200 (2)	200 (2)
<i>F</i> (000)	1456	832	2512	1536
μ , mm ⁻¹	1.772	1.375	2.193	1.654
\mathcal{G}_{\max}	30	27.5	27.5	22.4
Reflections				
Total	48903	14696	36672	11119
Unique	3980	3473	10033	3795
Observed	3359	3221	7630	2112
<i>R</i> _{int}	0.061	0.044	0.044	0.14
Parameters	201	226	730	381
<i>R</i> (<i>F</i>) (obs) ^a	0.041	0.032	0.0393	0.0661
<i>wR</i> (<i>F</i> ²) (all) ^a	0.1063	0.0809	0.1047	0.1069
<i>S</i> (all) ^a	1.13	1.13	1.06	1.03

^a $R(F) = \sum ||F_O| - |F_C|| / \sum |F_O|$; $wR(F^2) = [\sum w(F_O^2 - F_C^2)^2 / \sum w(F_O^2)^2]^{1/2}$; *S* = goodness-of-fit on $F^2 = [\sum w(F_O^2 - F_C^2)^2 / (n - p)]^{1/2}$, where *n* is the number of reflections and *p* is the number of parameters refined.

Table 6. Crystal data for compounds **52-54**.

Compound	52	53	54
Formula	C ₂₄ H ₁₆ AgF ₆ N ₂ Sb	C ₂₂ H ₁₂ Ag ₂ F ₆ N ₄ O ₆ S ₂	C ₃₈ H ₁₈ Ag ₄ F ₁₂ N ₈ O ₁₂ S ₄
Fw	676.01	822.22	1566.32
Crystal system	Triclinic	Triclinic	Monoclinic
Space group	<i>P</i> $\bar{1}$	<i>P</i> $\bar{1}$	<i>Cc</i>
<i>a</i> , Å	8.1200(5)	5.6658(3)	14.3560(2)
<i>b</i> , Å	9.0071(7)	7.0053(4)	14.8368(1)
<i>c</i> , Å	15.7747(12)	16.9762(10)	23.1128(3)
α , deg.	89.013(2)	82.532(2)	90
β , deg.	82.112(3)	81.470(3)	97.6915(5)
γ , deg.	87.916(4)	88.056(4)	90
<i>V</i> , Å ³	1141.96(14)	660.62(6)	4878.67(10)
<i>Z</i>	2	1	4
ρ (calcd.), g cm ⁻³	1.966	1.73	2.133
crystal size	0.05 x 0.08 x 0.21	0.02 x 0.09 x 0.19	0.13 x 0.15 x 0.20
<i>T</i> , K	200 (2)	200 (2)	200 (2)
<i>F</i> (000)	652	400	3032
μ , mm ⁻¹	2.104	1.73	1.868
ϱ_{\max}	27.5	22.5	27.5
Reflections			
Total	14227	6379	63248
Unique	5243	1731	11223
Observed	4138	1314	9208
<i>R</i> _{int}	0.042	0.097	0.059
Parameters	362	190	704
<i>R</i> (<i>F</i>) (obs) ^a	0.0372	0.0482	0.0459
<i>wR</i> (<i>F</i> ²) (all) ^a	0.0966	0.1358	0.1276
<i>S</i> (all) ^a	1.03	1.08	1.06

^a $R(F) = \frac{\sum ||F_O| - |F_C||}{\sum |F_O|}$; $wR(F^2) = [\frac{\sum w(F_O^2 - F_C^2)^2}{\sum w(F_O^2)^2}]^{1/2}$; *S* = goodness-of-fit on $F^2 = [\frac{\sum w(F_O^2 - F_C^2)^2}{(n - p)}]^{1/2}$, where *n* is the number of reflections and *p* is the number of parameters refined.

1-(2,2-Dicyanovinyl)naphthalene silver hexafluoroantimonate from benzene or toluene (48).

The crystals (colorless prisms) are tetragonal, space group $p4_32_12$, and the metal-ligand ratio was found to be 1:2. Four different ligands are attached to one silver atom, resulting in a distorted trigonal pyramidal geometry that largely forms a cationic 3D network (Figures 19 and 20). The bond angles (N–Ag–N) averaged 106.5° (Table 7). The observed bond distance C(12)–C(13) was 1.460 \AA , whereas the literature value for C(sp²)–CN is 1.427 \AA .⁵⁴ This bond distance is slightly elongated but probably due to the effect of the coordination of the CN group to Ag. The Ag(1)–N(15)–C(13) and Ag(1)–N(16)–C(14) bond angles are $170.3(4)$ and $164.7(4)$ (deg.), respectively. This interesting infinite network displays no solvent in the moiety, and counterions are not attached.

Table 7. Selected bond lengths (Å) and angles (deg.) for C₂₈H₁₆AgF₆N₂Sb (48).

Ag(1)–N(16)	2.251(3)	N(16)–C(14)	1.167(5)
Ag(1)–N(15)	2.309(3)	N(15)–C(13)	1.137(6)
N(15)–Ag(1)–N(15)	89.0(2)	N(16)–Ag(1)–N(15)	114.2(2)
N(15)–Ag(1)–N(16)	116.7(2)	Ag(1)–N(16)–C(14)	164.7(4)
N(16)–Ag(1)–N(16)	106.0(2)	Ag(1)–N(15)–C(13)	170.3(4)
C(2)–C(1)–C(11)–C(12)	40.5(7)	C(10)–C(1)–C(11)–C(12)	-139.9(5)

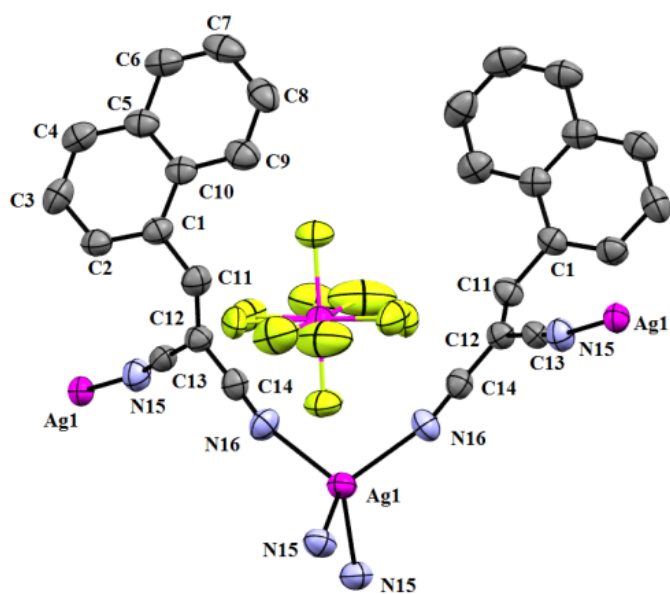


Figure 19. ORTEP representation of complex **48** showing the coordination geometry.

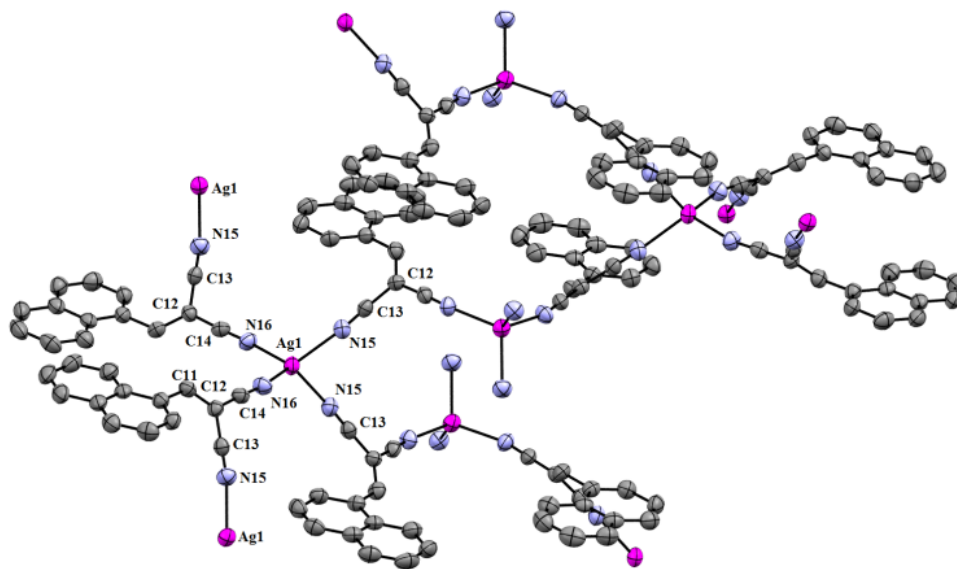


Figure 20. A complementary view of complex **48**.

4-(2,2-Dicyanovinyl)biphenyl silver tetrafluoroborate from benzene (**49**).

The sample (colorless prisms) consisted of orthorhombic crystals, space group $p2_12_12_1$, and the silver-ligand ratio was 1:1. This structure is made of alternating head-tail (CN–arene) units of ligands and silver forming a cationic 3D network (Figure 21). Cyclic motifs formed by five silver atoms and alternating head-tail ligands are observed in this arrangement (Figure 22). Silver exhibits coordination of approximately trigonal planar, taking the attachments on C(14)–C(15) as one ligand as described by Turner and Hasegawa.^{55,56} The Ag(1)–N bond distances are 2.228 Å (N18) and 2.186 Å (N17), and the N(17)–Ag(1)–N(18) bond angle is 124.2° (Table 8). Solvent was not found in the lattice but silver increases its coordination number by attaching effectively to the rear part of the ligand (arene region). Short interactions $X\cdots Y$ were observed between F(2)–C(9) and F(2)–C(10) with values of 2.90 and 2.93 Å, respectively. The observed bond distances for C(8)–C(9) and C(8)–C(10) were 1.447 and 1.435 Å, respectively (literature value for C(sp²)–CN is 1.427 Å).^{54,57} The counterion was not coordinated to the silver ion.

Table 8. Selected bond lengths (Å) and angles (deg.) for C₁₆H₁₀AgBF₄N₂ (**49**)

Ag(1)–N(18)	2.228(3)	Ag(1)–N(17)	2.186(3)
Ag(1*)–C(14)	2.433(9)	Ag(1*)–N(17)	2.336(3)
Ag(1)–C(14)	2.532(4)	N(17)–C(9)	1.130(4)
Ag(1)–C(15)	2.584(4)	N(18)–C(10)	1.139(4)
Ag(1*)–N(18)	2.217(9)		
C(9)–N(17)–Ag(1*)	176.2(3)	N(17)–Ag(1*)–C(14)	115.9(4)
C(9)–N(17)–Ag(1)	166.2(3)	N(17)–Ag(1*)–N(18)	117.9(3)
Ag(1)–N(18)–C(10)	157.3(3)	C(13)–C(14)–Ag(1)	96.5(2)
N(17)–Ag(1)–C(14)	117.8(1)	C(16)–C(15)–Ag(1)	98.2(2)
N(17)–Ag(1)–N(18)	124.2(1)	N(18)–Ag(1*)–C(14)	121.7(4)
N(18)–Ag(1)–C(15)	110.6(1)	C(14)–Ag(1*)–C(15)	30.8(2)
N(18)–Ag(1)–C(14)	117.0(1)	C(10)–N(18)–Ag(1*)	166.7(3)
N(17)–Ag(1)–C(15)	121.1(1)	C(13)–C(14)–Ag(1*)	88.7(3)
C(14)–Ag(1)–C(15)	31.6(1)		
C(3)–C(4)–C(11)–C(12)	31.2(5)	C(2)–C(1)–C(7)–C(8)	-24.8(5)
C(5)–C(4)–C(11)–C(16)	27.7(5)	C(6)–C(1)–C(7)–C(8)	156.0(3)

4-(2,2-Dicyanovinyl)biphenyl silver hexafluoroantimonate from benzene (**50**).

The silver-ligand complex (colorless prisms) produced monoclinic crystals, space group $p2_1/c$, and the composition ratio of ligand-metal was 1:1. This structure is comprised of two antiparallel sheets that are not connected. Each of these sheets define infinite cyclic dimers where silver exhibits trigonal planar coordination (Figures 23 and 24). The dimers are a direct consequence of the ligand binding head-tail (CN–arene) as in structure **49**, but in this case, a small ring is formed. In addition, the connection of four dimers forms an even larger ring that hosts two molecules of benzene. The Ag(1)–N(18), Ag(1)–N(17), and Ag(2)–N(36) bond distances are 2.226 Å, 2.201 Å, and 2.197 Å, respectively (Table 9). The silvers in the macro-ring are in a diagonal position, and the separation across is 13.9 Å. The counterion, hexafluoroantimonate ion, is not attached to silver. However, benzene, which is contained in the lattice, has a small interaction with the silver (I) (2.95 Å). In addition, small interactions (X···Y) contact were observed between C(15) and F(1) (2.97 Å). Overall, this complex is well described as cationic 2D sheets.

Table 9. Selected bond lengths (Å) and angles (deg.) for C₂₂H₁₆AgF₆N₂Sb (**50**).

Ag(1)–N(18)	2.226(3)	Ag(2)–N(35)	2.181(5)
Ag(1)–N(17)	2.201(3)	N(17)–C(9)	1.147(5)
Ag(1)–C(13)	2.610(4)	N(18)–C(10)	1.133(4)
Ag(2)–N(36)	2.197(5)	N(35)–C(27)	1.147(5)
Ag(2)–C(32)	2.598(5)	N(36)–C(28)	1.136(5)
N(17)–Ag(1)–N(18)	136.3(1)	N(36)–Ag(2)–C(32)	114.5(2)
C(13)–Ag(1)–N(17)	109.4(1)	N(36)–Ag(2)–N(35)	136.7(2)
C(13)–Ag(1)–N(18)	113.2(1)	C(32)–Ag(2)–N(35)	103.4(2)
Ag(1)–N(18)–C(10)	169.1(3)	Ag(2)–N(36)–C(28)	161.3(4)
C(9)–N(17)–Ag(1)	159.9(3)	C(27)–N(35)–Ag(2)	151.0(4)
C(2)–C(1)–C(7)–C(8)	-1.1(7)	C(16)–C(11)–C(4)–C(3)	-152.2(4)
C(6)–C(1)–C(7)–C(8)	177.2(4)	C(16)–C(11)–C(4)–C(5)	27.5(5)

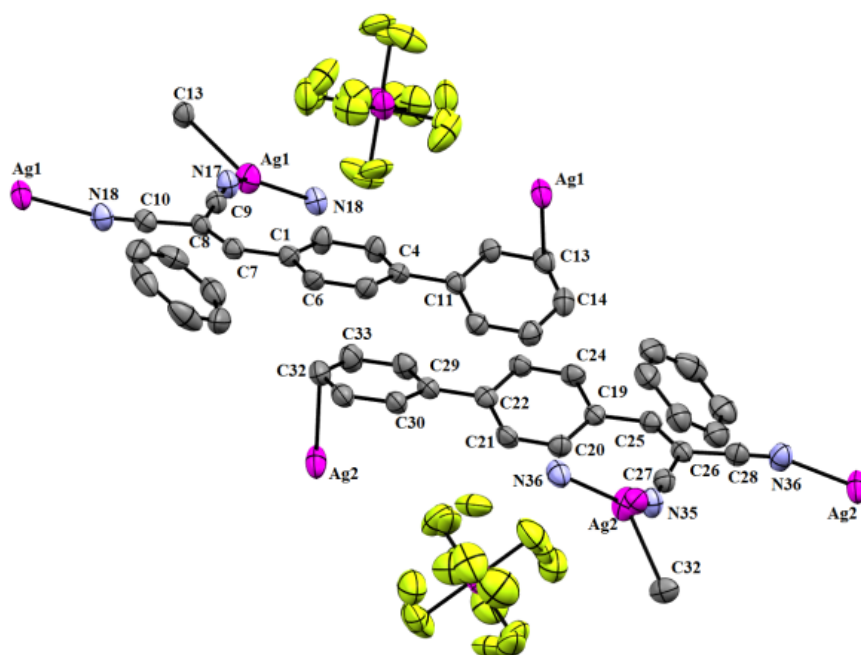


Figure 23. ORTEP representation showing the coordination geometry of complex **50**.

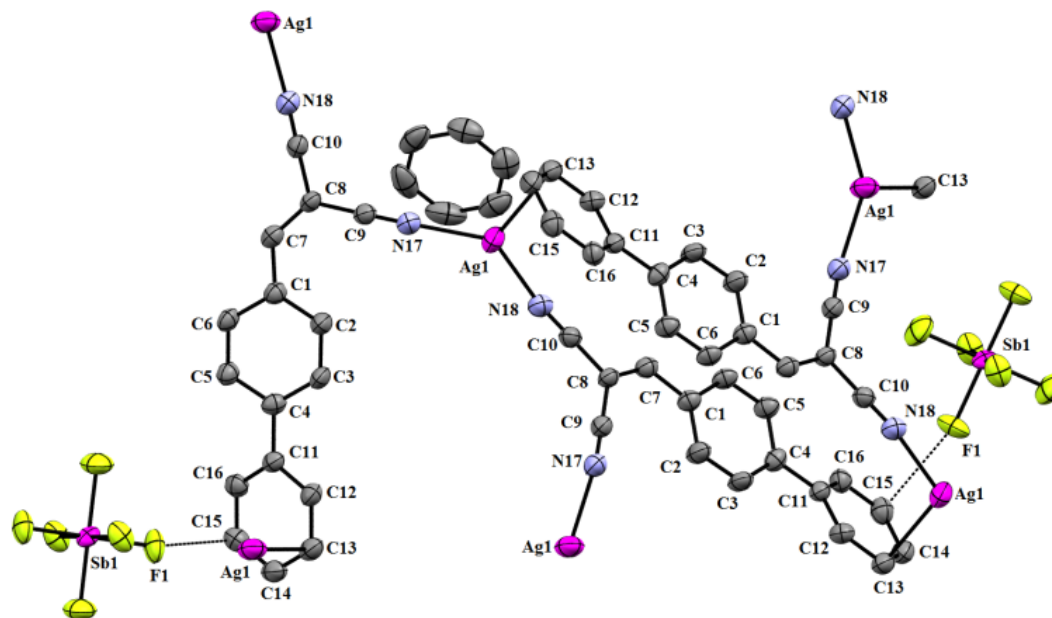


Figure 24. ORTEP representation of a dimer of complex **50**.

9-(2,2-Dicyanovinyl)anthracene silver hexafluoroantimonate from toluene (**51**).

Normal “thermodynamic” driving forces for crystallization (i.e., using heating and slow cooling) did not result in crystallization. However, heating with a heat gun or mixing with a sonicator resulted in the formation of “kinetic” crystals in a matter of 10 – 15 min. The crystals were *a priori* considered very poor (thin needles with very weak scattering), however, a good data set was eventually collected. The silver complex consisted of monoclinic crystals, space group $p2_1/c$, and the metal-ligand ratio is 1:1. The overall structure is a 2D ribbon, and silver atom coordination is approximately tetrahedral (Figure 25). This silver atom is coordinated to two cyano groups from different anthracene molecules and two toluene solvent molecules. These binding toluene molecules displayed an arrangement where their methyl groups are pointing in opposing directions (Figure 26). The Ag(1)–N(19) and Ag(1)–N(20) bond distances are 2.297 Å, and 2.285 Å, respectively (Table 10). Short X··Y contacts were observed between atom F(3) and atom C(18) (2.89 Å).

Table 10. Selected bond lengths (Å) and angles (deg.) for C₃₂H₂₆AgF₆N₂Sb (**51**).

Ag(1)–N(19)	2.297(8)	Ag(1)–C(9S)	2.668(12)
Ag(1)–N(20)	2.285(9)	C(10S)–C(9S)	1.356(16)
Ag(1)–C(3S)	2.534(11)	C(2S)–C(3S)	1.382(13)
Ag(1)–C(2S)	2.632(11)	N(19)–C(17)	1.121(10)
Ag(1)–C(10S)	2.555(14)	N(20)–C(18)	1.156(11)
Ag(1)–N(19)–C(17)	159.8(9)	N(20)–Ag(1)–C(9S)	93.8(4)
C(18)–N(20)–Ag(1)	170.8(8)	N(20)–Ag(1)–C(10S)	115.5(4)
C(9S)–Ag(1)–N(20)	93.8(4)	Ag(1)–C(2S)–C(3S)	31.0(4)
C(2S)–Ag(1)–N(20)	129.9(4)	Ag(1)–C(10S)–C(9S)	79.6(10)
C(3S)–Ag(1)–N(20)	100.2(4)	Ag(1)–C(2S)–C(3S)	70.6(7)
N(19)–Ag(1)–N(20)	105.6(3)	Ag(1)–C(9S)–C(10S)	30.0(5)
N(19)–Ag(1)–C(2S)	98.3 (3)	Ag(1)–C(3S)–C(2S)	78.4(7)
N(19)–Ag(1)–C(3S)	119.8(4)	C(2S)–Ag(1)–C(10S)	100.9(5)
N(19)–Ag(1)–C(10S)	102.4(5)	C(3S)–Ag(1)–C(10S)	113.8(6)
N(19)–Ag(1)–C(9S)	130.4(4)		
C(11)–C(9)–C(15)–C(16)	-38.7(17)	C(14)–C(9)–C(15)–C(16)	140.5(12)

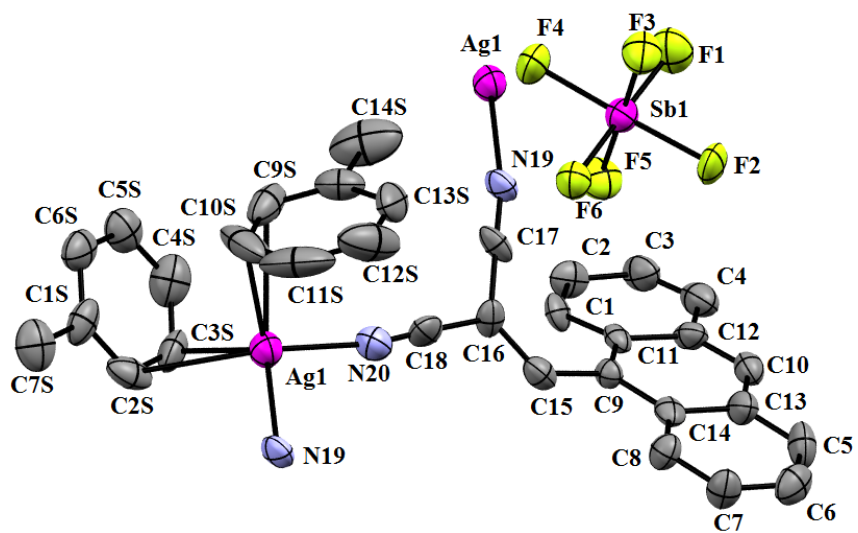


Figure 25. ORTEP representation showing the coordination environment of complex **51**.

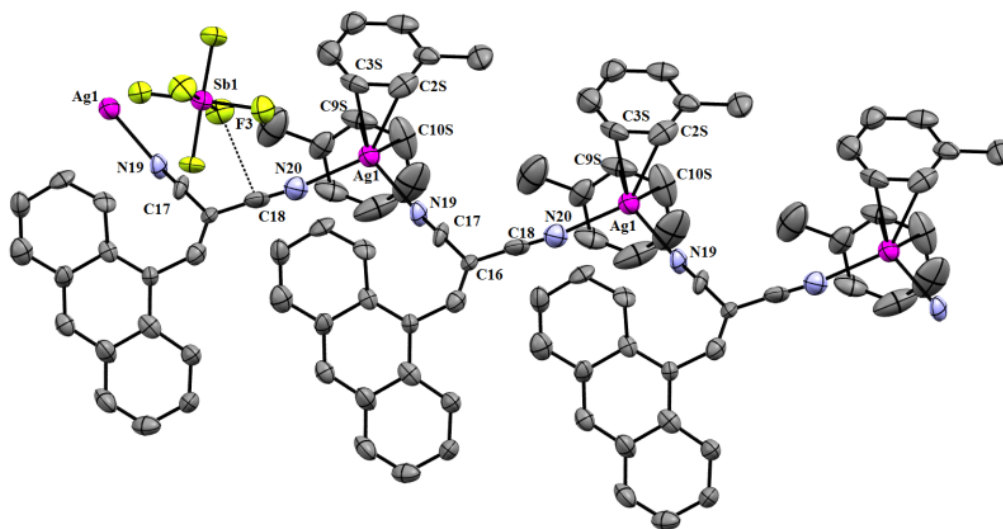


Figure 26. ORTEP representation of complex **51** emphasizing the orientation of the solvent.

9-(2,2-Dicyanovinyl)anthracene silver hexafluoroantimonate from benzene (**52**).

As in structure **51**, these red crystals were formed using a heat gun/sonicator and posed possibly unsatisfactory X-ray quality; nonetheless a data completeness of 99.3% was achieved. The crystals are triclinic, space group $P\bar{1}$, and the silver-ligand composition was found to be 1:1. Silver, which is attached to two cyano groups from different anthracenes and two benzene solvent molecules, exhibits approximately a trigonal pyramidal coordination (assuming that the attachments on C(1S)–C(2S) and (C(4)–C(5) are counted as one ligand).^{55,56} This structure displays macro rings containing four silver atoms, which are bridged by benzene and the cyano groups. The Ag(1)–N(19) and Ag(1)–N(20) bond distances are 2.286 Å, and 2.275 Å, respectively (Table 11). The distance between the antipodal silvers is 10.8 Å. Compound **52** is ultimately described as a structure having 2D cationic sheets (Figures 27 and 28).

Table 11. Selected bond lengths (Å) and angles (deg.) for $C_{24}H_{16}AgF_6N_2Sb$ (**52**).

Ag(1)–N(19)	2.286(3)	Ag(1)–C(5S)	2.588(19)
Ag(1)–N(20)	2.275(3)	Ag(1)–C(4S)	2.566(14)
Ag(1)–C(1S)	2.647(13)	N(19)–C(17)	1.145(5)
Ag(1)–C(2S)	2.673(14)	N(20)–C(18)	1.140(5)
Ag(1)–N(19)–C(17)	159.1(3)	C(1S)–Ag(1)–C(4S)	104.0(6)
Ag(1)–N(20)–C(18)	173.8(3)	C(1S)–Ag(1)–C(5S)	131.8(6)
N(20)–Ag(1)–N(19)	113.9(1)	C(1S)–Ag(1)–N(19)	115.0(5)
N(20)–Ag(1)–C(4S)	110.3(5)	C(2S)–Ag(1)–C(4S)	112.4(7)
N(20)–Ag(1)–C(5S)	94.8(4)	C(2S)–Ag(1)–C(5S)	142.2(6)
N(20)–Ag(1)–C(1S)	90.5(3)	C(2S)–Ag(1)–N(19)	86.6(4)
N(20)–Ag(1)–C(2S)	112.6(5)	C(4S)–Ag(1)–C(5S)	30.4(4)
C(2S)–Ag(1)–C(1S)	30.2(5)	C(4S)–Ag(1)–N(19)	119.2(3)
Ag(1)–C(1S)–C(2S)	75.9(8)	C(5S)–Ag(1)–N(19)	106.2(5)
C(11)–C(9)–C(15)–C(16)	-45.0(6)	C(14)–C(9)–C(15)–C(16)	136.6(4)

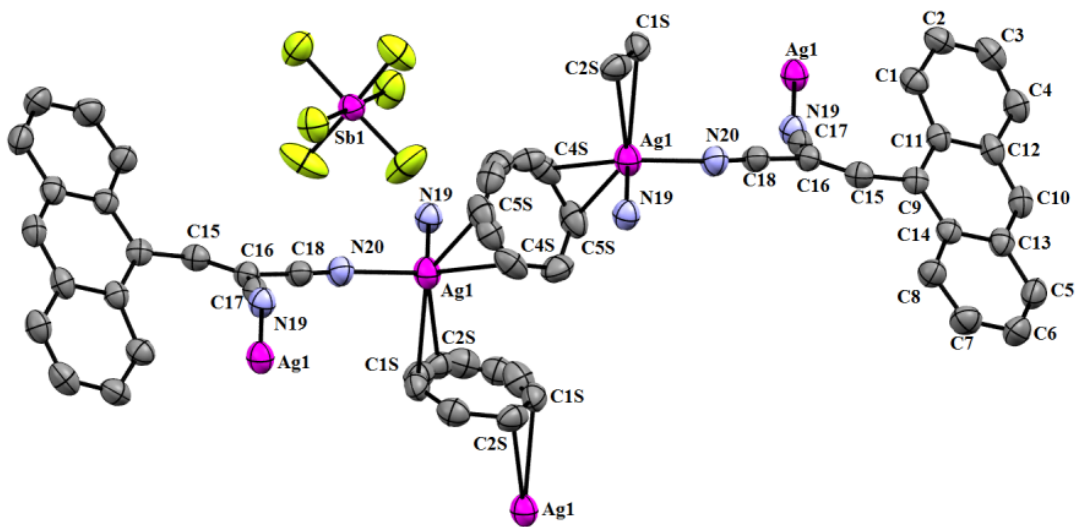


Figure 27. ORTEP representation showing the coordination geometry of complex **52**.

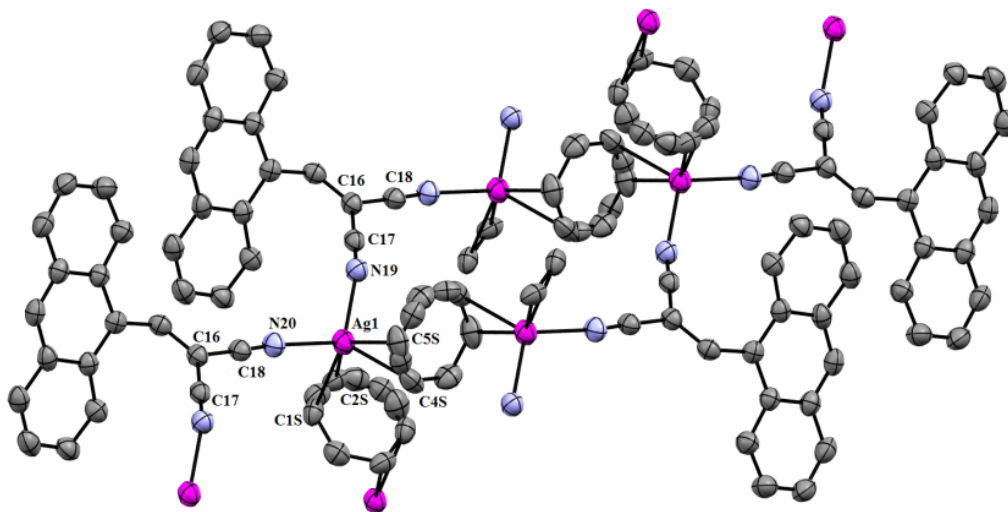


Figure 28. Representation of the cyclic unit observed in complex **52**.

1,4-Bis(cyanovinyl)benzene silver triflate from benzene (**53**).

These crystals (pale yellow plates) are triclinic, space group $P\bar{1}$ and present a 2:1 silver:ligand composition. Complex (**53**), which consists of neutral 2D sheets, displays silver attached to benzene, triflate ion, and ligand defining approximately a trigonal pyramidal environment. The attachment of silver to triflate enables the formation of imperfect-rectangular macrocyclic arrangements which contain four silvers along with two ligands interconnected by two bridges of O-S-O (Figure 29 and 30). This arrangement formed infinite rows that are additionally interconnected on both sides by bridges of benzene. The Ag(1)–O(1), Ag(1)–O(2), Ag(1)–N(9) bond distances are 2.446 Å, and 2.327 Å, and 2.206 Å, respectively (Table 12). The silver···silver distances are 17.0 Å and 5.6 Å, respectively.

Table 12. Selected bond lengths (Å) and angles (deg.) for $C_{22}H_{12}Ag_2F_6N_4O_6S_2$ (**53**).

Ag(1)–O(1)	2.446(5)	N(9)–C(7)	1.128(10)
Ag(1)–O(2)	2.327(5)	Ag(1)–C(1S)	2.522(9)
N(8)–C(6)	1.137(10)	Ag(1)–C(2S)	2.662(9)
Ag(1)–N(9)	2.206(8)	C(1S)–C(2S)	1.363(13)
O(1)–Ag(1)–N(9)	97.6(2)	N(9)–Ag(1)–C(1S)	112.9(3)
O(1)–Ag(1)–O(2)	113.2(2)	N(8)–C(6)–C(5)	176.8(9)
N(9)–Ag(1)–O(2)	116.8(2)	C(1S)–Ag(1)–C(2S)	30.3(3)
O(1)–Ag(1)–C(1S)	99.5(3)	C(2S)–Ag(1)–O(2)	94.8(3)
O(1)–Ag(1)–C(2S)	86.9(2)	Ag(1)–N(9)–C(7)	170.0(7)
O(1)–S(1)–O(2)	113.7(3)	S(1)–O(2)–Ag(1)	120.4(3)
O(1)–S(1)–O(3)	116.1(3)	Ag(1)–O(1)–S(1)	124.6(3)
O(2)–S(1)–O(3)	114.8(3)		
C(2)–C(1)–C(4)–C(5)	-4.3(13)	C(3)–C(1)–C(4)–C(5)	177.1(8)

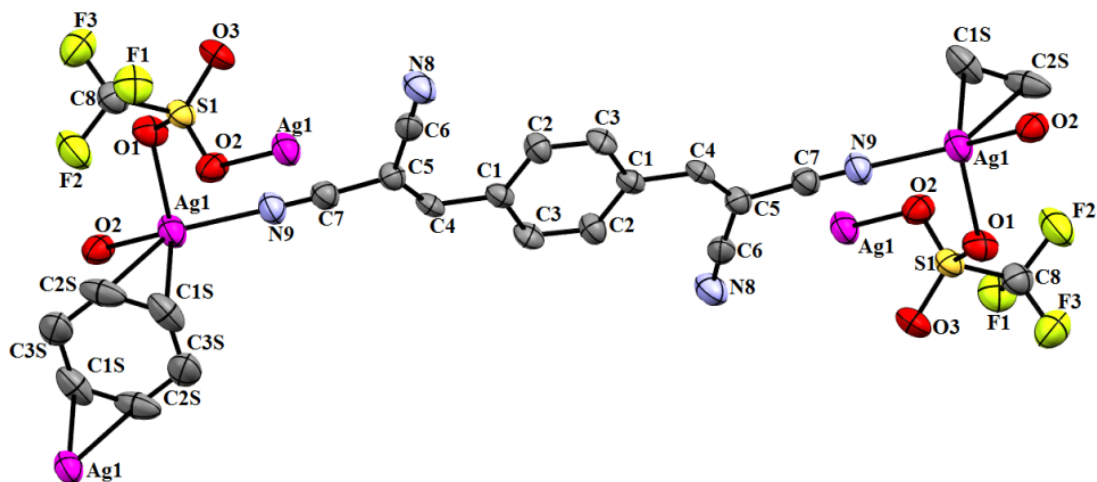


Figure 29. ORTEP representation showing the coordination geometry of complex 53.

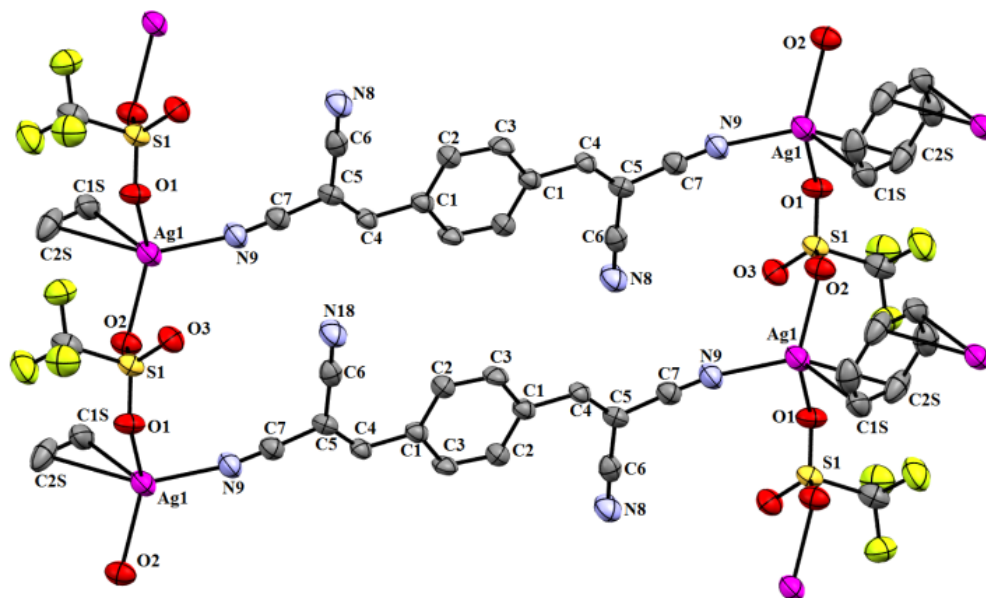


Figure 30. ORTEP representation showing a macrocyclic unit of 53.

1,3-Bis(cyanovinyl)benzene silver triflate from benzene (**54**).

The crystals (colorless plates) are monoclinic, space group Cc , and the composition formed from silver and ligand is 4:2. This neutral 3D network displayed four distinct silver atoms, Ag(1), Ag(2), Ag(3), and Ag(4). The bond distances, and bond angles are listed in Table 13. Ag(1) and Ag(2) display almost a trigonal planar coordination; however Ag(3) and Ag(4) are approximately trigonal pyramidal (Figure 31). This intriguing assembly is formed by two interconnected rings (Figure 32). The complexation of two ligands (using seven of the eight available cyano groups) and two distinctive silvers (Ag(1) and Ag(2)) delineated a macrocycle, which exhibits a Ag(1)···Ag(2) distance of 7.7 Å across the ring. The triflate ions are bonded to their respective silvers, and pointing in opposite directions. On the other hand, an eight-membered ring is formed by the connection of two silvers (Ag(3) and Ag(4)) through two bridges of O-S-O units as in structure **53**. The separation Ag(3)···Ag(4) across the ring is 5.3 Å. Solvent is coordinated to Ag(3). Eight-membered rings and similar structures connecting by bridging triflates have been reported previously,^{44,45} but this present structure has the particular characteristic that only one eight-membered ring has been formed when two were possible. Ag(1) and Ag(2) could have formed a second ring like the ring formed by Ag(3) and Ag(4).

The average distances between Ag···O in the eight-membered ring are 2.42 Å compared with the separations between Ag(1)···O(6) and Ag(2)···O(2) which are 2.89 and 2.75 Å. Solvent attached to Ag(3), which is favored by π interactions with the ligand, could have helped in the formation of the ring since the increase of coordination number could have imparted more flexibility to the system. Alternatively, Ag(1) and Ag(2) are not able to create a similar situation, so they are prevented from fusing together to form a ring.

Table 13. Selected bond lengths (Å) and angles (deg.) for C₃₈H₁₈Ag₄F₁₂N₈O₁₂S₄ (**54**).

Ag(1)–O(1)	2.474(5)	Ag(4)–O(8)	2.458(5)
Ag(1)–N(16)	2.216(6)	Ag(4)–O(11)	2.413(6)
Ag(1)–N(33)	2.196(6)	Ag(4)–N(34)	2.224(6)
Ag(2)–O(4)	2.479(6)	Ag(4)–N(18)	2.207(6)
Ag(2)–N(17)	2.224(6)	N(15)–C(9)	1.128(9)
Ag(2)–N(36)	2.227(6)	N(16)–C(10)	1.153(9)
Ag(3)–O(7)	2.368(5)	N(17)–C(13)	1.145(9)
Ag(3)–O(10)	2.446(5)	N(18)–C(14)	1.142(8)
Ag(3)–N(15)	2.234(6)	N(33)–C(27)	1.164(9)
Ag(3)–C(1S)	2.453(7)	N(34)–C(28)	1.153(9)
Ag(3)–C(2S)	2.402(6)	N(36)–C(32)	1.139(9)
O(1)–Ag(1)–N(33)	114.3(2)	C(1S)–Ag(3)–O(7)	118.2(2)
N(16)–Ag(1)–N(33)	146.0(2)	C(1S)–Ag(3)–N(15)	147.4(2)
O(1)–Ag(1)–N(16)	97.6(2)	C(2S)–Ag(3)–O(7)	151.5(2)
N(17)–Ag(2)–N(36)	143.8(2)	C(2S)–Ag(3)–O(10)	92.0(2)
O(4)–Ag(2)–N(17)	112.0(2)	O(11)–Ag(4)–N(34)	104.4(2)
O(4)–Ag(2)–N(36)	103.7(2)	O(11)–Ag(4)–N(18)	98.2(2)
O(7)–Ag(3)–N(15)	82.0(2)	O(8)–Ag(4)–O(11)	100.7(2)
O(7)–Ag(3)–O(10)	92.6(2)	N(34)–Ag(4)–N(18)	141.8(2)
N(15)–Ag(3)–C(2S)	122.7(2)	O(8)–Ag(4)–N(34)	95.8(2)
O(10)–Ag(3)–N(15)	109.0(2)	N(18)–Ag(4)–O(8)	109.9(2)
C(1S)–Ag(3)–O(10)	96.1(2)		
C(6)–C(1)–C(7)–C(8)	165.9(6)	C(20)–C(19)–C(25)–C(26)	23.4(12)
C(2)–C(1)–C(7)–C(8)	-11.5(10)	C(24)–C(19)–C(25)–C(26)	156.5(7)
C(4)–C(3)–C(11)–C(12)	163.3(7)	C(22)–C(21)–C(29)–C(30)	-170.7(6)
C(2)–C(3)–C(11)–C(12)	-15.4(11)	C(20)–C(21)–C(29)–C(30)	10.3 (11)

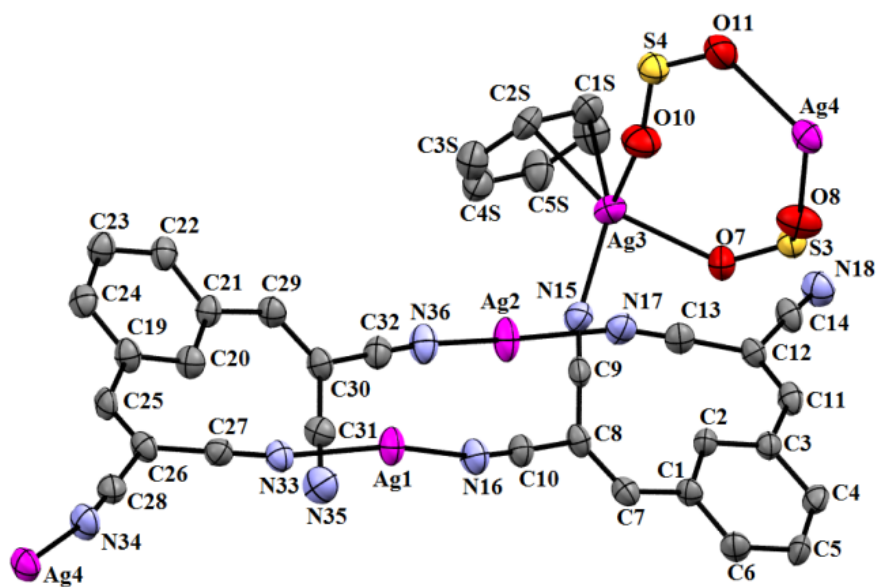


Figure 31. ORTEP representation showing the coordination geometry of complex **54**.

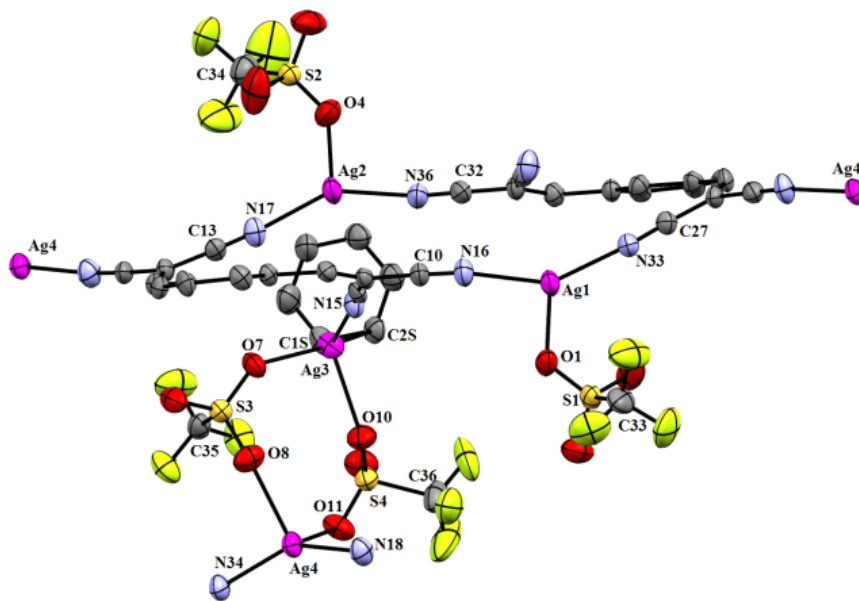


Figure 32. ORTEP representation showing the two ring units, which are part of structure **54**.

Summary

New coordination complexes of cyanovinyl arenes have been assembled with silver salts and analyzed by single-crystal X-ray crystallography. The observed coordination geometries are summarized in Table 14. Assembly of 1-(2,2-dicyanovinyl)naphthalene (**43**) with silver hexafluoroantimonate delineated a cationic 3D network **48** that exhibits an increased coordination number of 4. Complexation of 4-(2,2-dicyanovinyl)biphenyl (**44**) with silver tetrafluoroborate and hexafluoroantimonate from benzene generated two similar structures **49** and **50**, respectively. These complexes are comprised of alternating head-tail (CN–arene) ligands and silver atoms. In both cases, the counterions were nonbonding. Solvent was only present in complex **50**. The overall structure of **49** is quite different from **50**. While the former displays a cationic 3D network the latter is defined by cationic 2D sheets.

Complexation of 9-(2,2-dicyanovinyl)anthracene (**45**) with silver hexafluoroantimonate from toluene afforded a cationic 2D ribbon **51**, and from benzene yielded cationic 2D sheets **52**. Complexes **51** and **52** contained solvent bonded to their structures, which contributed to increasing the coordination number to four. In both cases, the hexafluoroantimonate ion is nonbonding. One of the differences between these complexes is that a macro-ring is only formed in complex **52**.

The crystal association of 1,4-bis(cyanovinyl)benzene (**46**) with silver triflate from benzene yielded complex (**53**). This complex consists of neutral 2D sheets that include imperfect-rectangular macrocyclic arrangements that are interconnected on both sides by bridges of benzene. On the other hand, the assembly of 1,3-bis(cyanovinyl)benzene (**47**) with

silver triflate from benzene gave compound **54**, which is a neutral 3D network formed by two interconnected rings. Solvent and triflate counterions are bonded in both complexes.

Table 14. Summary of topological features of the cyanovinylarene-silver(I) complexes.

Compound	Solvent	Coord. geometry	Coord. no	Structure description
$\{[(C_{14}H_8N_2)_2Ag]SbF_6\}_n$ (48)	Benzene or toluene	Trigonal pyramidal	4	Cationic 3D network
$\{[(C_{16}H_{10}N_2)Ag]BF_4\}_n$ (49)	Benzene	Trigonal planar	3	Cationic 3D network
$\{[(C_{16}H_{10}N_2)Ag]SbF_6 \cdot C_6H_6\}_n$ (50)	Benzene	Trigonal planar	3	Cationic 2D sheets
$\{[(C_{18}H_{10}N_2)(C_7H_8)_2Ag]SbF_6\}_n$ (51)	Toluene	Tetrahedral	4	Cationic 2D ribbon
$\{[(C_{18}H_{10}N_2)(C_6H_6)Ag]SbF_6\}_n$ (52)	Benzene	Trigonal pyramidal	4	Cationic 2D sheets
$[(C_{14}H_6N_4)(C_6H_6)(AgCF_3SO_3)_2]_n$ (53)	Benzene	trigonal pyramidal	4	Neutral 2D sheets
$[(C_{14}H_6N_4)_2(C_6H_6)(AgCF_3SO_3)_4]_n$ (54)	Benzene	Trigonal planar and trigonal pyramidal	3 and 4	Neutral 3D network

Conclusions

As expected, in all of the structures, tetrafluoroborate and hexafluoroantimonate counterions were not bonded while triflate was bonded. The π system length helped to stabilize the formation of the complexes. Using this approach, no silver complexes were formed using ligand **42**. Therefore, the π -stabilization and aromatic solvents did not lend enough stability to form a complex. In addition, ligands **43** and **45** formed complexes with high coordination number by incorporating an additional ligand or solvent in their structures. Even though the units in compounds **46** and **47** (tetratopic ligands) are not strictly flexible, the positions of the chelate sites confers a certain degree of flexibility and results in complexation with silver. Therefore, these compounds were able to accommodate additional ligands and solvent increasing their coordination number.

All metal–organic frameworks (MOFs) synthesized here were indeed affected by the nature of the counterions in combination with the topology of the organic ligands. These results reinforce our previous investigation in this area,⁴⁵ and the observed trends reported by Moore,²² which may be our most important contribution in ICE.

Experimental Section

General Procedures. Melting points were uncorrected. Proton NMR spectra were recorded on a Varian AC 400 spectrometer. Carbon NMR spectra were recorded on a Varian AC 400 spectrometer operating at 100 MHz. Commercial chemicals were used as supplied, unless otherwise stated. The silver salts: hexafluoroantimonate, triflate, and tetrafluoroborate were purchased from Aldrich. All the ligands were synthesized using a procedure adapted from Corson and Stoughton,⁴⁹ with the exception of dicyanovinylanthracene that was provided by Pascal Jr. Vials with Teflon-lined caps were purchased from Fisher. They were washed with distilled water and oven dried at 110 °C before use. No special steps were taken to exclude oxygen or moisture during the growth of X-ray quality crystals.

X-ray data were collected by using graphite monochromated Mo K α radiation (0.71073 Å) on a Nonius KappaCCD diffractometer. The diffraction data were processed and reduced with DENZO-SMN,⁵⁸ PLATON,⁵⁹ and Siemens SHELXTL.⁶⁰ All structures were solved by the charge flipping algorithm^{59,61} or direct methods.⁶⁰

2,2-Dicyanovinylbenzene (42). Malononitrile (3.10 g, 46.9 mmol) and *t*-butyl alcohol (25 mL) were added to a 125-mL Erlenmeyer flask. The solution was stirred and gently heated until all of the malononitrile dissolved. While stirring, benzaldehyde (5.02 g, 47.3 mmol) was added to the flask. Piperidine (3 drops) was then added causing the solution to become orange. The solution was stirred and gently heated for seven min. Formation of solid occurred when the stirring was stopped. The solid was filtered and washed with a water/acetic acid mixture to produce white crystals (6.09 g, 39.5 mmol, 84%); mp 82-83 °C (lit.⁶² mp 84-85 °C). ¹H NMR

(400 MHz, CDCl₃): δ (ppm) 7.55 (t, $J = 8$ Hz, 2H), 7.64 (t, $J = 8$ Hz, 1H), 7.79 (s, 1H), 7.91 (d, $J = 4$ Hz, 2 H). ¹³C NMR (100 MHz, CDCl₃): δ (ppm) 82.8, 112.5, 113.7, 129.6, 130.7, 130.9, 134.6, 160.0.

1-(2,2-Dicyanovinyl)naphthalene (43). 1-Naphthaldehyde (1.00 g, 6.40 mmol) was placed into a 250-mL Erlenmeyer flask and a solution of malononitrile (0.422 g, 6.40 mmol) and *t*-butyl alcohol (25 mL) was added. The resulting solution was stirred, and piperidine (5 drops) was added to the colorless solution. After three min, the solution became yellow with precipitate formation. The color of the solution then changed to a fluorescent green. The solution was vacuum, filtered, and allowed to dry overnight. The resulting product was fluorescent yellow in color (0.936 g, 4.58 mmol, 71%), mp 167-169 °C (lit.^{63,64} mp 168-169 °C). ¹H NMR (400 MHz, CDCl₃): δ (ppm) 7.59-7.71 (m, 3H), 7.95 (d, $J = 8$ Hz, 2 H), 8.10 (d, $J = 8$ Hz, 1H), 8.27 (d, $J = 8$ Hz, 1 H). ¹³C NMR (100 MHz, CDCl₃): δ (ppm) 85.2, 112.5, 113.7, 122.3, 125.4, 127.3, 127.5, 128.5, 128.6, 129.4, 131.0, 133.5, 135.0, 157.7.

4-(2,2-Dicyanovinyl)biphenyl (44). Malononitrile (0.412 g, 6.20 mmol) and ethanol (10 mL) were added to a 125-mL Erlenmeyer flask. The solution was stirred and gently heated until all of the malononitrile dissolved. While stirring, 4-biphenylcarboxaldehyde (1.01 g, 5.50 mmol) and piperidine (3 drops) were added causing the formation of a yellow product. The solid was filtered and recrystallized from ethanol to yield (0.719 g, 3.12 mmol, 57%): mp 139.5-140 °C (lit.⁶⁵ mp 142-143 °C). ¹H NMR (400 MHz, CDCl₃): δ (ppm) 7.42-7.52 (m, 3H), 7.64 (d, $J = 8$ Hz, 2H), 7.76 (t, $J = 8$ Hz, 3H), 7.98 (d, $J = 8$ Hz, 2H). ¹³C NMR (100 MHz, CDCl₃): δ (ppm) 81.8, 112.8, 113.9, 127.2, 127.9, 129.0, 129.1, 129.7, 131.4, 138.8, 147.2, 159.2.

9-(2,2-Dicyanovinyl)anthracene (45). This compound was synthesized by a collaborator following the same procedure outlined above. Mp 205-206 °C (lit.⁶⁶ mp 203-205 °C). ¹H NMR (400 MHz, CDCl₃): δ(ppm) 7.57 (t, *J* = 8.0 Hz, 2H), 7.67 (t, *J* = 8.0 Hz, 2H), 7.92 (d, *J* = 8.0 Hz, 2H), 8.08 (d, *J* = 8.0 Hz, 2H), 8.63 (s, 1H), 8.92 (s, 1H). ¹³C NMR (100 MHz, CDCl₃): δ (ppm) 92.3, 111.4, 113.0, 123.3, 123.8, 126.0, 128.3, 129.0, 129.5, 130.8, 132.5, 160.6.

1,4-Bis(2,2-dicyanovinyl)benzene (46). Malononitrile (5.20 g, 78.7 mmol) and *t*-butyl alcohol (25 mL) were added to a 50-mL Erlenmeyer flask containing terephthalaldehyde (5.00 g, 37.7 mmol). Piperidine (3 drops) was added to the stirring solution. The addition caused the solution to become red in color. The solution was then heated approximately three min, and the resulted solid was filtered and allowed to dry. The solid was recrystallized from a mixture of acetone/water (2.91 g, 12.6 mmol, 34%), mp 259-262 °C (lit.⁶⁷ mp 264 °C). ¹H NMR (400 MHz, CDCl₃): δ(ppm) 7.82 (s, 2H), 8.05 (s, 4 H). ¹³C NMR (100 MHz, CDCl₃): δ (ppm) 86.7, 111.8, 112.8, 131.2, 135.1, 157.1.

1,3-Bis(2,2-dicyanovinyl)benzene (47). Malononitrile (5.40 g, 81.7 mmol) and *n*-butyl alcohol (25 mL) were placed in a 50-mL Erlenmeyer flask. Isophthalaldehyde (5.00 g, 37.3 mmol) was added to the flask. Piperidine (8 drops) was added to the swirling solution. The reaction mixture was heated, and its color turned reddish-orange. After 15 min, the reaction mixture became thick. This material was filtered and washed with distilled water. The resulting pale-orange product was recrystallized from acetone/water (4.87 g, 21.2 mmol, 57%), mp 174-176 °C (lit.⁶⁷ mp 175 °C). ¹H NMR (400 MHz, CDCl₃): δ (ppm) 7.78 (t, *J* = 8 Hz, 1 H), 7.85 (s,

2 H), 8.19 (s, 1H), 8.21 (d, $J = 4$, 2 H). ^{13}C NMR (100 MHz, CDCl_3): δ (ppm) 86.2, 111.8, 112.7, 131.1, 132.0, 132.4, 134.6, 157.5.

Complexation of cyanovinyl ligands with silver salts. Using a typical experimental procedure the ligand, the silver salt and the solvent were combined in a screw-capped vial. If the solids did not dissolve, the mixture was heated with a heat gun. Then, the vial was placed in a sand bath for six hours. The material was heated using a temperature gradient of $20\text{ }^\circ\text{C}$ /two hour period until a maximum temperature of $120\text{ }^\circ\text{C}$ was reached. The heat was turned off and the vial was allowed to cool to room temperature for 12 hours. Those vials that afforded good quality crystals were submitted for X-ray analysis.

CHAPTER 2
SYNTHESIS OF POLYCYCLIC AROMATIC HYDROCARBONS
INTRODUCTION AND LITERATURE REVIEW

This part of the dissertation addresses the synthesis of medium size polycyclic aromatic hydrocarbons (PAHs), including ones that contain a perylene structure in their centers. Perylene is an alternant PAH constituted of two fused naphthalene molecules bridged at the one and eight positions (Figure 32). PAHs is a term used to describe bonded aromatic rings, which are exclusively constituted by carbon and hydrogen atoms.⁶⁸ The size of rings in PAHs may vary, however compounds having five- or six-membered rings are the most common. Naphthalene is frequently included as a PAH, although the International Union of Pure and Applied Chemistry (IUPAC) has defined anthracene (**55**) and phenanthrene (**56**) as the simplest PAHs.⁶⁹

PAHs are grouped in two major categories: alternant and nonalternant PAHs. In general, PAHs containing only six-membered benzenoid rings are called alternant PAHs (e.g., benzo(*a*)pyrene (**57**), [6]helicene (**58**), coronene (**59**), 9,10,11,12,13,14-hexaphenylbenzo[*f*]tetraphene (**60**), perylene (**61**), 9,18-diphenyltribenzo[*f,k,m*]tetraphene (**62**), and 9,10,11,20,21,22-hexaphenyltetrabenzo[*a,c,l,n*] pentacene (**63**) (Figure 33).

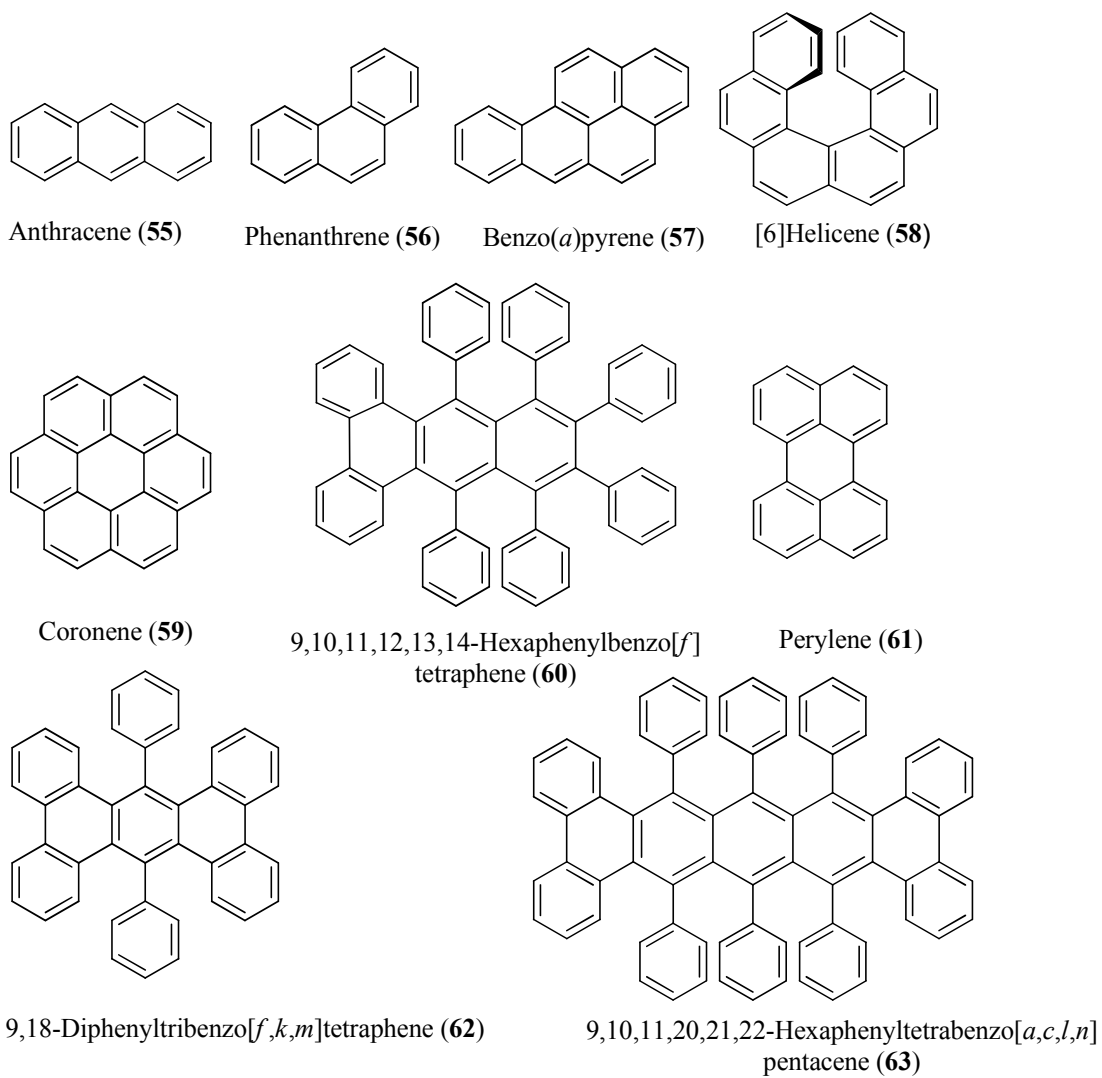


Figure 33. Examples of alternant PAHs.

On the other hand, nonalternant PAHs most likely contain rings other than six carbon atoms as well as up to six-membered rings (e.g., periflanthene (**64**), corannulene (**65**), fluoranthene (**66**), benzo[*mno*]fluoranthene (**67**), 7*H*-benzanthrene (**68**), [7]circulene (**69**), 6*H*-benzo[*cd*]pyrene (**70**), and 7,12-diphenylbenzo[*k*]fluoranthene (**71**)) (Figure 34).

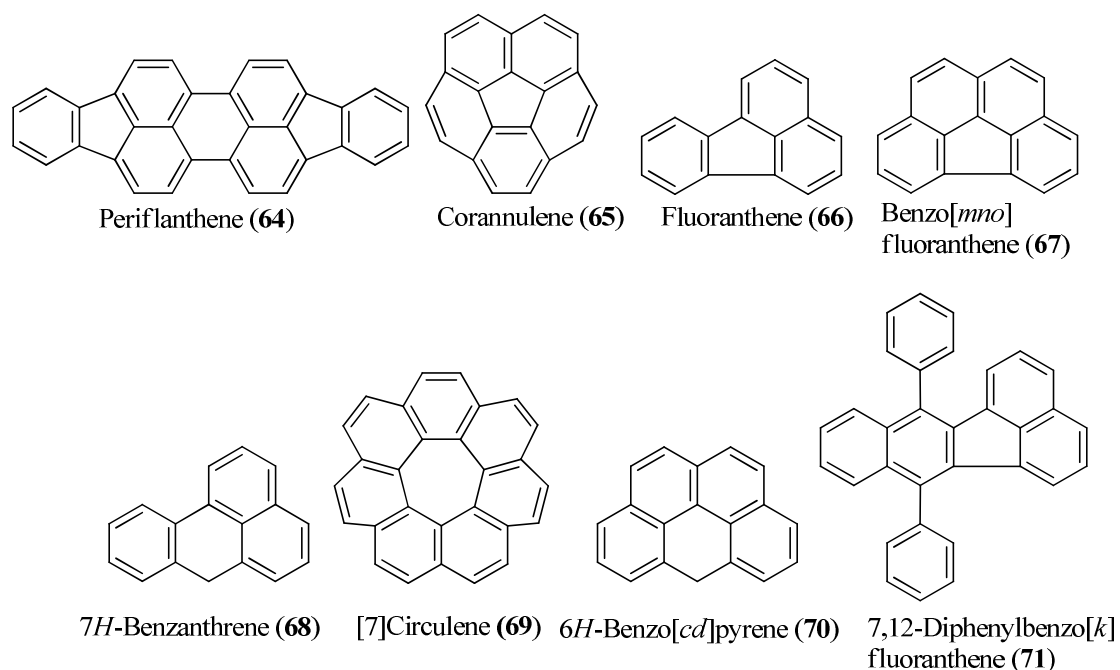


Figure 34. Examples of nonalternant PAHs.

Another classification, based on the size of the fused aromatic rings, distinguishes small PAHs from large PAHs. Those containing less than 24 carbons in the aromatic cores are

considered small PAHs. Examples include compounds **55-57**, while compounds containing 24 or more carbons are counted as large PAHs (e.g., **58-63**).⁶⁸

From planar to highly twisted PAHs

Small PAHs are generally planar as compounds **55-56**. However, as the molecule becomes more convoluted, and sterically congested, then deformations in the geometry of the molecule are expected to happen. This is the case of helicenes, which exhibit corkscrew-like structures formed by *ortho*-merged aromatic rings.⁷⁰ As the name suggests, helicenes are helical structures, which is a direct consequence of nonbonded repulsions between the faces of their aromatic rings. The interplanar angle between the terminal rings in helicenes increases from $n = 4$ (26.7°) to $n = 6$ (58.5°).⁷⁰ However, this angle decreases with larger values of n . Helicenes twist in opposite directions defining a C_2 -symmetric axis that coincides with the spiral axis. As a result, these molecules exhibit chirality without having a stereogenic center (axial chirality).⁷¹ Cahn, Ingold and Prelog proposed to label a left-handed helix as “minus” (represented by M) while a right-handed helix is labeled “plus” and is represented by P (Figure 35).⁷² [n]Helicenes have a tendency to racemize, especially among the lower members in the homologous series. The free energy barriers for racemization increase with n and with introduction of bulky substituents at the inner terminal rings. Consequently, the free energy barriers (kcal mol^{-1} at 300 K) for [n]helicenes increase in this order: 24.1 ($n = 5$), 36.2 ($n = 6$), 41.7 ($n = 7$), 42.4 ($n = 8$), and 43.5 ($n = 9$).^{71,73}

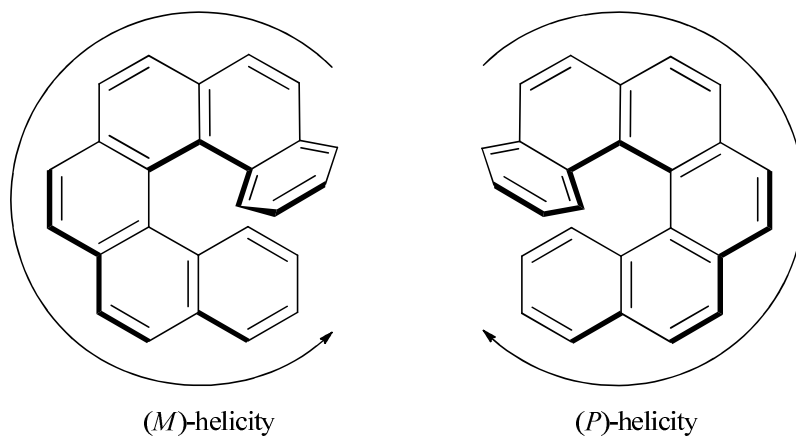


Figure 35. Schematic representation of helicity for [6]helicene (**58**).

Another deviation from planarity was evidenced by the X-ray crystallographic characterization of polycyclic aromatic hydrocarbon derivatives of anthracene and pentacene. These structures are highly twisted without losing their conjugation. For instance, the anthracene nucleus of molecule **62** is twisted longitudinally by 65.7° .⁷⁴ Variable-temperature NMR experiments of derivatives of compound **62** show that the barrier to twist is approximately 16.7 kcal/mol, which is too low to allow the separation of enantiomers. The next example compound **63** that claims to be “the most highly twisted PAH ever synthesized” shows an end-to-end twist of 144° . This value is attributed to the steric repulsion of substituents, the phenyl groups, on the conjugated fused rings. The barrier to racemization that was determined by the half-life for the decay of optical rotation, and for the loss of enantiomeric excess was 23.8 kcal/mol.⁷⁵

Extraordinary structures with high curvature are exemplified by corannulene (**65**)⁷⁶ and [7]circulene (**69**).^{77,78} Even though these two molecules belong to the same family as coronene (**59**), which has a planar structure, compound **65** exhibits a bowl-shaped nonplanar geometry with two nonequivalent faces: concave and convex, while compound **69** adopts a saddle-shaped nonplanar structure. These curvatures observed in compounds **65** and **69** are the result of the incompatibility of adjoining hexagons with pentagons or heptagons, respectively.

The absence of planarity reaches its maximum expression with two classes of compounds: fullerenes and carbon nanotubes. These structures are not strictly speaking PAHs; rather, they form part of a distinct group of carbon allotropes along with diamond and graphite (Figure 36).

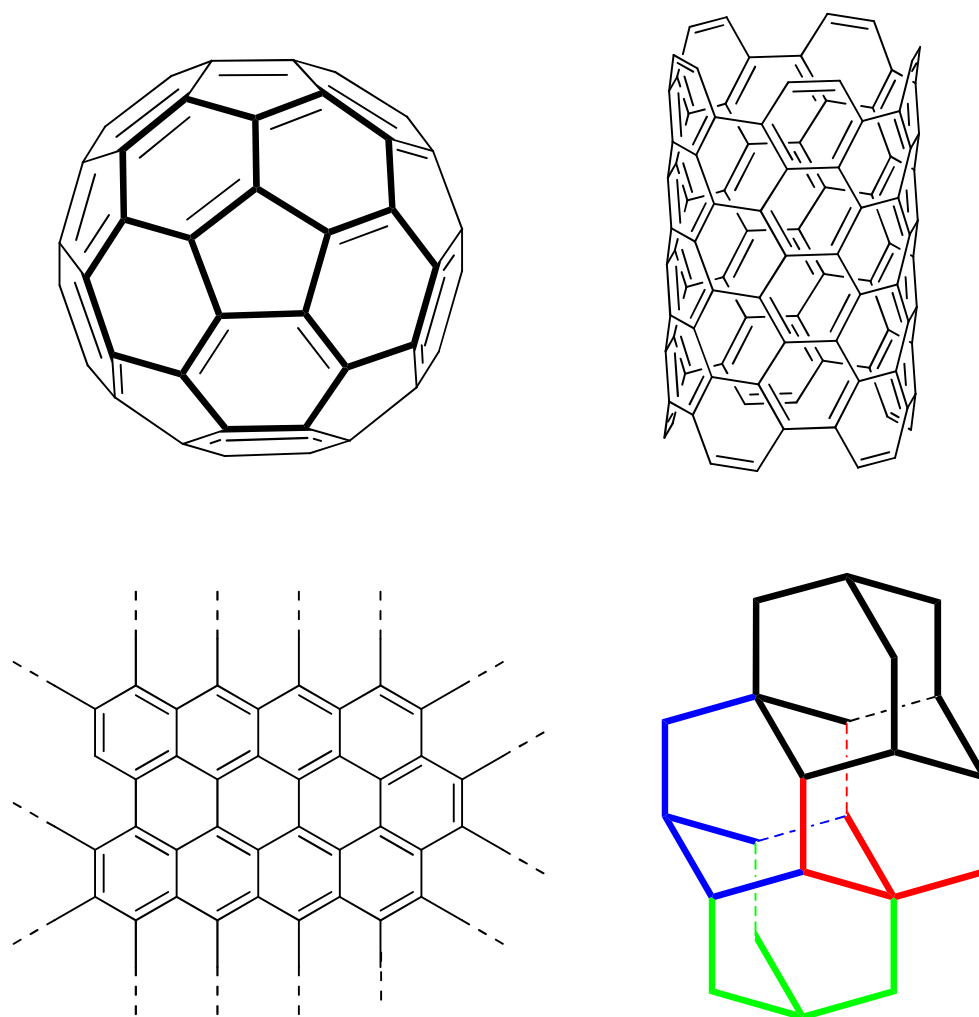


Figure 36. Pictorial representation of carbon allotropes from top-left to bottom-right: fullerene (C_{60}) (**72**), nanotube (armchair), graphite “layer” (graphene), and four caged structure of the diamond lattice.

Fullerenes are hollow spherical carbon clusters built-up predominantly of hexagonal and pentagonal rings, the latter being responsible for the curvature.⁷⁹ The best known fullerene is buckminsterfullerene (C_{60}) (**72**) which was first prepared at Rice University, Houston, Texas.⁸⁰ This cage is composed of 20 six-membered rings and 12 five-membered rings, where all

pentagons are isolated by hexagons.⁸¹ As a result, some recognizable bowed fragments as corannulene (**65**) appear depicted on the surfaces of these structures (Figure 36). This fact invigorated the interest for building bowl-shaped PAHs and other curved structures since these fragments may be used as intermediates for step-wise syntheses of carbon nanocages.

Fullerene chemistry has found application in the construction of materials such as superconductors.⁸² In addition, various fullerene derivatives with promising biological activity have been synthesized, such as compound **73** which is an inhibitor of HIV-protease, HIV-1, and HIV-2 reverse transcriptase (Figure 37).^{83,84}

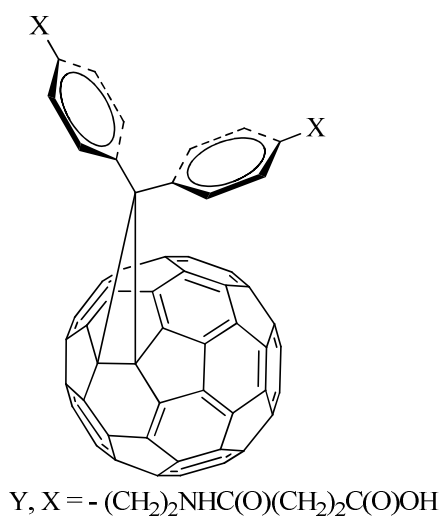


Figure 37. Chemical structure of fullerene derivative **73** (HIV enzyme inhibitor).

On the other hand, carbon nanotubes are hollow cylindrical carbon clusters constructed of hexagonal rings. In other words, these structures resemble graphite sheets (graphene) that have been rolled up into nanoscale tubes (Figure 36).⁸⁵ Carbon nanotubes can be chiral or achiral depending on the orientation of the graphene sheets along the tube, and achiral nanotubes are further divided in two subgroups: zigzag and armchair. Moreover, nanotubes sharing more than one common axis are called multiwalled nanotubes.⁸⁶

One of the most remarkable characteristic of carbon nanotubes is their outstanding strength. They exhibit tensile strengths, which is the force needed to pull the material apart, between ~18,000 to ~63,000 MPa.⁸⁷ The magnitude of this value pales the values of other known materials as pine wood or structural steel, which have tensile strengths of 40 and 400 MPa, respectively.⁸⁶ In addition, carbon nanotubes can act as conductors (armchair nanotubes) or semiconductors (zig-zag and chiral nanotubes). The conduction of electricity makes them eligible for the building of nanowires, which are a fundamental part of molecule-scale electronic materials.^{88,89}

There is a lot of concern about these types of compounds due to the potential damage that they may cause to the environment and the detrimental consequences on people's health. PAHs are formed relatively easily from the incomplete combustion of fossil oil, wood, cigarette or chargrilled food, and many of those are believed to be cancer-causing agents.⁹⁰ For instance, benzo(*a*)pyrene (**57**), which has been detected in smoked food is frequently referred as the most harmful PAH.⁹¹

Despite their harmful effects some PAHs have been used as intermediates in pharmaceutical and agricultural applications, and in the manufacture of dyes and pigments.⁹²

In addition, due to the extended π conjugated system, PAHs molecules can be easily excited by light in the visible spectral range and they provide an excellent alternative to the design of electronic and optoelectronic devices.⁹³ For instance, 7,12-diphenylbenzo[*k*]fluoranthene (**74**) has been incorporated in the structure of three novel organic sensitizers.⁹⁴ The resulting moieties, **74a**, **74b**, and **74c**, contain a fluoranthene **74** unit acting as an electron donor, phenyl and thiophene cores as electron spacers, and a carboxylic acid as an electron acceptor (Figure 38). These three molecules were anchored to nanocrystalline TiO₂-based solar cells to create dye-sensitized solar cells (DSSCs). Electrochemical measurements evidenced a maximum solar energy to electricity conversion efficiency of 4.4% under an AM 1.5 solar simulator (100 mW cm⁻²) for **74a**.

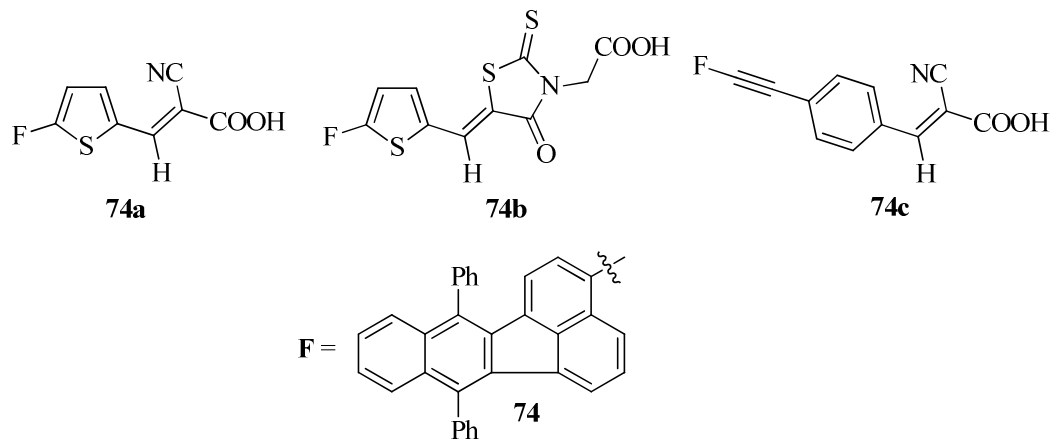


Figure 38. Molecular representations of dyes **74a-74c**

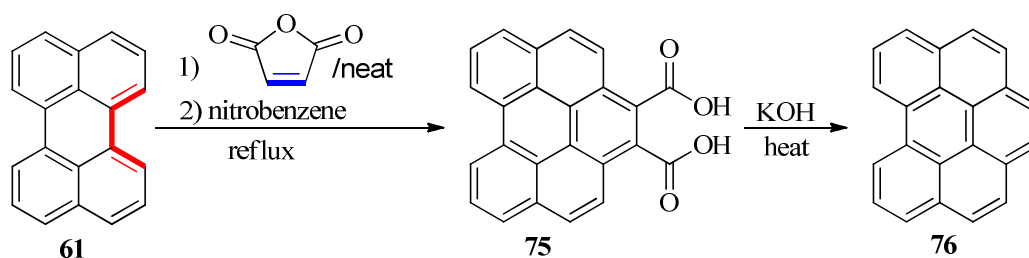
Concisely summarizing, the chemistry of PAHs includes small planar compounds as anthracene (**55**), highly twisted structures as 9,10,11,20,21,22-hexaphenyltetrabenzo[*a,c,l,n*]pentacene (**63**), and spherical compounds as buckminsterfullerene **72**. Some PAHs have been culprits of environmental damage and toxic effects on people's health. However, the aromatic core in these compounds also translates into unique properties that have found beneficial applications as those cited above.

Methods used for the building of PAHs

The most useful methods for the construction of PAHs have involved the Diels-Alder, ring closing metathesis (RCM), flash vacuum pyrolysis (FVP), oxidative cyclohydrogenation, and diaryl coupling reactions.

Diels-Alder reaction

This method that honors its discoverers Otto Diels and Kurt Alder, offers an easy and convenient choice for creating six-membered rings.⁹⁵ The Diels-Alder reaction is a concerted [4+2] cycloaddition where a reactant acts as diene (e.g., compound **61**), and the other reactant, which usually contains an electron-withdrawing group conjugated to the double bond, acts as a dienophile (e.g., maleic anhydride). One drawback of this method is that the dienes have to exist in the *s-cis* conformation.⁹⁶ For instance, cycloaddition between perylene (diene) (**61**) and maleic anhydride (dienophile) using a high boiling point solvent such as nitrobenzene (dehydrogenating agent) afforded intermediate **75**. The latter was decarboxylated by sublimation with potassium hydroxide to generate benzo[*ghi*]perylene (**76**) (Scheme 7).⁹⁷



Scheme 7. Diels-Alder cycloaddition of maleic anhydride to perylene (**61**).

Ring-closing olefin metathesis (RCM)

RCM is a type of olefin metathesis, whose proposed mechanism involves sequences of [2+2] cycloaddition and cycloreversion steps.⁹⁸ This carbon-carbon bond-forming reaction represents a great tool for the construction of medium- or large-sized rings from noncyclic diene precursors.⁹⁹ The right selection of the catalyst system (more appropriately described as initiators due to their transformation in the course of the reaction) constitutes a critical issue for this reaction. The Grubbs second-generation catalyst (**2-Ru**) is one of the most used metal-based catalytic agent (e.g., compounds **77-78**, Figure 39).^{100,101} Unlike first generation catalyst, these catalysts display larger functional group tolerance, thermal stability, and decent levels of activity.¹⁰²

RCM is prone to olefin isomerization/migration that ultimately diminishes the yield of the expected product, and makes its separation almost impossible.¹⁰³ Normally, in a typical procedure, the olefin is mixed with a transition-metal catalyst in a dry solvent (e.g., methylene chloride or toluene). For example, in an investigation by King,¹⁰⁴ compounds **79** and **80**

underwent double RCM in dichloromethane to afford PAHs **81** and **82** in 98 and 83% yield, respectively) (Scheme 8).

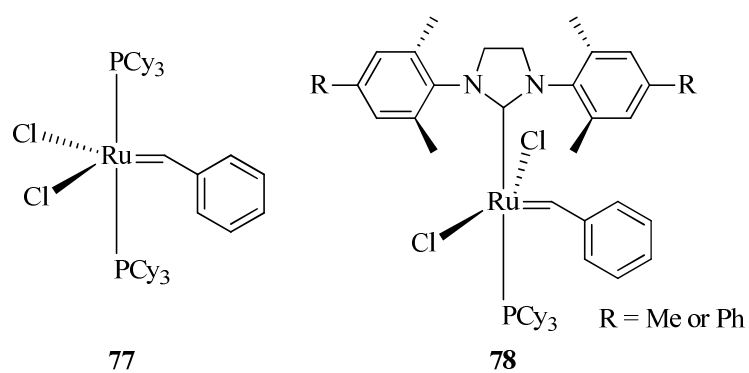
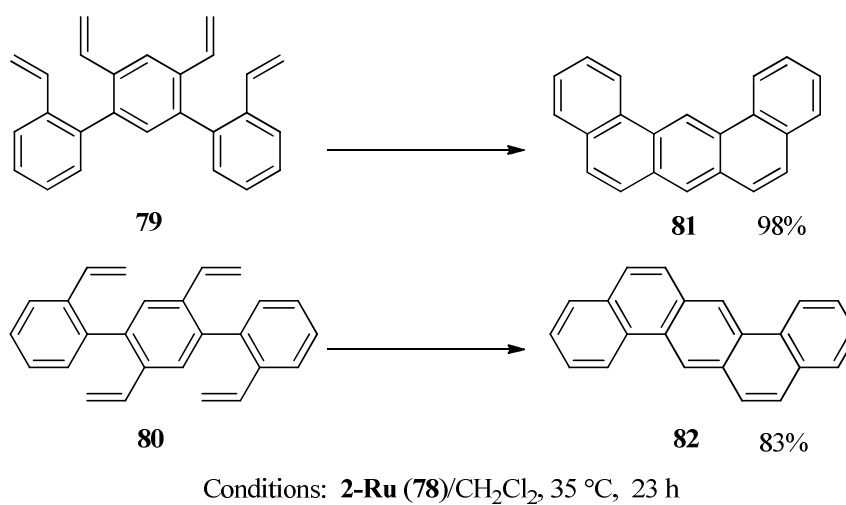


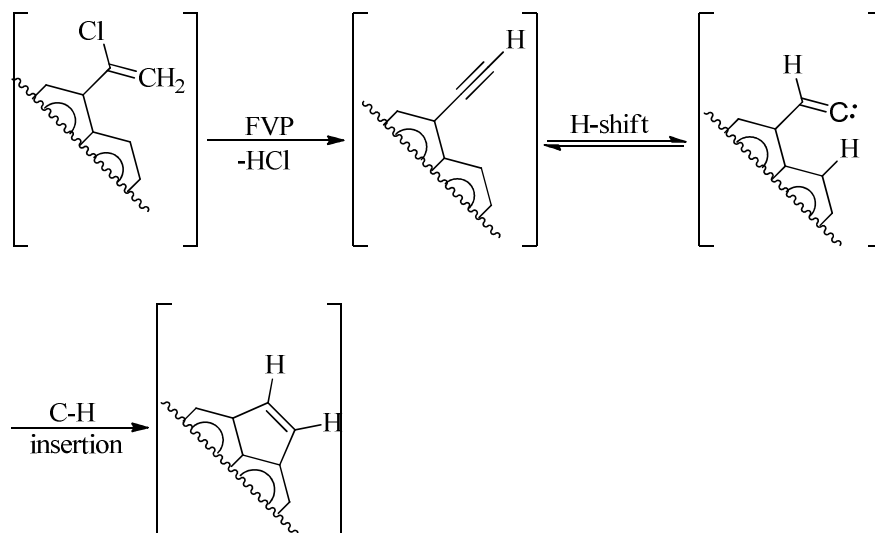
Figure 39. Second-generation Grubbs catalyst.



Scheme 8. Examples of PAHs obtained through RCM.

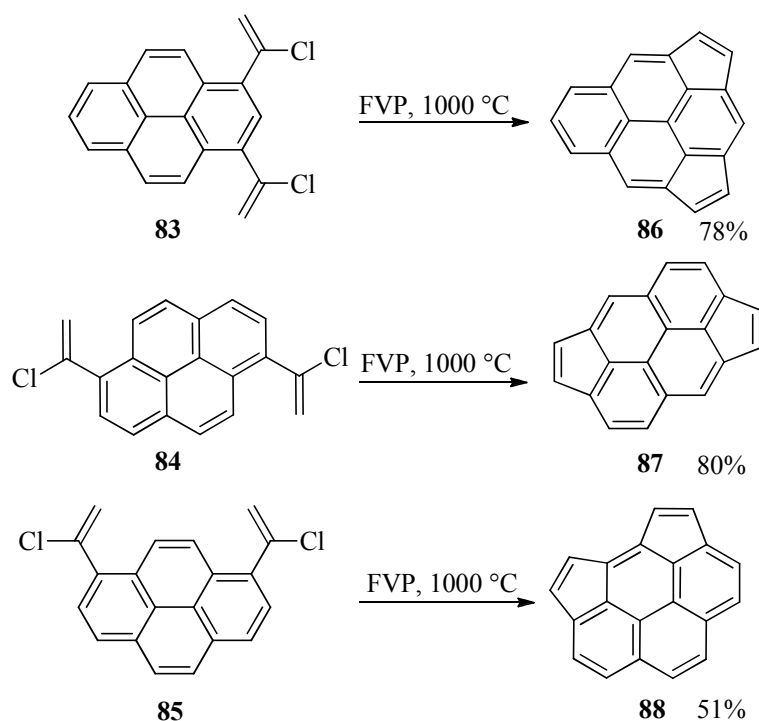
Flash Vacuum Pyrolysis (FVP)

This technique is very convenient for construction of PAHs that exhibit a curved bowl-like structure. It roughly consists of passing a compound through a hot quartz tube (800-1300 °C) under vacuum conditions (10^{-4} -1 Torr) for a very short time.⁷⁹ The success of this technique relies on the nature of the precursors, which requires having thermal stability and appropriately positioned reactive sites.⁶⁹ Compounds displaying terminal alkynes or “masked acetylenes” that can lose HCl and generate the alkyne structure *in situ* are optimal candidates for this process. The terminal alkynes under FVP are apparently in equilibrium with vinyl carbene intermediates (1,2-shifts of hydrogen), which eventually insert into adjacent *peri*-positions to form the cyclopentene annulated products (Scheme 9).^{79,105}



Scheme 9. The proposed pathway in FVP.

The major limitation of this strategy is that starting materials have to be very resistant to the high heating needed to bring them into the gas phase.¹⁰⁶ This fact is reflected in yields that rarely surpass 35%. Another drawback of FVP is the tendency to form polymeric side products that also diminish the efficiency of this technique. An example that illustrates how this method has been used in the synthesis of PAHs was reported by Scott.¹⁰⁵ His investigation tests the abilities of bis-vinyl halides **83-85** (“masked acetylenes”) in the cyclization reaction under FVP conditions. The starting materials **83-85** effectively underwent double ring closing to afford nonalternant PAHs **86-88** in 78, 80, and 51% yields, respectively (Scheme 10).



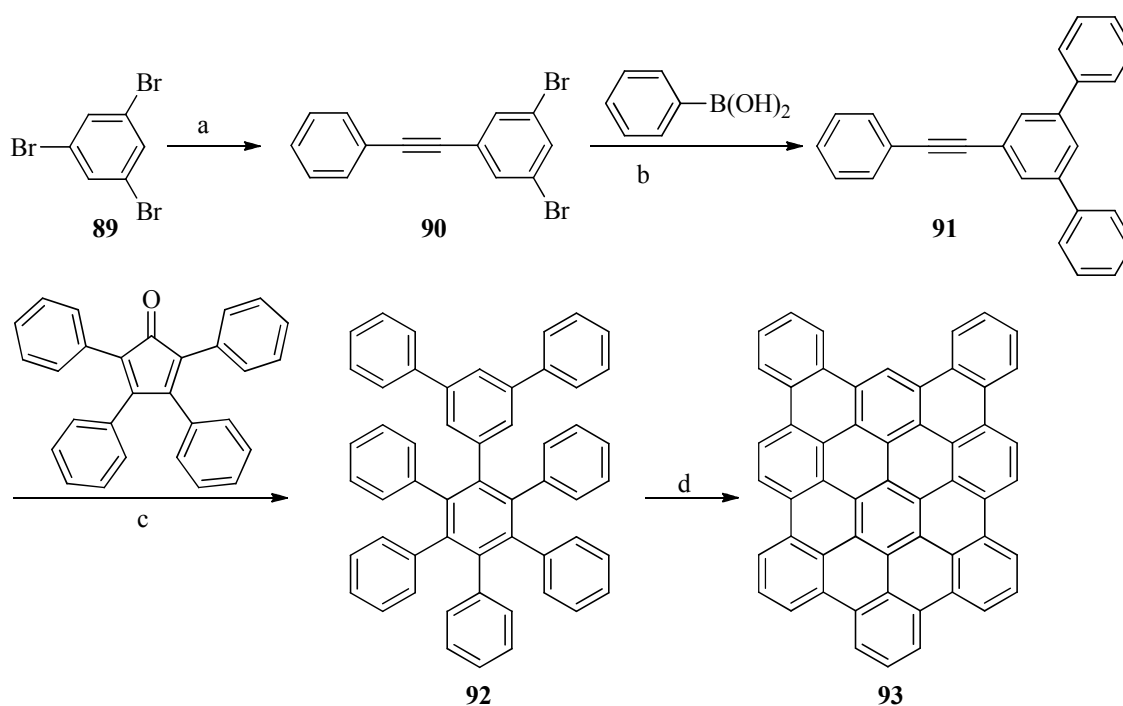
Scheme 10. Three dicyclopentapyrenes obtained using FVP.

Oxidative cyclodehydrogenation

This type of reaction is usually the last step in a synthetic pathway, and consists of the coupling of two aromatic rings using Lewis acid catalysts (Scholl reaction), platinum or palladium metals. The classical Scholl reaction has inherent limitations of low yields, and the formation of multiple products. As a result, other catalytic systems that require mild conditions have been implemented such as $\text{Cu}(\text{OSO}_2\text{CF}_3)_2/\text{AlCl}_3$ in CS_2 .

An example of this route is illustrated in the last step of the synthesis of “Arrowlike” PAH.¹⁰⁷ 1,3,5-Tribromobenzene (**89**) and phenylacetylene under Pd(0)-catalyzed reaction afforded compound **90** in 77% yield. Subsequently, a Suzuki coupling of compound **90** with

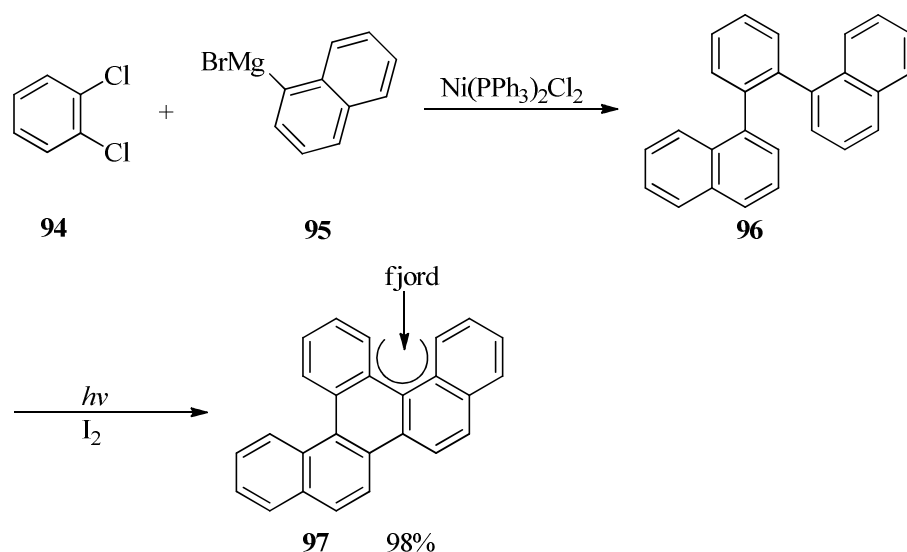
phenylboronic acid formed intermediate **91** in 99% yield. Compound **92** was obtained in 77% yield from a Diels-Alder reaction between **91** and tetraphenylcyclopentadienone. Finally, cyclodehydrogenation reaction of **92** with copper(II)trifluoromethanesulfonate/aluminum(III) chloride yielded PAH **93** in 75% yield (Scheme 11).



Scheme 11. Synthesis of an "Arrowlike" PAH. Conditions: (a) phenylacetylene, Pd(PPh₃)₄, CuI, piperidine, 25 °C, 24 h, 77%; (b) Pd(PPh₃)₄, toluene, K₂CO₃, EtOH, H₂O, reflux, 24 h, 99%; (c) tetraphenylcyclopentadienone, diphenyl ether, reflux, 16 h, 77%; (d) Cu(OSO₂CF₃)₂, AlCl₃, CS₂, 25 °C, 24 h, 75%.

Diaryl coupling

This method involves the coupling between an organometallic compound (OMC), e.g., aromatic Grignard molecule, and an aromatic halide, in the presence of a catalyst. The major limitation of this procedure is in the preparation of the OMC. Some OMCs are extremely sensitive to air and humidity, and they need to be treated with special care. Consequently, it is not surprising to find the nonhalogenated version of the starting material as a side product. For example,¹⁰⁸ *o*-dichlorobenzene (**94**) and 1-bromonaphthalene (**95**) in the presence of nickel (II) chloride triphenylphosphine were coupled to afford intermediate **96** in 79% yield. Subsequently, an oxidative photocyclization of **96** yielded benzo[*s*]picene (**97**) in 98% yield. Compound **97**, which contains two fjord regions, is likely to exhibit a nonplanar structure because of the steric hindrance between the hydrogen atoms in the aforementioned region (Scheme 12).



Scheme 12. Synthesis of benzo[*s*]picene.

Perylene structures

Structures containing perylene (**61**) (Figure 33), which is an alternant PAH made up of two fused naphthalene molecules bridged at the one and eight positions,⁶⁸ are well known for their extensive use as industrial colorants.¹⁰⁹⁻¹¹² One of the first group of compounds used as colorants included perylene-3,4,9,10-tetracarboxdiimides (PDIs). These pigments have outstanding chemical, thermal-resistance, and weather stability.¹¹³ In addition, PDIs exhibit high absorptivity and fluorescence quantum yield, high photochemical stability, and strong electron affinity.^{114,115} It has been reported that the extension of the aromatic rings along the molecular axis from perylene-tetracarboxdiimides (PDI, $n = 1$) **98** to quaterrylene-tetracarboxdiimides (QDI, $n = 3$) **100** provokes a bathochromic shift of approximately 100 nm per added n unit with an absorbance maximum of 780 nm for quaterrylene **100** (Figure

40).¹¹⁶ Furthermore, a linear increase in the extinction coefficient up to $170000 \text{ M}^{-1} \text{ cm}^{-1}$ for this series has been observed.¹¹¹ As result of their particular physical, optical and electronic properties, PDIs also have found applications in organic field-effect transistors (OFETs),^{117,118} organic photovoltaic cells (OPVCs),¹¹⁹ light harvesting arrays,^{120,121} and dye lasers.¹²²

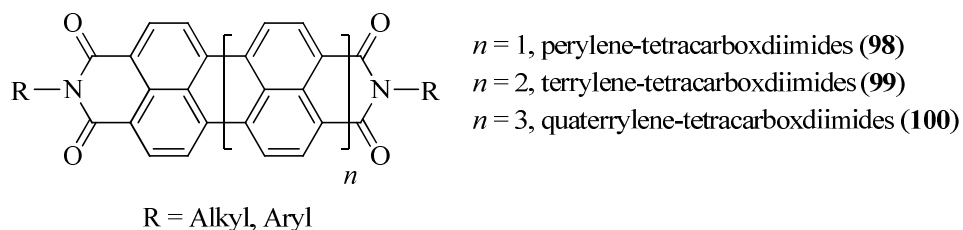
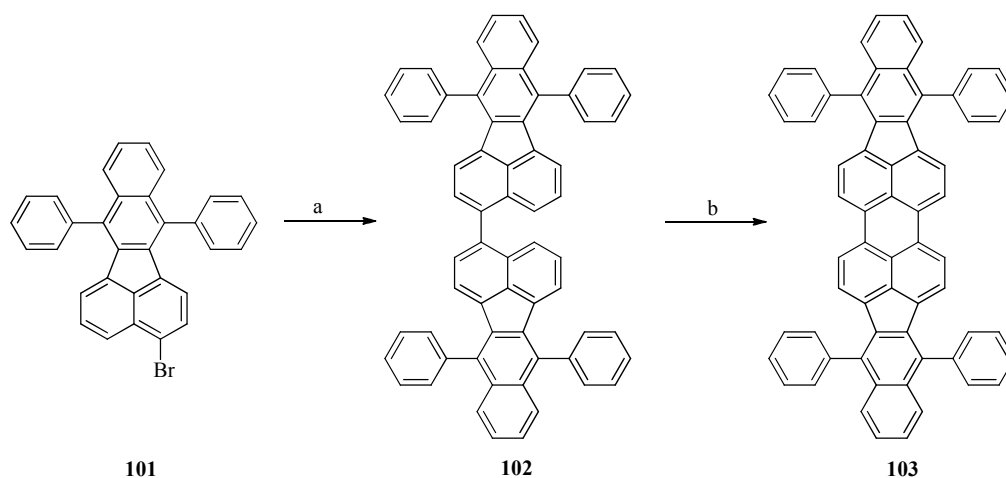


Figure 40. Chemical structures of peryleneimide chromophores.

Our motivation in this area has been nourished by a myriad of excellent papers conducted by renowned researchers, such as Bard and Müllen.^{123,124} Even though their work diverges in style, their purpose converges on the way to construct the perylene center in a straightforward manner, with manageable amounts to carry out the pertinent analysis.

Bard was particularly interested in mechanistic and kinetic studies of coupling reactions of large PAHs using electrochemical methods. However, he carried out a chemical synthesis in order to compare the products. In the proposed chemical synthesis, Bard employed brominated fluoranthene units (monomers). Subsequently, a coupling between two of those monomers formed the intermediate units (dimers), and finally an intramolecular ring closure of the dimers

generated the perylene core. For instance, 3-bromo-7-12-diphenylbenzo[*k*]fluoranthene (**101**) was used as starting material to obtain 7,7',12,12'-tetraphenyl-3,3'-bibenzo[*k*]fluoranthene (**102**) and ultimately 5,10,15,20-tetraphenylbenzo[5,6]indeno[1,2,3-*cd*]benzo[5,6]indeno[1,2,3-*lm*]perylene (**103**) (Scheme 13).¹²⁵ Compound **103** showed an absorption band with a maximum at 582 nm.

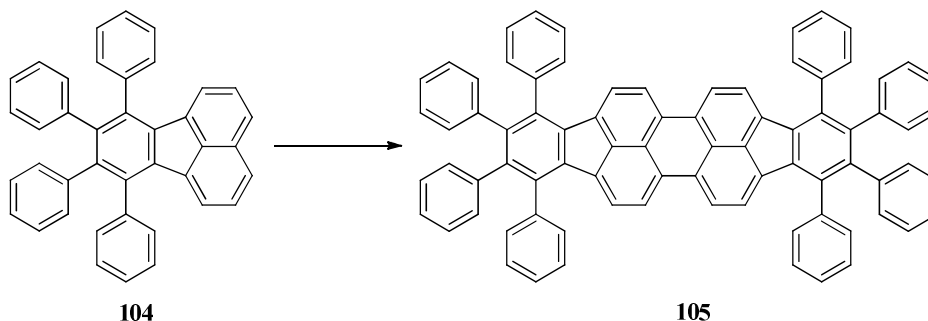


Scheme 13. Synthesis of 5,10,15,20-tetraphenylbenzo[5,6]indeno[1,2,3-*cd*]benzo[5,6]indeno[1,2,3-*lm*]perylene (**103**). Conditions: (a) NiCl₂, Zn, DMF, NaBr/PPh₃, 80 °C, 40%; (b) CoF₃/trifluoroacetic acid, 70%.

On the other hand, Müllen has stated that the motivation behind the syntheses of PAHs is due in part to their potential applications in optoelectronics and dyes/pigments chemistry.¹²⁴ In his synthetic approach, soluble PAH intermediates undergo an *intramolecular* dehydrogenative coupling reaction to afford symmetrical enlarged PAHs. For instance, 7,8,9,10-tetraphenylfluoranthene (**104**) was used as starting material to obtain

1,2,3,4,9,10,11,12-octaphenyldiindeno[1,2,3-*cd*:1',2',3'-*lm*]perylene (**105**) (Scheme 14).¹²⁴

Compound **105** showed an absorption band with a maximum at 564 nm ($\log \varepsilon = 4.94 \text{ L mol}^{-1} \text{ cm}^{-1}$).



Scheme 14. Synthesis of 1,2,3,4,9,10,11,12-octaphenyldiindeno[1,2,3-*cd*:1',2',3'-*lm*]perylene (**105**). Conditions: FeCl_3 , $\text{CH}_3\text{NO}_2/\text{CH}_2\text{Cl}_2$, rt, 90%.

Objectives and synthetic approaches

One subset of our research group, which focuses on the elaboration of PAHs, undertakes on the synthesis of these symmetric, linear, medium-sized perylene networks. The goal of this investigation encompasses a rigorous study of the resulting moieties, including physical and chemical properties, followed by a comparison between our collected data and the data previously reported for perylene chromophores.

We proposed to synthesize compounds **106-109** (Figure 41). They share similarities with those studied by the researchers mentioned previously. However, we wanted to introduce a differentiation by means of extending the fluoranthene units. To achieve this task phenyl and *tert*-butyl groups were added with an expectation of making our final frameworks more soluble

in typical solvents. Therefore, we anticipated achieving better separation, purification, and characterization by mass spectrometry, UV/Vis, ^1H NMR, and ^{13}C NMR spectroscopy.

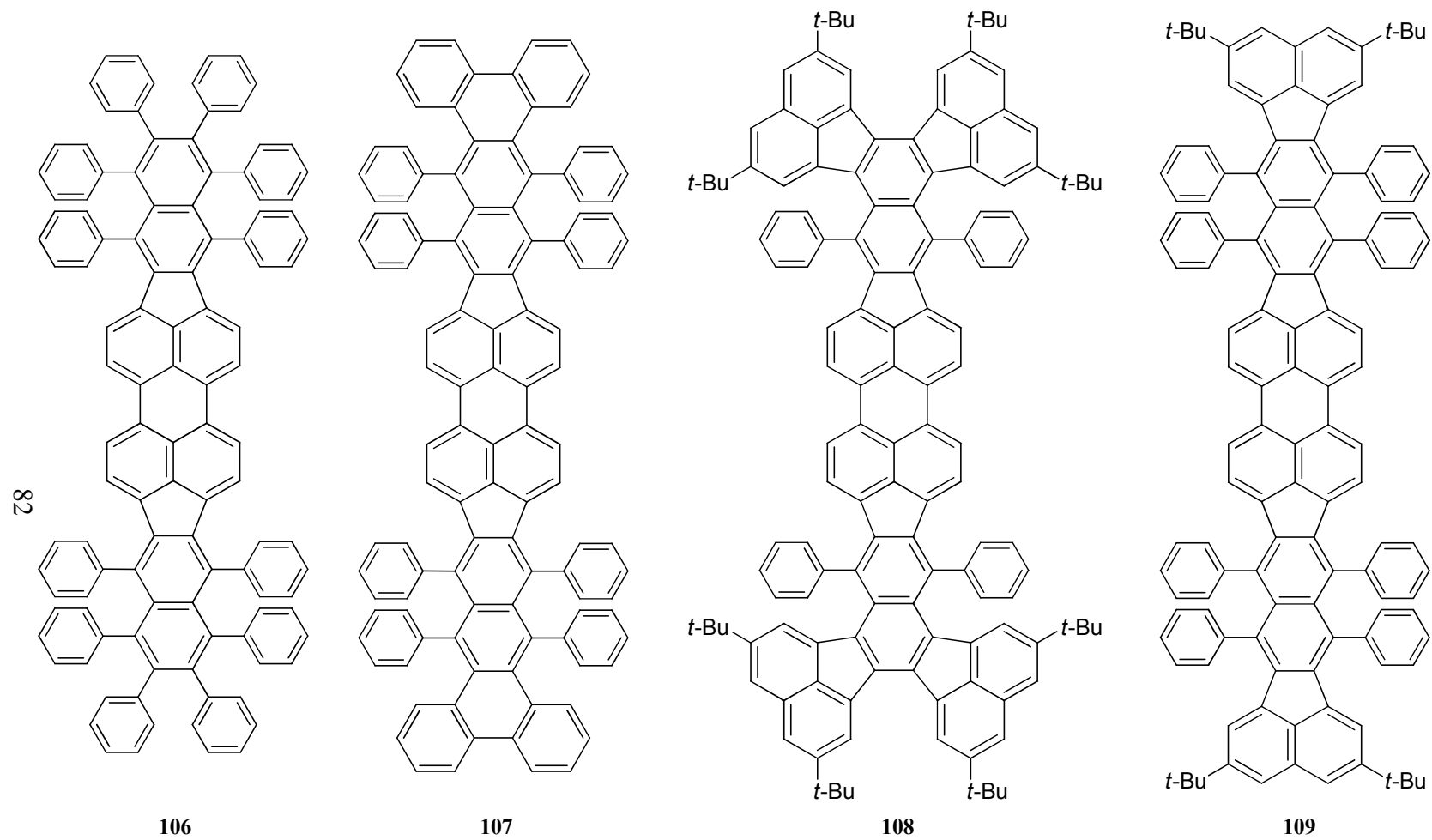
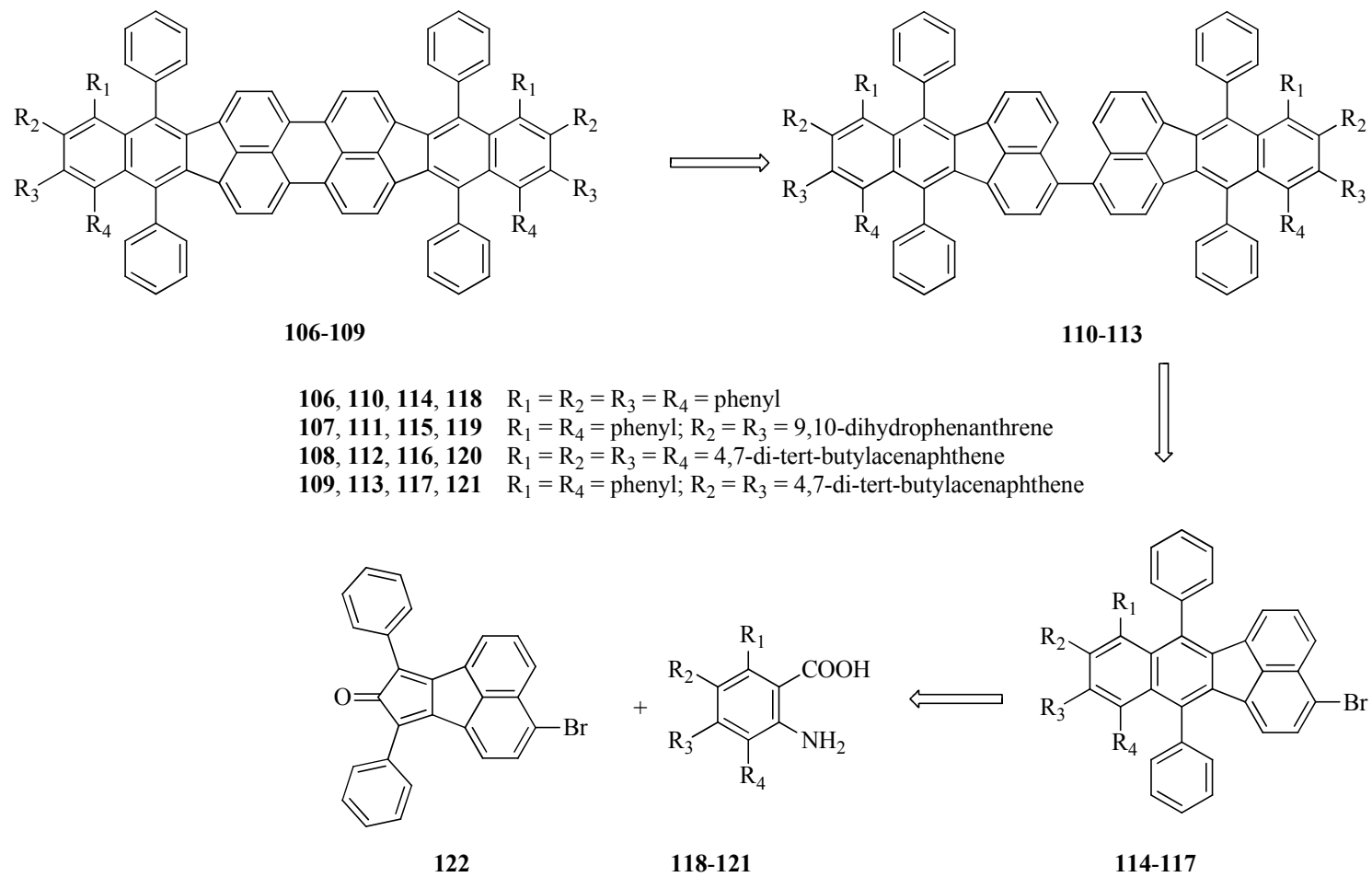


Figure 41. Target molecules 106-109.

Retrosynthetic Analysis.

The symmetric shape of these structures suggests that a well-defined retrosynthetic route should start with double splits in the core of these molecules (Scheme 15). The first split generates the dimers and the second two identical monomers. These monomers, the fluoranthene units, must contain a halogen substituent such as bromine (the anchor position) as a precondition that aids in the progress of the molecule for its imminent dimerization. A reasonable disconnection of the fluoranthene units reveals the crucial participation of anthranilic acid derivatives and substituted cyclopentadienones in the synthesis of this type of molecule as was demonstrated by Pascal's study.^{126,127}



Scheme 15. Retrosynthetic analysis of perylene molecules.

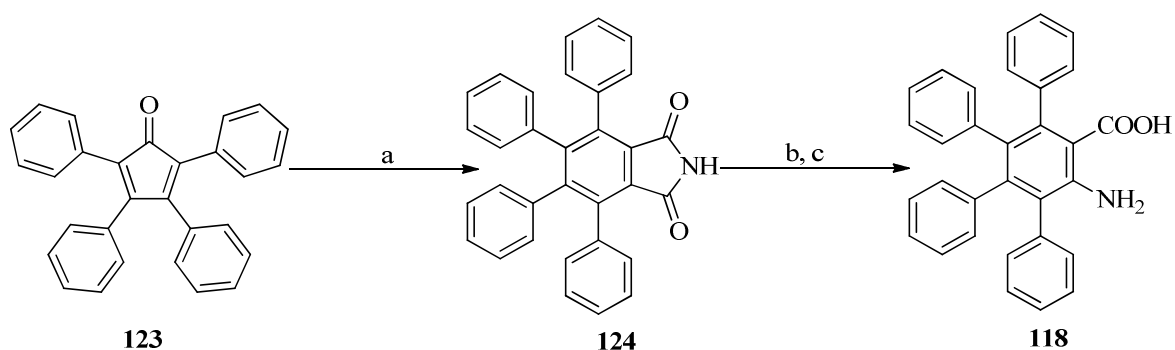
Results and discussions

To facilitate a better understanding of the process, we decided to divide the synthesis in three stages: 1) synthesis of the monomers, 2) synthesis of the dimers, and 3) ring closure for formation of targets.

1) Synthesis of the monomers.

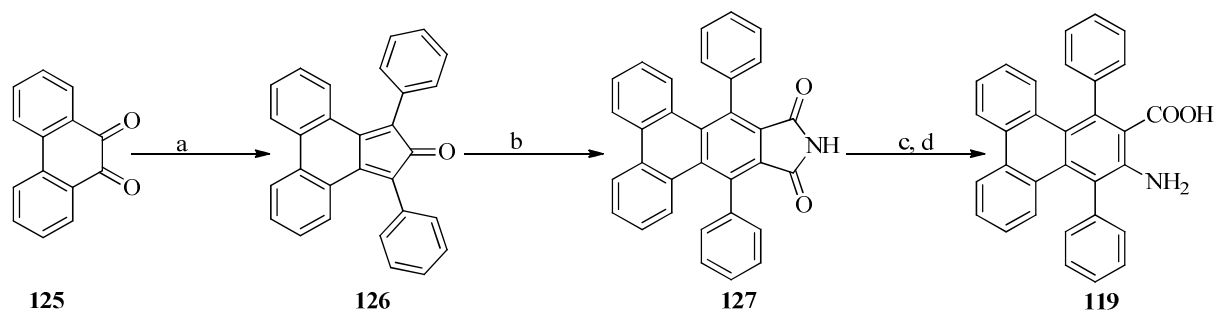
The synthesis of the monomers required a unique design of four amino acids and phenylcyclopentadienone.¹²⁶ A close look of the retrosynthetic analysis shows that the structure of the amino acids provides the distinction of the target molecules. The amino acids were all obtained using a similar pathway with several differentiations intrinsically attributed to their specific shapes.

Amino acid **118** was synthesized under Diels-Alder conditions using commercially available tetraphenylcyclopentadienone (**123**) and maleimide to afford compound (**124**), and then a Hoffman rearrangement was followed by a basic hydrolysis reaction (Scheme 16).



Scheme 16. Construction of amino acid **118**. Conditions: (a) maleimide/nitrobenzene, reflux, 61%; (b) NaOCl, NaOH/MeOH, reflux, (not isolated); (c) KOH, propanol, reflux, 84% (b, c combined).

The synthesis of amino acid **119** first included an aldol condensation reaction between commercially available phenanthrene-9,10-dione (**125**), and 1,3-diphenylacetone to afford compound **126**. Subsequently, compound **126** and maleimide underwent a Diels-Alder reaction to yield compound **127**, and then a Hoffman rearrangement followed by a basic hydrolysis reaction gave amino acid **119** (Scheme 17).

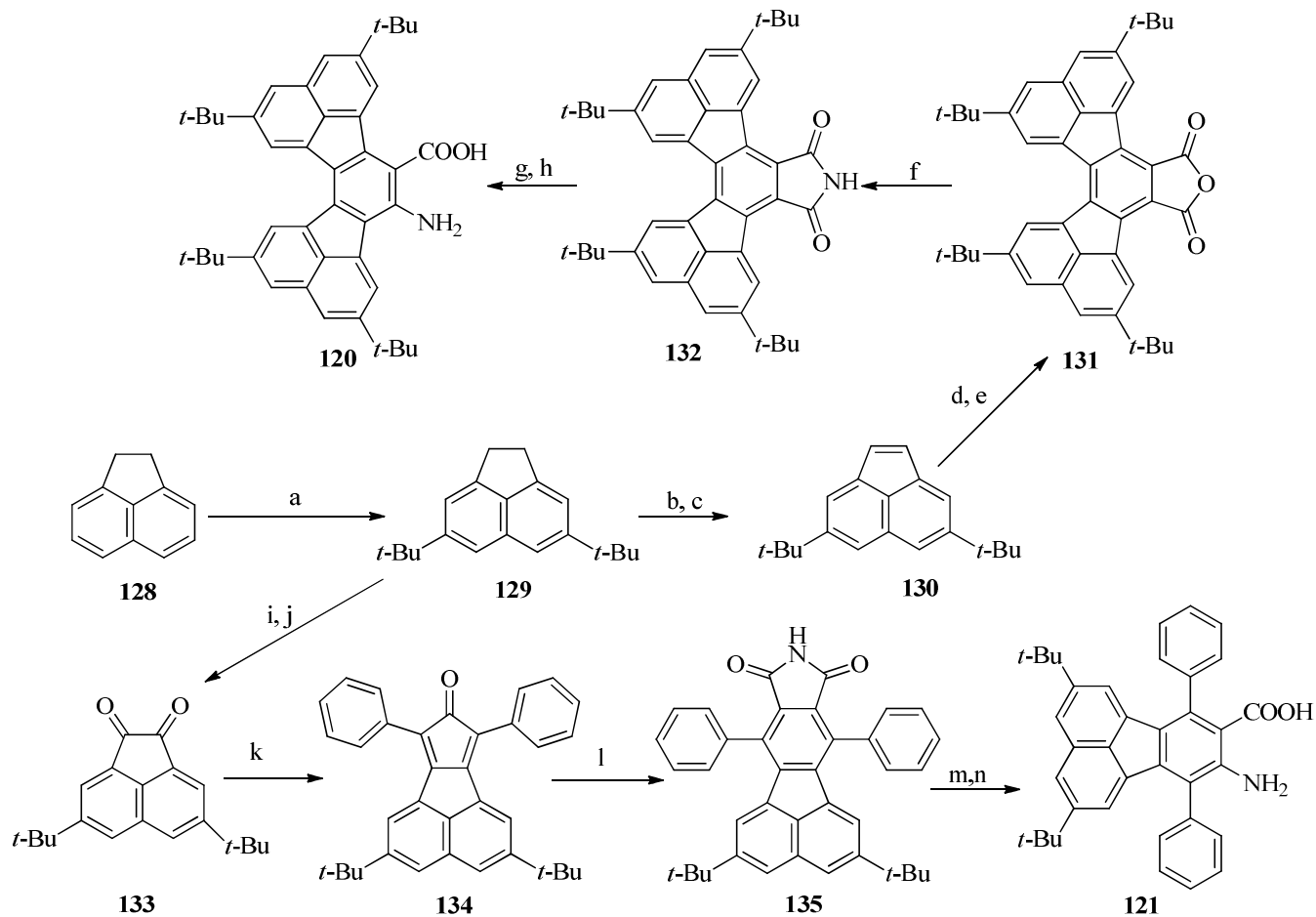


Scheme 17. Construction of amino acid **119**. Conditions: (a) 1,3-diphenylacetone/NaOH, EtOH, heat, 78%; (b) maleimide/nitrobenzene, reflux, 68%; (c) NaOCl, NaOH/MeOH, reflux, (not isolated); (d) KOH, propanol, reflux, 40% (c, d combined).

The synthesis of amino acids **120** and **121** was more convoluted, and, of course, required additional steps. Their syntheses started using commercially available and inexpensive acenaphthene (**128**) that was treated with *tert*-butylchloride in a Friedel-Crafts fashion reaction to form 4,7-di-*tert*-butylacenaphthene (**129**). Compound **129** was the mutual intermediate for both amino acid **120** and **121**. In the route to form **120**, 4,7-di-*tert*-butylacenaphthene (**129**) was

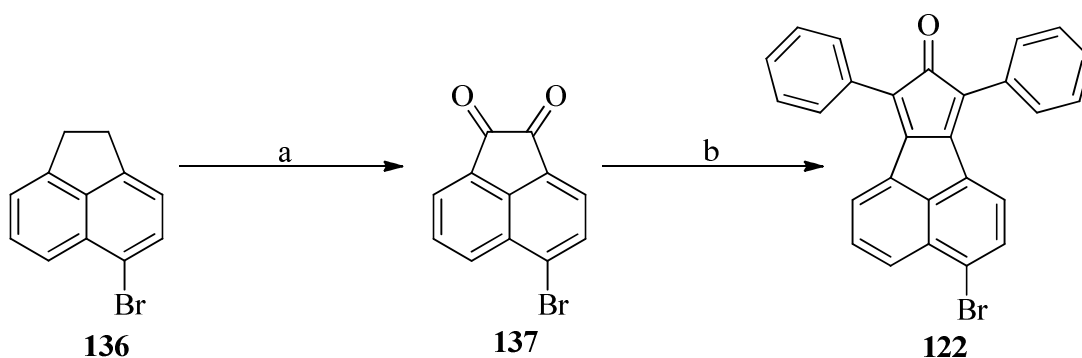
first brominated and then debrominated to form compound **130**.¹²⁸ Then, compound **130** was treated first with sulfur and next with maleic anhydride to produce **131**. The latter compound was then reacted with maleimide to give **132**. Finally, in the last two steps, a common denominator in the building of these amino acids, a Hoffman rearrangement was followed by a basic hydrolysis reaction, yielded amino acid **120**.

In the path to build **121**, 4,7-di-*tert*-butylacenaphthene (**129**) was oxidized to form dione **133**, and subsequently, treatment with 1,3-diphenylacetone in basic conditions gave **134**. A Diels-Alder reaction between **134** and maleimide yielded **135**. Finally, the last two steps as in the previous reaction scheme afforded amino acid **121** (Scheme 18).



Scheme 18. Construction of amino acids **120** and **121**. Conditions: (a) *tert*-butylchloride, $\text{AlCl}_3/\text{CS}_2$, 28%; (b) dibenzoyl peroxide, NBS/benzene (not isolated); (c) Zn, acetic acid/THF, 66% (b, c combined); (d) S_8/DMF (not isolated); (e) maleic anhydride, 55% (d, e combined); (f) urea/DMF, 81%; (g) NaOCl, NaOH/MeOH, reflux, (not isolated); (h) KOH, propanol, reflux, 90% (g, h combined); (i) dibenzoyl peroxide, NBS/ CCl_4 , (j) DMSO, 30% (i, j combined); (k) 1,3-diphenylacetone/NaOH, EtOH, heat, 92%; (l) maleimide/nitrobenzene, heat, 52%; (m) NaOCl, NaOH/MeOH, reflux, (not isolated); (n) KOH, propanol, reflux, 85% (m, n combined).

Alternatively, the synthesis of phenylcyclopentadienone **122** required two steps: oxidation of the commercially available 5-bromoacenaphthene (**136**) to give dione **137**, and an aldol condensation reaction between compound **137** and 1,3-diphenylacetone to afford **122** (Scheme 19).¹²⁹



Scheme 19. Synthesis of phenylcyclopentadienone **122**. Conditions: (a) $\text{CrO}_3/\text{Ac}_2\text{O}$, 59%; (b) 1,3-diphenylacetone/ NaOH , EtOH, heat, 73%.

The anthranilic acids (**118-121**) formerly depicted were deliberately synthesized as a convenient source of highly reactive arynes. Pascal has successfully used compound **119** in the course of the synthesis of twisted PAHs as compound **60** (Figure 42).^{126,127} The X-ray crystallographic analysis of compound **60** showed that the central anthracene is twisted by approximately 60.0° .

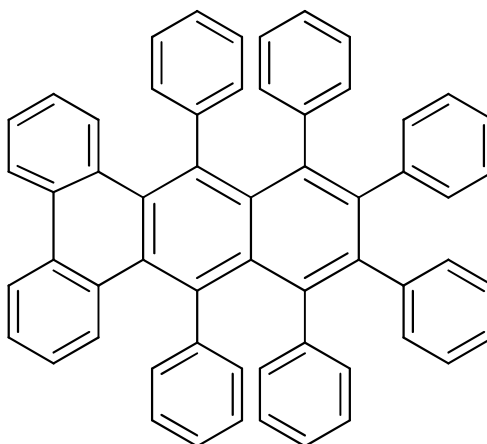
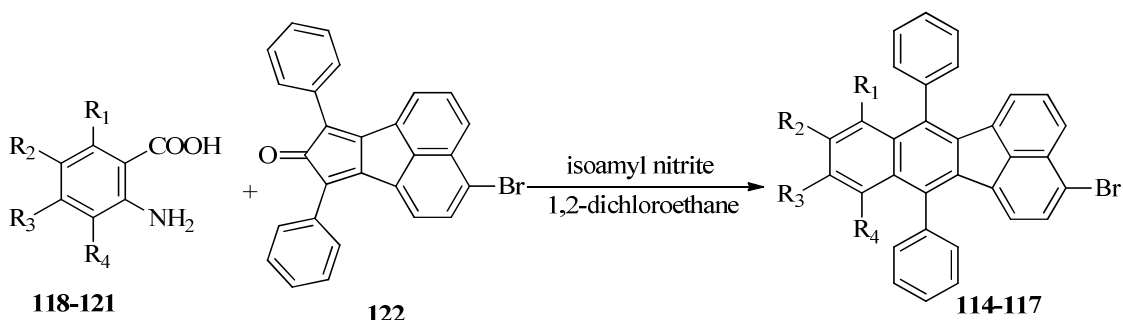


Figure 42. Structure of twisted compound **60**.

Our anthranilic acids **118-121** were treated with phenylcyclopentadienone **122** *via* benzyne addition conditions (Scheme 20). The products, fluorene units **114-117**, were obtained in 84%, 77%, 83% and 76% yields, respectively. Compounds **114**, **115**, and **117** were yellow powders, and **116** was an orange solid. All of them exhibited high melting points. In addition, they showed satisfactory solubility in chloroform, methylene chloride and toluene, and were scarcely soluble in hexanes. They amino acid were further characterized by mass spectrometry, and ^1H NMR, and ^{13}C NMR spectroscopy.

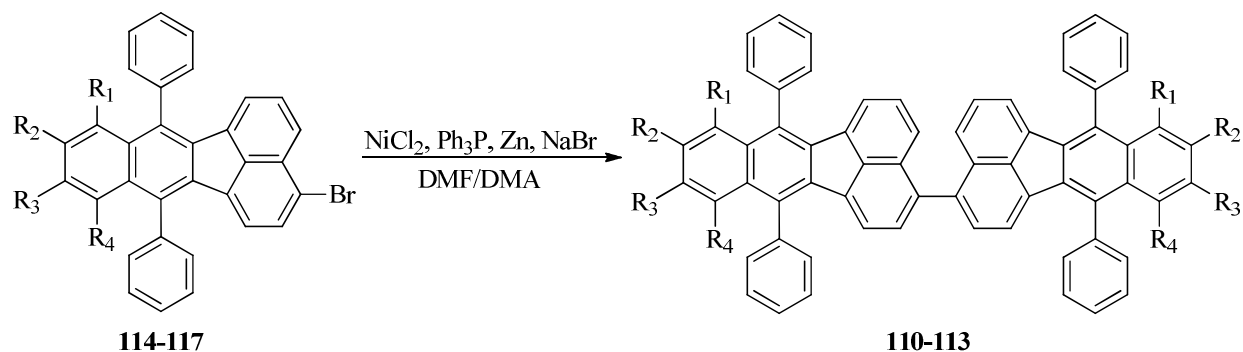


- 114, 118** $R_1 = R_2 = R_3 = R_4 = \text{phenyl}$
115, 119 $R_1 = R_4 = \text{phenyl}; R_2 = R_3 = 9,10\text{-dihydrophenanthrene}$
116, 120 $R_1 = R_2 = R_3 = R_4 = 4,7\text{-di-}i\text{-tert-butylacenaphthene}$
117, 121 $R_1 = R_4 = \text{phenyl}; R_2 = R_3 = 4,7\text{-di-}i\text{-tert-butylacenaphthene}$

Scheme 20. Synthetic pathway through the fluoranthenes.

2) Synthesis of the dimers.

This first attempt to synthesize the dimers involved the homocoupling of aryl halides mediated by a nickel agent. The monomers were mixed with anhydrous nickel chloride, triphenyl phosphine, zinc powder, and sodium bromide in a solution of dimethylformamide (DMF) and dimethylacetamide (DMA) (Scheme 21).



- 110, 114** $R_1 = R_2 = R_3 = R_4 = \text{phenyl}$
111, 115 $R_1 = R_4 = \text{phenyl}; R_2 = R_3 = 9,10\text{-dihydrophenanthrene}$
112, 116 $R_1 = R_2 = R_3 = R_4 = 4,7\text{-di-}i\text{-tert-butylacenaphthene}$
113, 117 $R_1 = R_4 = \text{phenyl}; R_2 = R_3 = 4,7\text{-di-}i\text{-tert-butylacenaphthene}$

Scheme 21. Synthesis of the dimers.

Under these conditions, only compound **110** was obtained in a quantifiable amount (56.6 mg, 21%). However, this result could not be duplicated as confirmed by mass spectrometry. The other three monomers were obtained in trace amounts only. Most of the recovered products in these syntheses consisted of starting material and presumably the nonbrominated versions of the starting material (verified by NMR spectroscopy). The conditions were changed slightly to a mixture of $\text{Ni}(\text{PPh}_3)_2\text{Br}_2$, $(n\text{Bu})_4\text{NI}$ in THF. The results were similar to that previously discussed.

After this failed attempt, we tried Müllen's strategy, which consists of an oxidative coupling of the nonbrominated monomers to afford the final compound in a single step. The reaction was run using a mixture of iron trichloride and nitromethane in dichloromethane

(DCM). The results comprised multiple unidentifiable products. The previously mentioned outcomes are summarized in Table 15.

Table 15. Results for the coupling of monomers **114-117** under different conditions.

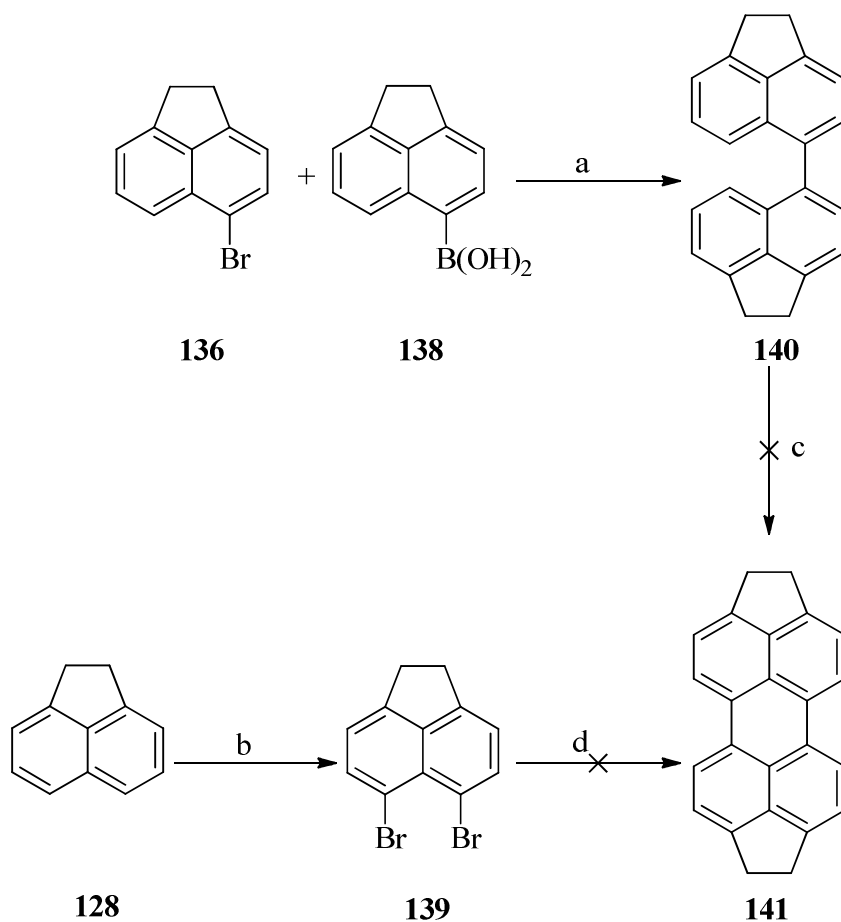
Conditions	Monomers			
	114	115	116	117
NiCl ₂ , Ph ₃ P, Zn, NaBr/DMF-DMA	positive	negative	negative	negative
Ni(PPh ₃) ₂ Br ₂ , (<i>n</i> Bu) ₄ Ni/THF	negative	negative	negative	negative
FeCl ₃ , CH ₃ NO ₂ /CH ₂ Cl ₂	negative	negative	negative	negative

The next proposed synthetic route diverges from the route depicted in Scheme 21. This approach illustrates a challenging attempt to integrate the perylene moiety at the beginning of the synthesis, followed by the incorporation of fluoranthene units on both sides of the perylene center. In order to accomplish this task, it was first necessary to synthesize 1,2,7,8-tetrahydrodicyclopenta[*cd,lm*]perylene (**141**) (Scheme 22).

Commercially available 5-bromoacenaphthene (**136**) and its boronic acid form **138** were reacted under Suzuki-Miyaura conditions to afford intermediate **140**.^{130,131} Then, compound **140** was treated with a catalytic mixture of CuSO₄ and Al₂O₃ (SCAT)¹³² in a failed attempt to obtain **141**. In addition, compound **140** was mixed with lithium metal in THF and allowed to heat to reflux overnight.¹³³ In both cases, only starting material **140** was recovered. These results were very disappointing taking into account that previously a model reaction was carried

out with a positive outcome. The model reaction consisted of the synthesis of perylene (**61**) employing 1-bromonaphthalene and naphthalen-1-ylboronic acid as starting materials, and following the same pathway outlined in Scheme 22 (steps a and c) perylene (**61**) was obtained over 50% in overall yield.

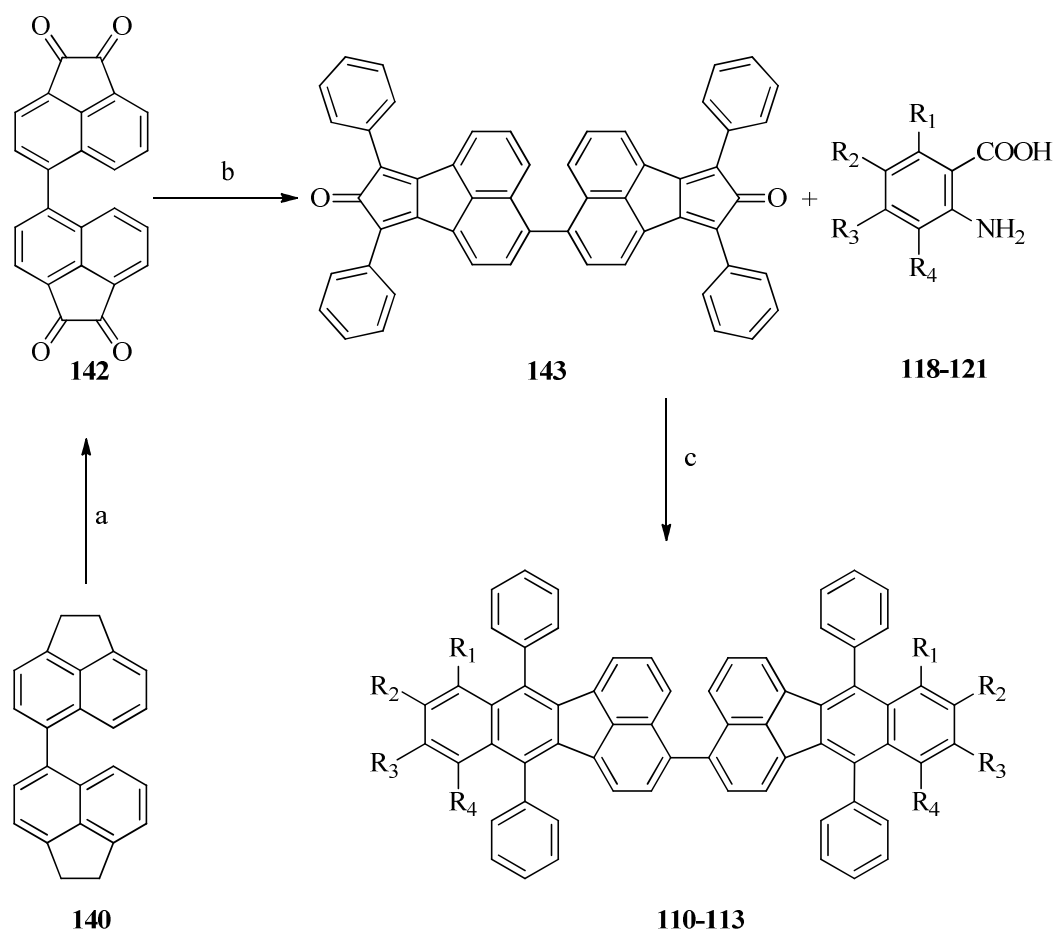
After these futile outcomes, we tried Tanaka^{134,135} and Mitchell procedures.¹³⁶ Under these conditions (Scheme 22, step d), it was expected that 5,6-dibromoacenaphthene (**139**) undergoes an oxidative homo coupling to yield compound **141**. The unsuccessful results showed primarily the presence of starting material (**139**).



Scheme 22. Synthetic route through 1,2,7,8-tetrahydrodicyclopenta[cd,lm]perylene (**141**). Conditions: (a) Pd(PPh₃)₄, 2M K₂CO₃/toluene, reflux, 2 d, 64%; (b) NBS/DMF; (c) CuSO₄/Al₂O₃ (SCAT), chlorobenzene, reflux, 24 h or Li/THF, 24 h; (d) TMEDA, *n*-butyllithium, 9,10-phenanthrenequinone/ether, -78 °C (Tanaka procedure)^{134,135} or Ni(acac)₂/ether, -78 °C (Mitchell procedure).¹³⁶

The previously outlined route failed to yield compound **141**, however it indicated an easy way to synthesize compound **140**. We took advantage of this result to design a new way to obtain the dimers and consequently the target molecules (Scheme 23). The previously synthesized compound **140** was oxidized to the corresponding tetraone **142** using benzeneseleninic anhydride in chlorobenzene.¹³⁷ The latter was treated with 1,3-diphenylketone

to yield compound **143**.¹³⁸ Finally, anthranilic acids **118-121** and cyclopentadienone derivative **143** were reacted under benzyne addition conditions to afford compounds **110-113**, in 50, 30, 64, and 30%, respectively. These dimers are insoluble in hexanes but soluble in halogenated hydrocarbons and benzene. Compounds **110**, **111**, and **113** are yellow solids, and compound **112** exhibits a deep red coloration. All of them have mp points above 300 °C. The presence of the dimers was corroborated by mass spectrometry.

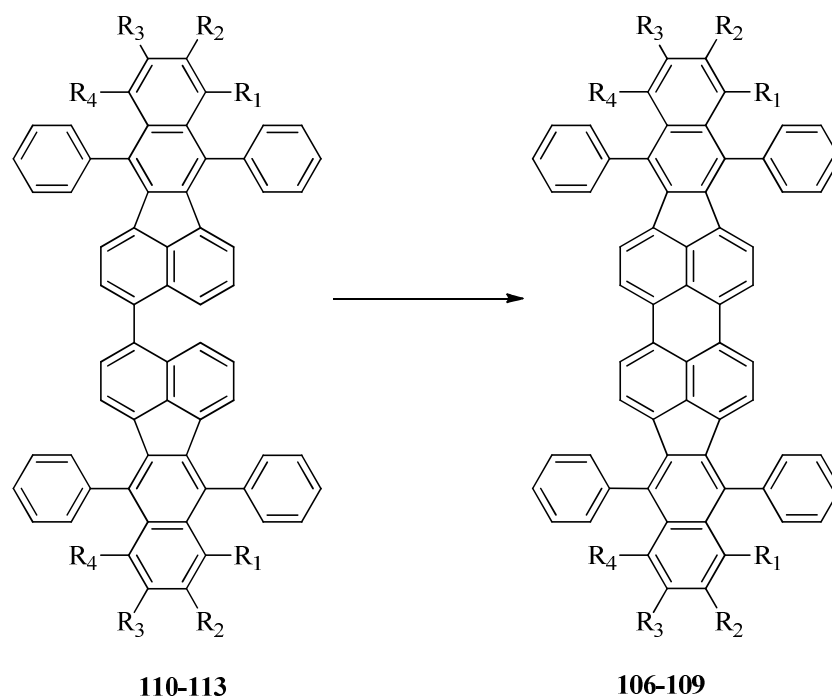


- 110, 118** $R_1 = R_2 = R_3 = R_4 = \text{phenyl}$
111, 119 $R_1 = R_4 = \text{phenyl}; R_2 = R_3 = 9,10\text{-dihydrophenanthrene}$
112, 120 $R_1 = R_2 = R_3 = R_4 = 4,7\text{-di-}i\text{-tert-butylacenaphthene}$
113, 121 $R_1 = R_4 = \text{phenyl}; R_2 = R_3 = 4,7\text{-di-}i\text{-tert-butylacenaphthene}$

Scheme 23. An alternative route to the synthesis of the dimers. Conditions: (a) benzeneseleninic anhydride/chlorobenzene, refluxed for 2 d, 80%; (b) 1,3-diphenylketone, KOH/MeOH, 1 h, 83%; (c) isoamyl nitrite/dichloroethane, heated for 30 min, yields: 50% for **110**, 30% for **111**, 64% for **112**, and 30% for **113**.

3) Ring closure

The ring closure of the dimers **110-113** through products **106-109** (Scheme 24) was initially performed using oxidative coupling reactions. One of the first reaction systems employed was cobalt trifluoride in trifluoroacetic acid.^{123,125} Under this condition, only compound **106** was obtained in moderate yield (52%). Other catalytic systems used include $\text{AlCl}_3/\text{Cu}(\text{OTf})_2/\text{CS}_2$ (Kovacic conditions),^{139,140} 2,3-dichloro-5,6-dicyano-1,4-benzoquinone (DDQ)/ $\text{AlCl}_3/\text{CH}_2\text{Cl}_2$,¹⁴¹ and $\text{Sc}(\text{OTf})_3/\text{DDQ}$.¹⁴² None of these conditions progressed to the desired products. In addition, dissimilar classes of systems as sodium naphthalenide/THF,¹⁴³⁻¹⁴⁵ lithium/THF,¹⁴⁶ and potassium *t*-butoxide/1,5-diazabicyclo(4.3.0)non-5-ene (DBN)/diglyme¹⁴⁷ were tested. Once again, these conditions did not yield the expected products. The results are summarized in Table 16.



- 106, 110,** $R_1 = R_2 = R_3 = R_4 = \text{phenyl}$
107, 111, $R_1 = R_4 = \text{phenyl}; R_2 = R_3 = 9,10\text{-dihydrophenanthrene}$
108, 112, $R_1 = R_2 = R_3 = R_4 = 4,7\text{-di-}i\text{-tert-butylacenaphthene}$
109, 113, $R_1 = R_4 = \text{phenyl}; R_2 = R_3 = 4,7\text{-di-}i\text{-tert-butylacenaphthene}$

Scheme 24. Ring closure of the dimers.

Table 16. The different conditions employed to obtain products **106-109** from dimers **110-113**

Conditions	Dimers			
	110	111	112	113
CoF ₃ /F ₃ CCO ₂ H	positive	negative	negative	negative
AlCl ₃ , Cu(OTf) ₂ /CS ₂	negative	negative	negative	negative
DDQ, AlCl ₃ /CH ₂ Cl ₂	negative	negative	negative	negative
Sc(OTf) ₃ /DDQ	negative	negative	negative	negative
Sodium Naph/THF	negative	negative	negative	negative
Li/THF	negative	negative	negative	negative
<i>t</i> BuOK, DBN/diglyme	negative	negative	negative	negative

The only obtained product, compound **106**, is a purple solid, which displays partial solubility in chloroform and benzene, and forms a light pink solution in those organic solvents. Under UV irradiation, the solution emits a bright reddish fluorescence (Figure 43). UV/Vis absorption and fluorescence spectra evaluated in chloroform are shown in Figure 44. Absorption bands at 318, 352, 518, 558, and 606 nm were observed along with emission bands at 615 and 667 nm. The fluorescence quantum yield at 558 nm is $\phi_F = 0.21$, and at 606 nm is $\phi_F = 0.4$. The absorption band at 606 nm represents a bathochromic shift (red shift) of 66 nm from perflanthene (**64**) ($\lambda_{\max} = 540$ nm) or 42 nm from compound **105** ($\lambda_{\max} = 564$ nm) (Table 17).¹²⁴ This shift is not pronounced due to the rotation out of the plane of the phenyl substituents, preventing more extensive delocalization.¹²⁴ However, the spectroscopic characteristics of compound **106** are similar to those exhibited for chromophore **98**, which is an excellent fluorescent material.¹⁴⁸ The emission band with a maximum at 615 nm is shifted by 9 nm to a longer wavelength (lower frequency) with respect to the absorption band ($\lambda_{\max} = 606$ nm). According to Holtrup,¹⁴⁸ a small Stokes shift such as 9 nm suggests that the transition state and the ground state geometries are very similar. This is a consequence of the rigidity of the planar structures.



Figure 43. Compound **106** under regular light (top), and under UV-Vis light (bottom).

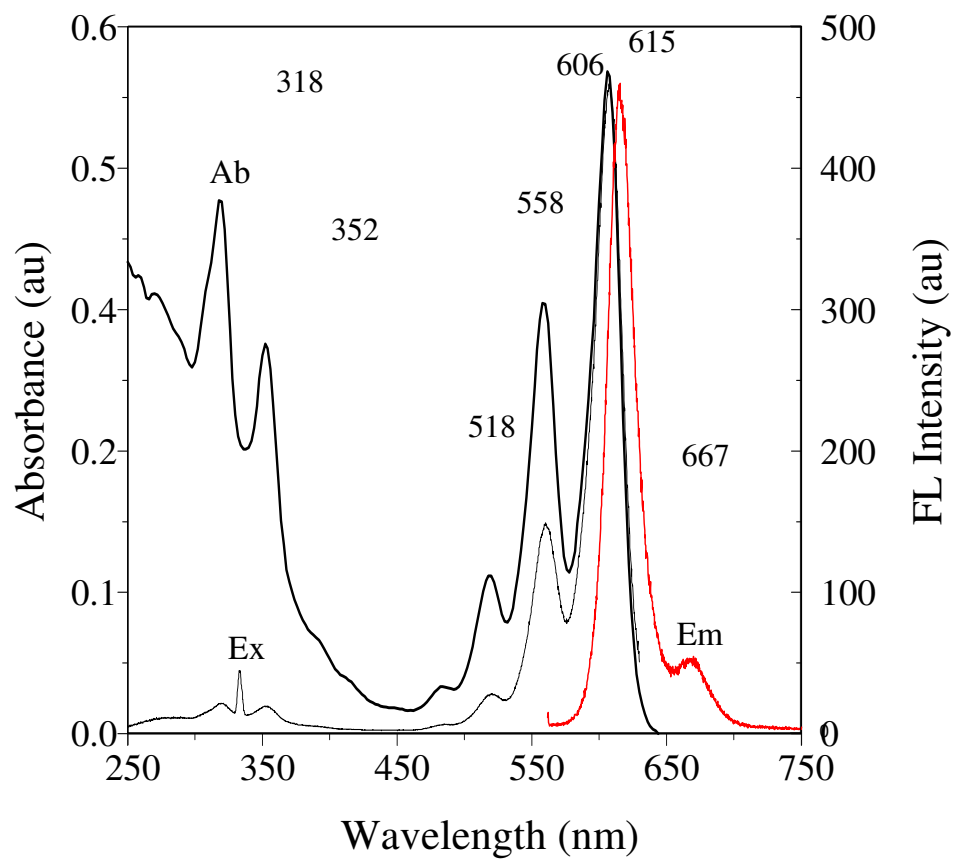
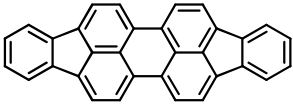
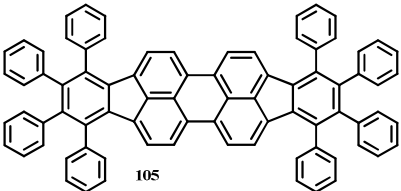
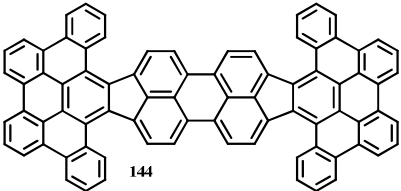
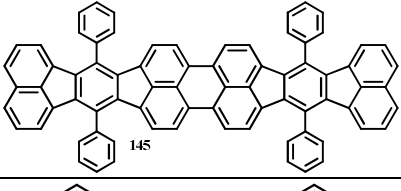
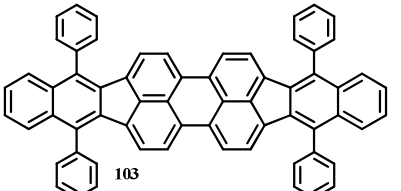
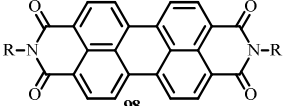
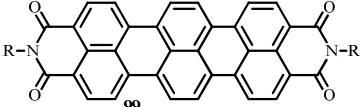
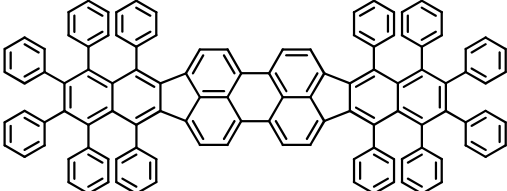


Table 17. UV data of compounds **64**, **105**, **144**, **145**, **103**, **98**, **99**, and **106**.¹²⁴

	λ_{\max} [nm]	$\log \varepsilon$ [L mol ⁻¹ cm ⁻¹]	Max. of Fl [nm] ^a
 64	540	3.79	<i>b</i>
 105	564	4.94	587
 144	670	4.99	696
 145	602	5.06	632
 103	582	<i>b</i>	<i>b</i>
 98	525	4.67	556
 99	664	5.08	707
 106	606	<i>b</i>	615

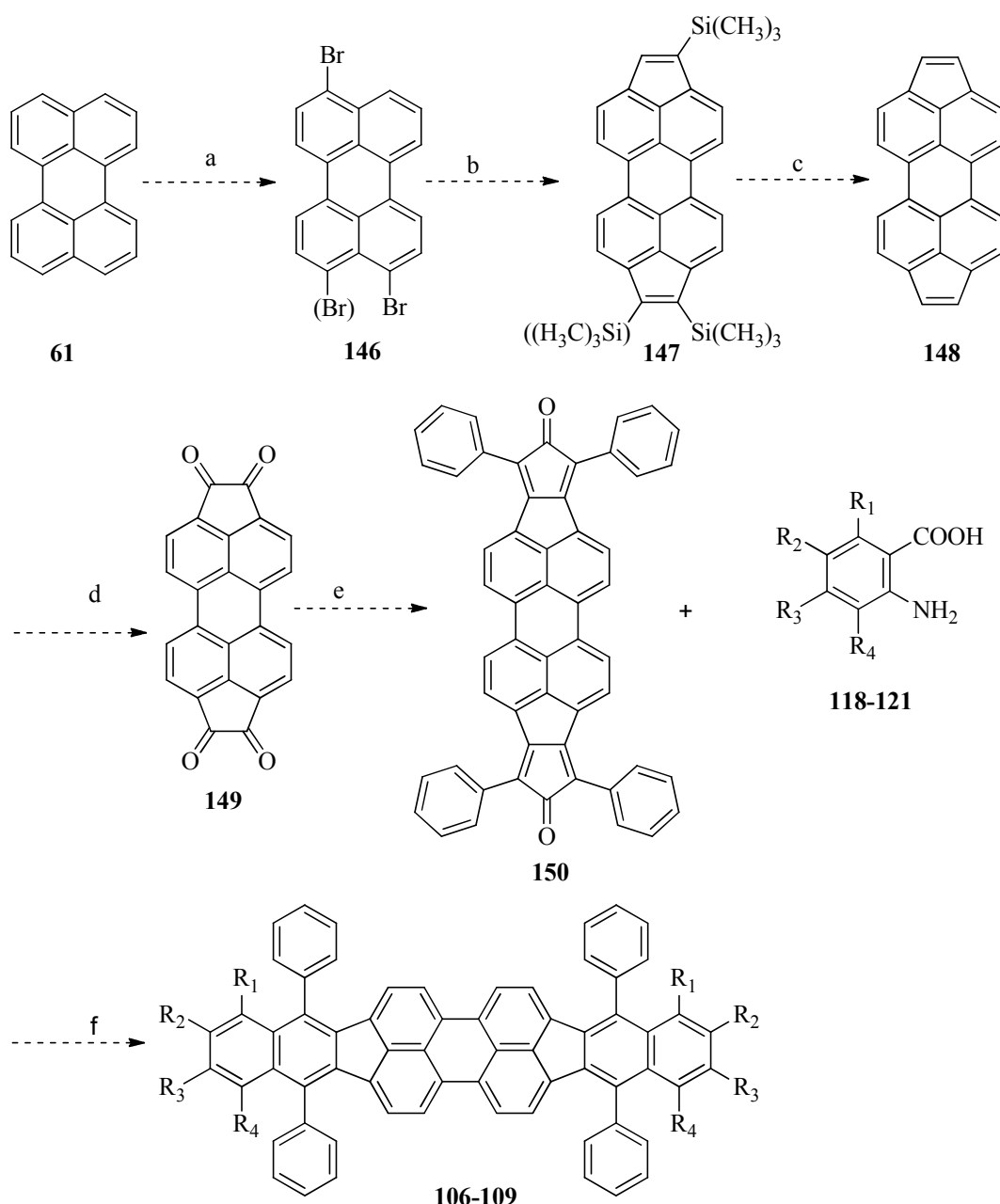
^a Excitation in the maximum of absorption. *b* Not available. R = Alkyl, Aryl

Conclusion

We have found a convenient synthetic pathway for the formation of the fluoranthene dimers, which represents a step prior to the building of the target molecules. Nevertheless, more experimentation needs to be carried out in order to find the appropriate conditions for the *intramolecular* ring closure. We did synthesize compound **106**, which is very similar to compound **105** (structure previously synthesized by Müllen). However, when the terminal phenyl groups in the fluoranthene backbone were substituted with either phenanthracenyl or *t*-butylated acenaphthenyl groups, the ring closure step did not proceed successfully. This result suggests that changes in the fluoranthene moiety cause changes in the reactivity (electronic or steric) in the coupling reaction. Given the interesting spectroscopic characteristics of compound **106** (absorption at 606 nm and emission at 615 nm), that positioned it at the level of those compounds tested for fluorescent applications, it is important to keep surveying for ways to obtain the target molecules. Because the results indicated that the substitution on the fluoranthene units affects the coupling steps, it is prudent in future investigations to concentrate our effort in obtaining pentacycloperylene **141** or related derivatives.

We have considered two possible routes (A and B) starting with commercially available perylene **61**. In route A (Scheme 25), perylene (**61**) is first treated under bromination conditions (step a) resulting in the formation of an isomeric mixture of 3,9- and 3,10-dibromoperylene (**146**). The investigators involved in this synthesis found that the isomeric mixture could not be resolved using column chromatography or HPLC. The reported percent yield for the isomeric mixture **146** is 94%.¹⁴⁹ The next step consists of a palladium-catalyzed reaction between compound **146** and trimethyl silane to form an isomeric mixture of silylated cyclopenta-fused

PAH **147**.¹⁵⁰ The latter compound **147** (step c) would then be desilylated using tetrabutylammonium fluoride in dichloromethane to yield compound **148**.¹⁵¹ Subsequently, compound **148** could be oxidized by means of benzeneseleninic anhydride in chlorobenzene to the corresponding tetraone **149**.¹⁵² Finally, the last two steps (e and f) are the same previously outlined in Scheme 23.



- 106, 118** $R_1 = R_2 = R_3 = R_4 = \text{phenyl}$
107, 119 $R_1 = R_4 = \text{phenyl}; R_2 = R_3 = 9,10\text{-dihydrophenanthrene}$
108, 120 $R_1 = R_2 = R_3 = R_4 = 4,7\text{-di-}t\text{-butylacenaphthene}$
109, 121 $R_1 = R_4 = \text{phenyl}; R_2 = R_3 = 4,7\text{-di-}t\text{-butylacenaphthene}$

Scheme 25. Proposed route A for future investigation. Conditions: (a) Br_2 , HCl/AcOH , $40\text{ }^\circ\text{C}$, 5 h; (b) $\text{HCCSi}(\text{CH}_3)_3$, $\text{PdCl}_2(\text{PPh}_3)_2$, $\text{PPh}_3/\text{Et}_3\text{N}$, benzene, reflux; (c) $\text{Bu}_4\text{NF}/\text{CH}_2\text{Cl}_2$, rt; (d) benzeneseleninic anhydride/chlorobenzene, reflux; (e) 1,3-diphenylketone, KOH/MeOH ; (f) isoamyl nitrite/dichloroethane.

In route B, (Scheme 26), electrophilic substitution of perylene (**61**) first using oxalyl chloride in carbon disulfide (step a) would afford quinone intermediate (**151**).¹⁵³ Following step a, a double Wolff-Kishner reduction (step b) of quinone **151** would yield intermediate **152**.¹⁵⁴ Again, oxalyl chloride is reacted with compound **152** (step c) to form quinone **153**. Subsequently, quinone **153** is further oxidized to tetraone **149** using benzeneseleninic anhydride in chlorobenzene (step d). Finally, the last two steps (e and f) are the same previously outlined in Schemes 23 and 25.

Experimental section

General Procedures. Melting points were uncorrected. Proton NMR spectra were recorded on a Varian INOVA AC 400 spectrometer. Carbon NMR spectra were recorded on a Varian INOVA AC 400 spectrometer operating at 100 MHz. UV-Vis absorption spectra were measured on a Hewlett-Packard 8452A diode array spectrophotometer. Maldi analysis was performed using an Applied Biosystems 4700 Proteomics Analyzer with TOF/TOF options. Commercial chemicals were purchased from Aldrich and used as supplied, unless otherwise stated.

4,5,6,7-Tetraphenylisoindoline-1,3-dione (124). 2,3,4,5-Tetraphenylcyclopenta-2,4-dienone (**123**) (24.8 g, 64.5 mmol) and maleimide (6.28 g, 64.7 mmol) along with nitrobenzene (150 mL) were placed in a 500-mL Erlenmeyer flask and heated to reflux for 24 h. After cooling, the reaction mixture was vacuum filtered and washed with ethanol (200 mL) to yield a brown solid (17.3 g, 39.2 mmol, 61%); mp > 300 °C (lit.¹⁵⁵ mp 324–325 °C) ¹H NMR (400 MHz, CDCl₃): δ 6.74 (m, 4H), 6.88 (m, 2H), 7.11 (m, 4H), 7.19 (m, 6H), 7.79 (br s, 1H). ¹³C NMR (100 MHz, CDCl₃): δ 126.3, 127.0, 127.3, 127.4, 128.6, 129.8, 130.6, 135.4, 137.9, 139.6, 148.1, 166.8.

2-Amino-3,4,5,6-tetraphenylbenzoicacid (118). 4,5,6,7-Tetraphenylisoindoline-1,3-dione (**124**) (5.00 g, 11.1 mmol) and methanol (500 mL) were placed in a 1000-mL Erlenmeyer flask. Sodium hydroxide (1.75 g, 43.8 mmol) dissolved in the minimal amount of methanol was added and subsequently a solution of sodium hypochlorite, bleach, (17.6 mL, 14.2 mmol) was dropped into the flask. The mixture was refluxed for 30 min. After cooling, the solvent was

evaporated until one third of its original volume remained. The mixture was acidified and extracted with three portions of methylene chloride (~150 mL total). The organic layer was dried over anhydrous sodium sulfate and evaporated to dryness. The reaction was run one more time, and the products combined. The total isolated urethane was transferred into a 500- mL Erlenmeyer flask and combined with a mixture of potassium hydroxide (38.6 g, 688 mmol) in *n*-propanol (430 mL). After refluxing for 2 days, the bright orange mixture was poured into water (400 mL) and acidified until yellow solid started to precipitate. The crude yellow product was filtered (8.25 g, 18.7 mmol, 84%); mp 268–272 °C (lit.¹⁵⁵ mp 275–278 °C). ¹H NMR (400 MHz, DMSO-*d*₆): δ 6.71-6.83 (m, 10H), 7.01-7.24 (m, 10H). ¹³C NMR (100 MHz, DMSO-*d*₆): δ 118.4, 125.0, 125.4, 126.0, 126.4, 126.5, 125.6, 126.8, 126.9, 128.3, 129.8, 130.4, 130.6, 131.6, 137.2, 139.1, 139.7, 139.9, 140.5, 142.0, 142.5, 170.2.

1,3-Diphenyl-2*H*-cyclopenta[*l*]phenanthren-2-one (126). Phenanthrene-9,10-dione (**125**) (30.0 g, 0.144 mol), 1,3-diphenylacetone (30.3 g, 0.144 mol) and methanol (500 mL) were placed in a 1000-mL Erlenmeyer flask. Potassium hydroxide (17.0 g, 0.302 mmol) dissolved in methanol (50 mL) was added into the mixture. The resulting black solid was stirred at rt for 1 h. The product was filtered and washed with water (150 mL) and then with methanol (150 mL) to yield (48.4 g, 127 mmol, 88%); mp 240–247 °C (lit.¹⁵⁶ mp 245–255 °C). ¹H NMR (400 MHz, CDCl₃): δ 6.94 (t, *J* = 8, 3H), 7.29 (d, *J* = 8, 2H), 7.35-7.43 (m, 9H), 7.55 (d, *J* = 8, 2H), 7.80 (d, *J* = 8, 2H). ¹³C NMR (100 MHz, CDCl₃): δ 123.1, 124.4, 128.1, 128.2, 128.5, 128.6, 129.0, 130.0, 131.4, 132.2, 133.5, 148.2, 200.2.

9,10,12,13-Tetraphenyl-11,12-dihydro-10*H*-phenanthro[9,10-*f*]isoindole (127). 1,3-Diphenyl-2*H*-cyclopenta[*l*]phenanthren-2-one (**126**) (7.76 g, 20.3 mmol) and maleimide (1.98 g,

20.4 mmol) were placed in a 200-mL round bottomed flask. Nitrobenzene (45 mL) was added, and the solution was allowed to reflux for 24 h. Upon cooling, the reaction mixture was vacuum filtered and washed with ethanol (~60 mL) to yield a brown solid (5.27 g, 11.7 mmol, 58%); mp > 300 °C (lit.¹²⁶ mp 399–403 °C). ¹H NMR (400 MHz, CDCl₃): δ 6.94 (t, *J* = 8, 2H), 7.28 (d, *J* = 8.0 Hz, 2H), 7.37-7.45 (m, 10H), 7.54 (d, *J* = 8 Hz, 2H), 7.80 (d, *J* = 8 Hz, 2H). ¹³C NMR (100 MHz, CDCl₃): δ 30.0, 120.3, 125.5, 125.8, 131.3, 142.0, 145.8.

3-Amino-1,4-diphenyltriphenylene-2-carboxylic acid (119). 9,10,12,13-Tetraphenyl-11,12-dihydro-10*H*-phenanthro[9,10-*f*]isoindole (**127**) (5.27 g, 11.8 mmol) and methanol (500 mL) were placed in a 1000-mL Erlenmeyer flask. Sodium hydroxide (2.05 g, 51.3 mmol) and bleach (20.0 mL) were added, respectively, into the flask. The mixture was refluxed for 30 min. After cooling, the solvent was evaporated until one third of its original volume remained. The mixture was acidified and extracted with three portions of methylene chloride (~150 mL). The organic layer was dried over anhydrous sodium sulfate and evaporated to dryness. The reaction was run four more times. The accumulative intermediate (26.3 g, 59.0 mmol) and potassium hydroxide (89.7 g, 1.60 mmol) were refluxed for 2 days in *n*-propanol (1000 mL). The bright orange mixture was poured into water (650 mL) and acidified until a yellow solid started to precipitate. The crude yellow product was filtered to yield (17.4 g, 39.6 mmol, 77%), mp 225–235 °C (lit.¹²⁶ mp 220–230 °C). ¹H NMR (400 MHz, CDCl₃): δ 6.87 (t, *J* = 8 Hz, 1H), 6.95 (t, *J* = 8 Hz, 1H), 7.13 (d, *J* = 8 Hz, 1H), 7.20 (t, *J* = 8 Hz, 1H), 7.24-7.45 (m, 12 H), 8.38 (d, *J* = 8 Hz, 1H), 8.43 (d, *J* = 8 Hz, 1H). ¹³C NMR (100 MHz, *d*-DMSO): δ 120.3, 120.9, 123.2, 124.3, 125.1, 126.1, 126.7, 127.3, 128.2, 128.4, 129.0, 129.1, 129.7, 129.9, 130.4, 131.0, 131.1, 134.7, 140.3, 141.3, 142.9.

4,7-Di-*tert*-butyl-1,2-dihydroacenaphthylene (129). Carbon dioxide (500 mL) was placed in a three necks round flask. Aluminum trichloride (8.85 g, 66.4 mmol) and acenaphthene (**128**) (50.2 g, 326 mmol) were added. After 5 min, *tert*-butyl chloride (63.8 g, 689 mmol) was added dropwise for a period of 30 min. The reaction mixture was brought to a gentle reflux for 4 h. The mixture was poured into water (600 mL), and the organic layer was separated and evaporated to dryness. The solid was triturated with methanol and then recrystallized in hexanes yielding (24.0 g, 90.0 mmol, 28%); mp 161–164 °C (lit.¹⁵⁷ mp 162.5–163.5 °C). ¹H NMR (400 MHz, CDCl₃): δ 1.42 (s, 18H), 3.38 (s, 4H), 7.34 (s, 2H), 7.53 (s, 2H). ¹³C NMR (100 MHz, CDCl₃): δ 30.5, 31.7, 35.3, 117.3, 117.4, 130.7, 136.3, 145.1, 151.2.

4,7-Di-*tert*-butylacenaphthylene (130). In a typical procedure: addition-elimination of bromine, compound **129** (23.9 g, 89.9 mmol), *N*-bromosuccinimide (32.4 g, 182 mmol), and dibenzoyl peroxide (few pieces) were placed in a flask. Benzene (120 mL) was added, and the system was heated to reflux for 20 min. The reaction mixture was filtered and upon evaporation of the solvent, orange oil was obtained. The oil was dissolved in the minimal amount of THF and added dropwise to a refluxing mixture of zinc (15.2 g, 232 mmol), THF (60.0 mL) and acetic acid (10.0 mL). The resulting mixture was stirred for 24 h. After evaporation of the solvent, the crude orange product was purified by column chromatography (silica gel SG; solvent/Hexanes). The first band to elude, a yellow bright product, was collected to yield (15.7 g, 59.4 mmol, 66%); mp 110–112 °C (lit.¹⁵⁸ mp 114.5–117 °C). ¹H NMR (400 MHz, CDCl₃): δ 1.45 (s, 18H), 7.06 (s, 2H), 7.75 (s, 2H), 7.78 (s, 2H). ¹³C NMR (100 MHz, CDCl₃): δ 31.7, 35.5, 122.0, 122.5, 125.4, 127.3, 129.5, 139.0, 151.1.

2,8,11,14-tetra-*tert*-butylacenaphtho[1',2':9,10]fluorantheno[7,8-*c*]furan-4,6-dione (131). Combined procedures from Nakayama¹⁵⁹ and Clapp.¹⁶⁰ A mixture of 4,7-di-*tert*-butylacenaphthene (**130**) (15.7 g, 59.4 mmol) and sulfur (7.62 g, 29.7 mmol) in dimethylformamide (150 mL) was heated to reflux for 24 h. The crude product was vacuum filtered, washed with methanol, and transferred into a 500-mL Erlenmeyer flask. Maleic anhydride (21.0 g, 214 mmol) was added and the mixture was heated, keeping the flask loosely capped, for 2 h. After cooling, water was cautiously added into the mixture. The crude product was filtered and rinsed with ethanol to afford (10.2 g, 16.4 mmol, 55%); mp > 300 °C. ¹H NMR (400 MHz, CDCl₃): δ 1.58 (s, 18H), 1.68 (s, 18H), 8.05 (d, *J* = 1.2 Hz, 2H), 8.09 (d, *J* = 1.2 Hz, 2H), 9.05 (d, *J* = 1.2 Hz, 2H), 9.36 (d, *J* = 1.2 Hz, 2H). ¹³C NMR (100 MHz, CDCl₃): δ 31.6, 32.0, 35.8, 35.9, 122.5, 124.6, 124.7, 126.0, 129.4, 131.4, 132.4, 134.4, 139.0, 141.9, 151.3, 152.6, 164.1.

2,5,11,14-Tetra-*tert*-butyl-7*H*-diacenaphtho[1,2-*e*:1',2'-*g*]isoindole-7,9(8*H*)-dione (132). A combined procedure from Koch¹⁶¹ and Schindlbauer.¹⁶² Anhydride (**131**) (10.0 g, 16.1 mmol), urea (125 g) and dimethylformamide (300 mL) were heated to reflux for 1 h. After cooling, the green-brown solution was filtered and washed with ethanol yielding a yellow solid (8.06 g, 13.0 mmol, 81%); mp > 300 °C. ¹H NMR (400 MHz, CDCl₃): δ 1.60 (s, 18H), 1.67 (s, 18H), 7.74 (s, 1H), 8.01 (d, *J* = 1.2 Hz, 2H), 8.04 (d, *J* = 1.2 Hz, 2H), 9.02 (d, *J* = 1.2 Hz, 2H), 9.51 (d, *J* = 1.6 Hz, 2H). ¹³C NMR (100 MHz, CDCl₃): δ 31.7, 32.0, 35.8, 35.9, 123.8, 123.9, 124.0, 125.2, 126.2, 129.4, 131.7, 133.3, 135.1, 138.2, 141.0, 151.0, 152.3, 168.8.

8-Amino-2,5,10,13-tetra-*tert*-butylacenaphtho[1,2-*j*]fluoranthene-7-carboxylic acid (120). Imide **132** (7.92 g, 12.8 mmol) and methanol (600 mL) were placed in a 1000-mL

Erlenmeyer flask. Sodium hydroxide (2.07 g, 51.9 mmol) and bleach (22.0 mL) were respectively poured into the flask. The mixture was refluxed for 30 min. After cooling, the solvent was evaporated until one third of its original volume remained. The mixture was acidified and extracted with three portions of methylene chloride (~150 mL total). The organic layer was dried over anhydrous sodium sulfate and evaporated to dryness. The isolated urethane was transferred into a 500-mL Erlenmeyer flask and combined with a mixture of potassium hydroxide (22.3 g, 0.397 mol) in *n*-propanol (330 mL). After refluxing for 2 days, the bright orange mixture was poured into water (400 mL) and acidified until an orange-red solid started to precipitate. The crude red product was filtered (7.00 g, 11.5 mmol, 90%). ¹H NMR (400 MHz, CDCl₃): δ 1.49 (s, 9H), 1.55 (s, 9H), 1.63 (s, 9H), 1.65 (s, 9H), 7.82 (d, *J* = 1.2 Hz, 1H), 7.85 (d, *J* = 0.80 Hz, 1H), 7.86 (d, *J* = 1.2 Hz, 1H), 7.96 (d, *J* = 0.80 Hz, 1H), 8.03 (s, 1H), 8.59 (d, *J* = 1.2 Hz, 1H), 8.76 (d, *J* = 1.6 Hz, 1H), 8.95 (d, *J* = 1.2 Hz, 1H). ¹³C NMR (100 MHz, CDCl₃): δ 31.6, 31.7, 31.9, 32.0, 35.6, 35.7, 35.8, 111.4, 119.3, 121.1, 121.3, 123.2, 123.3, 123.8, 124.4, 128.9, 129.2, 129.3, 130.1, 130.7, 135.0, 135.8, 135.9, 136.1, 139.5, 141.7, 143.4, 150.6, 151.1, 151.2, 151.3, 174.6.

4,7-Di-*tert*-butylacenaphthylene-1,2-dione (133). Compound **129** (11.7 g, 43.9 mmol), *N*-bromosuccinimide (15.8 g, 88.9 mmol) and dibenzoyl peroxide (few pieces) were placed in a flask. Benzene (60 mL) was added, and the system was heated to reflux for 20 min. The reaction mixture was filtered and upon evaporation of the solvent, orange oil was obtained. The oil was poured into dimethyl sulfoxide (300 mL) and carefully heated at approximately 50 °C for 48 h. After cooling, the mixture was transferred into water (200 mL), and the yellowish precipitate was separated by vacuum filtration. The crude product was stirred in hexanes (200

mL) for 2 h to get rid of the excess starting material. Upon vacuum filtration, a bright yellow solid was obtained (3.81 g, 13.0 mmol, 30%); mp 185–180 °C. The compound was used for the next step without further purification. ¹H NMR (400 MHz, CDCl₃): δ 1.49 (s, 18H), 8.18 (s, 2H), 8.23 (s, 2H). ¹³C NMR (100 MHz, CDCl₃): δ 31.4, 35.9, 120.0, 127.9, 128.0, 131.4, 143.5, 152.4, 188.9.

2,5-Di-*tert*-butyl-7,9-diphenyl-8*H*-cyclopenta[*a*]acenaphthylen-8-one(134).

4,7-Di-*tert*-butylacenaphthylene-1,2-dione (**133**) (3.80 g, 12.9 mmol), 1,3-diphenylacetone (2.76 g, 13.1 mmol) and methanol (90 mL) were placed in a 250-mL Erlenmeyer flask. Potassium hydroxide (1.48 g, 26.4 mmol) dissolved in the minimal amount possible of methanol was added into the mixture. The resulting black solid was stirred at rt for 15 min. The crude product was filtered and washed with water (5.56 g, 11.9 mmol, 92%); mp > 300 °C. ¹H NMR (400 MHz, CDCl₃): δ 1.43 (s, 18H), 7.41 (t, *J* = 8 Hz, 2H), 7.53 (t, *J* = 8 Hz, 4H), 7.86 (t, *J* = 8 Hz, 6H), 8.15(s, 2H). ¹³C NMR (100 MHz, CDCl₃): δ 31.5, 35.5, 119.0, 121.1, 123.4, 128.1, 128.5, 129.0, 130.9, 131.5, 131.6, 142.1, 152.0, 155.0, 202.0.

2,5-Di-*tert*-butyl-7,11-diphenyl-8*H*-acenaphtho[1,2-*f*]isoindole-8,10(9*H*)-dione (135).

5-Di-*tert*-butyl-7,9-diphenyl-8*H*-cyclopenta[*a*]acenaphthylen-8-one (**134**) (5.56 g, 11.9 mmol), maleimide (1.20 g, 12.4 mmol), and nitrobenzene (40 mL) were placed in a 100-mL Erlenmeyer flask. The mixture was heated to reflux for 48 h, and upon to cooling down, methanol (300 mL) was added. The precipitate was vacuum filtered to yielded (3.27 g, 6.10 mmol, 52%); mp > 300 °C. ¹H NMR (400 MHz, CDCl₃): δ 1.20 (s, 18H), 6.88 (s, 2H), 7.57-7.64 (m, 11H), 7.77 (s, 2H). ¹³C NMR (100 MHz, DMSO-*d*₆): δ 31.2, 35.4, 123.5, 124.1, 128.0, 128.6, 128.7, 128.9, 130.4, 133.5, 135.6, 135.7, 144.0, 151.4, 167.3.

9-amino-2,5-di-tert-butyl-7,10-diphenylfluoranthene-8-carboxylic acid (121). 2,5-Di-tert-butyl-7,11-diphenyl-8*H*-acenaphtho[1,2-*f*]isoindole-8,10(9*H*)-dione (**135**) (3.27g, 6.10 mmol) was suspended in methanol (330 mL) in a 1000-m L Erlenmeyer flask. Sodium hydroxide (0.966 g, 24.2 mmol) dissolved in the minimal amount of water was added followed by the addition of commercial bleach (9.70 mL). The resulting solution was heated to reflux for 30 min on a hot plate. The mixture was concentrated, poured into 3M hydrochloric acid (70.0 mL) and then, extracted with three portions of methylene chloride (~150 mL). The combined organic layer was dried over sodium sulfate and concentrated to dryness. The brown crude product was transferred into a 500-mL Erlenmeyer flask and combined with a mixture of potassium hydroxide (10.6 g, 189 mmol) in *n*-propanol (300 mL). After refluxing for 2 days, the yellowish mixture was poured into water (400 mL) and acidified until a yellow solid started to precipitate. The product was filtered and rinsed firstly with water (150 mL), and subsequently with methanol (150 mL) to yield (2.72 g, 5.17 mmol, 85%). ¹H NMR (400 MHz, DMSO-*d*₆): δ 1.10 (d, *J* = 1.6 Hz, 18H), 6.4 (s, 1H), 6.36 (s, 1H), 7.41 (d, *J* = 7.2 Hz, 2H), 7.48–7.58 (m, 6H), 7.63–7.74 (m, 4H). ¹³C NMR (100 MHz, DMSO-*d*₆): 30.96, 31.02, 119.1, 119.5, 121.0, 122.2, 123.7, 126.3, 127.0, 128.2, 128.46, 128.54, 128.6, 130.0, 130.1, 134.5, 135.5, 136.3, 138.2, 139.9, 140.9, 145.6, 149.9, 150.4, 170.1.

5-bromoacenaphthylene-1,2-dione (137). 5-Bromoacenaphthene (**136**) (10.0 g, 42.9 mmol) was dissolved in acetic anhydride (400 mL) and cooled in an ice bath for 30 min. Chromium trioxide (21.9 g, 219 mmol), which was divided in three equal portions, was added to the iced solution at least every 1.5 h. The dark solution was kept in the ice bath and allowed to stir overnight. The solution was very carefully poured into water (~1000 mL), and the yellow

precipitate filtered, rinsed with water and air dried to yield (6.62 g, 25.4 mmol, 59%); mp 234–236 °C (lit.¹⁶³ mp 236.0–236.8 °C). ¹H NMR (400 MHz, DMSO-*d*₆): δ 7.95 (d, *J* = 8.0 Hz, 1H), 8.03 (t, *J* = 8.0 Hz, 1H), 8.14 (d, *J* = 8.0 Hz, 1H), 8.20 (d, *J* = 8.0 Hz, 1H), 8.38 (d, *J* = 8.0 Hz, 1H). ¹³C NMR (100 MHz, DMSO-*d*₆): 122.0, 122.1, 126.5, 128.9, 129.6, 129.7, 130.1, 130.6, 132.0, 144.3, 186.7, 186.8.

3-Bromo-7,9-diphenyl-8*H*-cyclopenta[*a*]acenaphthylen-8-one (122).

5-Bromoacenaphthylene-1,2-dione (**137**) (9.88 g, 37.8 mmol), 1,3-diphenylacetone (8.00 g, 38.0 mmol), and methanol (150 mL) were placed in a 500-mL Erlenmeyer flask. Potassium hydroxide (4.26 g, 75.9 mmol) dissolved in the minimal amount of methanol was added into the mixture. The resulting black solid was stirred at rt for 15 min. The product was filtered and washed with water to yield (11.6 g, 26.6 mmol, 70%); mp > 300 °C. ¹H NMR (400 MHz, CDCl₃): δ 7.42 (t, *J* = 8 Hz, 2H), 7.51-7.54 (m, 4H), 7.67 (t, *J* = 8 Hz, 1H), 7.78-7.81 (m, 5H), 7.87 (d, *J* = 4 Hz, 1H), 8.07 (dd, *J*₁ = 8 Hz, *J*₂ = 4 Hz 2H). ¹³C NMR (100 MHz, CDCl₃): δ 121.1, 121.6, 122.1, 122.3, 123.0, 127.0, 128.5, 128.6, 128.7, 129.0, 129.1, 129.6, 131.1, 131.2, 131.7, 131.8, 145.1, 152.9, 153.4, 201.5.

3-Bromo-7,8,9,10,11,12-hexaphenylbenzo[*k*]fluoranthene (114). 3-Bromo-7,9-diphenyl-8*H*-cyclopenta[*a*]acenaphthylen-8-one (**122**) (9.86 g, 22.6 mmol) in dichloroethane (350 mL) was heated to refluxed. To this mixture, a solution of isoamyl nitrite (7.90 mL, 59.3 mmol) in dichloroethane (100 mL) was added. Following a suspension of 2-amino-3,4,5,6-tetraphenylbenzoic acid (**118**) (8.25 g, 18.7 mmol) in dichloroethane (50 mL) was introduced. The reaction mixture was refluxed for 1 h. After cooling, the yellow precipitate was filtered to afford (9.02 g, 11.5 mmol, 61%); mp > 300 °C. ¹H NMR (400 MHz, CDCl₃): δ 5.75 (d, *J* = 8,

1H), 5.99 (d, $J = 4$ (d, $J = 8$ Hz, 1H), 6.61-6.72 (m, 20H), 6.95-7.03 (m, 10H), 7.19 (dd, $J_1 = 4$ Hz, $J_2 = 8$ Hz, 1H), 7.34 (d, $J = 8$, 1H), 7.75 (d, $J = 8$ Hz, 1H). ^{13}C NMR (100 MHz, CDCl_3): δ 120.9, 122.9, 123.0, 123.2, 124.6, 124.7, 124.9, 125.0, 125.9, 126.1, 126.3, 128.0, 128.6, 128.8, 129.4, 130.3, 130.8, 131.0, 131.8, 132.1, 133.0, 133.1, 135.8, 136.1, 136.3, 136.6, 136.7, 139.1, 139.2, 140.4, 140.7, 141.0, 141.8.

3-Bromo-7,8,17,18-tetraphenylacenaphtho[1,2-*l*]benzo[*f*]tetraphene (115).

3-Bromo-7,9-diphenyl-8*H*-cyclopenta[*a*]acenaphthylen-8-one (**122**) (19.1 g, 43.9 mmol) in dichloroethane (500 mL) was heated to reflux. To this mixture, a solution of isoamyl nitrite (15 mL, 13.1 g, 112 mmol) in dichloroethane (100 mL) was added. Then, a suspension of 3-amino-1,4-diphenyltriphenylene-2-carboxylic acid (**119**) (19.3 g, 43.9 mmol) in dichloroethane (200 mL) was added. The reaction mixture was refluxed for 2 h. After cooling, the orange precipitate was filtered to afford (11.6 g, 14.8 mmol, 34%); mp > 300 °C. ^1H NMR (400 MHz, CDCl_3): δ 6.41 (d, $J = 8$, 1H), 6.67 (d, $J = 8$, 1H), 6.79-7.13 (m, 23H), 7.25-7.33 (m, 4H), 7.43 (d, $J = 8$, 1H), 7.83 (d, $J = 8$, 1H), 8.15 (d, $J = 8$, 2H). ^{13}C NMR (100 MHz, CDCl_3): δ 120.9, 122.7, 122.9, 123.4, 125.0, 125.4, 126.2, 126.6, 126.9, 127.0, 127.8, 128.4, 128.7, 129.0, 129.3, 129.8, 130.9, 131.4, 132.2, 133.3, 135.1, 135.2, 135.3, 135.4, 135.5, 135.8, 136.0, 136.4, 136.9, 140.1, 142.3.

13-bromo-2,5,8,19-tetra-*tert*-butyl-10,17diphenylacenaphtho[1,2-*j*]fluorantheno [8,9-*l*]fluoranthene (116).

3-Bromo-7,9-diphenyl-8*H*-cyclopenta[*a*]acenaphthylen-8-one (**122**) (5.00 g, 11.5 mmol) in dichloroethane (110 mL) was heated to reflux. To this mixture, a solution of isoamyl nitrite (4.0 mL) in dichloroethane (45 mL) was added. Then, a suspension of 8-amino-2,5,10,13-tetra-

tert-butylacenaphtho[1,2-*j*]fluoranthene-7-carboxylic acid (**120**) (7.00 g, 11.5 mmol) in dichloroethane (45 mL) was added. The reaction mixture was refluxed for one h. After cooling, the precipitate was filtered to yield a red powder (9.10 g, 10.4 mmol, 83%); mp > 300 °C. ¹H NMR (400 MHz, CDCl₃): δ 1.25 (s, 18H), 1.61 (s, 18H), 7.27-7.95 (m, 21H), 8.94 (s, 2H). ¹³C NMR (100 MHz, CDCl₃): δ 31.8, 31.9, 35.66, 35.67, 121.0, 122.0, 122.2, 122.9, 123.1, 123.3, 125.2, 125.4, 128.4, 132.5, 137.3, 140.4, 150.4, 151.1.

11-bromo-2,5-di-*tert*-butyl-7,8,15,16-tetraphenylfluorantheno[8,9-*k*]fluoranthene (117).

3-Bromo-7,9-diphenyl-8*H*-cyclopenta[*a*]acenaphthylen-8-one (**122**) (5.00 g, 11.5 mmol) in dichloroethane (110 mL) was heated to reflux. To this mixture, a solution of isoamyl nitrite (2.6 mL) in dichloroethane (45 mL) was added. Then, a suspension of 9-amino-2,5-di-*tert*-butyl-7,10-diphenylfluoranthene-8-carboxylic acid (**121**) (2.72 g, 5.17 mmol) in dichloroethane (45 mL) was added. The reaction mixture was refluxed for 1 h. After cooling, the precipitate was filtered to yield a yellow powder (3.40 g, 3.90 mmol, 75%); mp > 300 °C. ¹H NMR (400 MHz, CDCl₃): δ 1.07 (s, 18H), 5.46 (d, *J* = 8, 1H), 5.70 (d, *J* = 8, 1H), 5.82 (d, *J* = 2, 1H), 7.07-7.23 (m, 23H), 7.33 (d, *J* = 8, 1H), 7.50 (s, 1H), 7.75 (d, *J* = 8, 1H). ¹³C NMR (100 MHz, *d*-DMSO): δ 31.1, 35.4, 120.9, 121.0, 122.0, 123.2, 123.4, 124.9, 126.2, 126.4, 128.1, 128.2, 128.7, 128.8, 129.3, 130.7, 132.0, 132.5, 135.4, 136.3, 136.6, 136.9, 137.2, 138.0, 141.5, 141.8, 150.6.

7,7',8,8',9,9',10,10',11,11',12,12'-Dodecaphenyl-3,3'-bibenzo[*k*]fluoranthene (110).

Nickel chloride (5.40 mg, 0.0420 mmol), triphenylphosphine (77.3 mg, 0.293 mmol), zinc (114 mg, 174 mmol), sodium bromide (129 mg, 1.24 mmol) and 3-bromo-7,8,9,10,11,12-hexaphenylbenzo[*k*]fluoranthene (**114**) (300 mg, 0.381 mmol) were placed in a 50-mL three

necks round bottomed flask. The system was degassed, and a stream of argon was flowing during the complete course of the reaction. To this mixture, *N,N*-dimethyl formamide (5 mL) and *N,N*-dimethylacetamide (5 mL) were added via syringe, and the reaction was left to go for 24 h. The reddish solution was filtered and diluted with methylene chloride. The solution was washed with 3 M hydrochloric acid (10 mL), water (10 mL), and saturated sodium chloride solution (10 mL). The yellowish solution was dried over anhydrous sodium sulfate, filtered and evaporated to dryness. The dark yellow solid was purified by column spectroscopy (methylene chloride/hexanes 2:8) to yield a bright yellow solid (56.6 mg, 21%). ¹H NMR (400 MHz, CDCl₃): δ 5.93 (d, *J* = 8Hz, 4H), 6.61-6.71 (m, 41H), 6.98-7.09 (m, 22H), 7.64 (d, *J* = 8Hz, 3H).

7,7',8,8',17,17',18,18'-Octaphenyl-3,3'-biacenaphtho[1,2-*l*]benzo[*f*]tetraphene (111).

Nickel chloride (3.02 mg, 0.0233 mmol), triphenylphosphine (42.5 mg, 0.162 mmol), zinc (62.8 mg, 0.960 mmol) and sodium bromide (71.1 mg, 0.691 mmol) were placed in a round-bottomed flask along with *N,N*-dimethylacetamide (1 mL). The mixture was heated until it turned deep red. 3-Bromo-7,8,17,18-tetraphenylacenaphtho[1,2-*l*]benzo[*f*]tetraphene (**115**) (165 mg, 0.210 mmol) in a mixture of *N,N*-dimethylacetamide (1 mL) and *N,N*-formamide (1 mL) was added. The combined reagents were heated overnight at 80 °C. The compound was isolated in trace amounts and characterized by MS. ¹H NMR (400 MHz, CDCl₃): δ. ¹³C NMR (100 MHz, CDCl₃): δ 121.8, 122.3, 123.4, 125.1, 125.4, 126.1, 126.5, 127.6, 128.4, 129.3, 129.7, 129.8, 131.0, 131.1, 131.5, 132.2, 133.2, 133.4, 134.9, 135.3, 135.7, 135.9, 136.1, 136.4, 136.7, 140.4, 142.4, 142.5.

2,2',5,5',8,8',19,19'-Octa-*tert*-butyl-10,10',17,17'-tetraphenyl-13,13'-biacenaphtho[1,2-*j*]fluorantheno[8,9-*l*]fluoranthene (112). Ni(PPh₃)Br₂ (47.0 mg, 0.0628 mmol), activated zinc (565 mg, 8.64 mmol) and (*n*Bu)₄Ni (154 mg, 0.418 mmol) were placed in a dried round 10 mL vessel under argon. Anhydrous tetrahydrofuran (4 mL) was added. 13-Bromo-2,5,8,19-tetra-*tert*-butyl-10,17-diphenylacenaphtho[1,2-*j*]fluorantheno[8,9-*l*]fluoranthene (**116**) (0.200 g, 0.209 mmol) was dissolved in THF (2 mL) and added dropwise to the mixture. The vessel was sealed and heated at 60 °C overnight. After cooling down, the reaction mixture was gravity filtered and rinsed out with methylene chloride. After evaporation of the solvent, the crude product was purified by column chromatography (alumina; solvent: hexanes–methylene chloride 10:0.5) to yield trace amounts of the product.

10,10',13,13'-Tetra-*tert*-butyl-7,7',8,8',15,15',16,16'-octaphenyl-3,3'-bifluorantheno[8,9-*k*]fluoranthene (113). Ni(PPh₃)Br₂ (0.0571 g, 0.0770 mmol), activated zinc (0.192 g, 2.94 mmol) and (*n*Bu)₄Ni were placed in a 50-mL round-bottomed flask under argon. Anhydrous tetrahydrofuran (4 mL) and a solution of 11-bromo-2,5-di-*tert*-butyl-7,8,15,16-tetraphenylfluorantheno[8,9-*k*]fluoranthene (**117**) (0.200 g, 0.229 mmol) in THF (2 mL) was added to the mixture. The flask was capped and heated at 60 °C overnight. After cooling down, the reaction mixture was filtered through a short pad of celite and rinsed out with methylene chloride (~20 mL). The filtrate was washed, in this order, with 10% hydrochloric acid (10 mL), saturated sodium bicarbonate (10 mL) and saturated sodium chloride solution (10 mL). The organic layer was dried over anhydrous sodium sulfate and evaporated to dryness. The crude product was purified by column chromatography (silica gel; solvent: hexanes–methylene chloride 10:2). Less than 1% of the product was recovered. ¹H NMR (400 MHz,

CDCl₃): δ 1.07 (s, 36H), 5.64 (d, $J = 8\text{Hz}$, 2H), 5.72 (d, $J = 8\text{Hz}$, 2H), 5.80 (d, $J = 4\text{Hz}$, 3H), 6.88 (t, $J = 8\text{Hz}$, 2H), 7.03-7.22 (m, 45H), 7.49 (d, $J = 4\text{Hz}$, 4H). ¹³C NMR (100 MHz, CDCl₃): δ 31.3, 35.4, 121.0, 122.1, 122.4, 123.0, 125.3, 126.3, 126.5, 127.7, 128.3, 128.4, 129.0, 129.5, 130.0, 131.0, 131.2, 131.3, 132.0, 132.8, 135.6, 135.8, 136.6, 136.7, 136.8, 137.0, 137.2, 137.3, 138.0, 142.0, 142.2, 150.8.

1,1',2,2'-Tetrahydro-5,5'-biacenaphthylene (140). 5-Bromoacenaphthene (**136**) (3.00 g, 12.9 mmol), boronic acid **138** (2.55 g, 12.9 mmol) and tetrakis(triphenylphosphine)palladium (0) (452 mg, 0.391 mmol) were refluxed in a mixture of toluene (125 mL) and aqueous solution of 2M potassium carbonate (125 mL) for 2 d. The organic layer was separated, washed with water, dried over sodium sulfate, and evaporated to dryness. The crude solid was purified by column chromatography (alumina, hexanes) to afford a slightly yellow product (2.51 g, 8.19 mmol, 64%), mp 178–180 °C (lit. mp 176–178 °C). ¹H NMR (400 MHz, CDCl₃): δ 3.48 (s, 8H), 7.28-7.30 (m, 6H), 7.39 (d, $J = 6.8$, 2H), 7.49 (d, $J = 7.2$, 2H). ¹³C NMR (100 MHz, CDCl₃): δ 30.1, 30.6, 119.0, 119.2, 121.5, 127.7, 129.5, 130.9, 133.5, 139.4, 145.5, 146.0.

[5,5'-Biacenaphthylene]-1,1',2,2'-tetraone (142). Biacenaphthylene **140** (600 mg, 1.96 mmol) and benzeneseleninic anhydride (2.82 g, 7.83 mmol) in chlorobenzene (50 mL) were heated to reflux for 3 d. After cooling, the precipitate was filtered, washed with aqueous sodium bicarbonate (10 mL), water (10 mL), methanol (20 mL) and methylene chloride (10 mL) to give an orange solid (567 mg, 80%). Due to low solubility, compound **142** was used for the next step without further purification. HRMS calcd for C₂₄H₁₀O₄ 362.0579, found 362.0789.

7',9,9'-Tetraphenyl-8H,8'H-[3,3'-bi(cyclopenta[*a*]acenaphthylene)]-8,8'-dione (143).

Tetraone **142** (567 mg, 1.56 mmol), and 1,3-diphenylacetone (727 mg, 3.46 mmol) in methanol (35 mL) were gently refluxed. Potassium hydroxide (363 mg, 6.48 mmol), dissolved in the minimal amount of methanol, was added dropwise and the mixture was stirred for 1 h. The dark precipitate was filtered, and subsequently washed with methanol (20 mL), water (20 mL), and methanol (20 mL) to afford a black solid (919 mg, 83%); mp > 300 °C. ¹H NMR (400 MHz, CDCl₃): δ 7.43-7.58 (m, 15H), 7.67 (d, *J* = 8.0 Hz, 2H), 7.84-7.89 (m, 7H), 8.10 (d, *J* = 8.0 Hz, 2H), 8.20 (d, *J* = 8.0 Hz, 2H). HRMS calcd for C₅₄H₃₀O₂ 710.2246, found 710.221.

7,7',8,8',9,9',10,10',11,11',12,12'-Dodecaphenyl-3,3'-bibenzo[*k*]fluoranthene (110).

Tetraphenylacenaphthylenedione **143** (200 mg, 0.281 mmol) in 1,2-dichloroethane (12 mL) was gently heated. Firstly a solution of isoamyl nitrite (0.2 mL) in 1,2-dichloroethane (2 mL) was added and then a dropwise addition of aminoacid **118** (248 mg, 0.563 mmol) in 1,2-dichloroethane (12 mL). The mixture was heated for 30 min and after cooling evaporated to dryness. The residue was purified by column chromatography (neutral alumina; solvent: 10:3 hexanes-dichloromethane) to give (200 mg, 0.141 mmol, 50%); mp > 300 °C. ¹H NMR (400 MHz, CDCl₃): δ 5.95 (d, *J* = 8Hz, 2H), 6.04 (d, *J* = 8 Hz, 2H), 6.60-6.74 (m, 40H), 6.93 (t, *J* = 8Hz, 2H), 6.98-7.06 (m, 20H), 7.08 (d, *J* = 8Hz, 2H), 7.18 (d, *J* = 8Hz, 2H). ¹³C NMR (100 MHz, CDCl₃): δ 122.0, 122.5, 124.7, 124.9, 125.0, 125.8, 125.9, 126.0 126.2, 127.5, 127.9, 128.0, 129.5, 129.7, 130.5, 130.6, 130.9, 131.0, 132.0, 133.0, 135.6, 136.0, 136.1, 136.4, 136.5, 136.7, 139.1, 140.4, 140.5, 141.3, 142.0.

7,7',8,8',17,17',18,18'-Octaphenyl-3,3'-biacenaphtho[1,2-*l*]benzo[*f*]tetraphene (111).

Tetraphenylacenaphthylenedione **143** (200 mg, 0.281 mmol) in 1,2-dichloroethane (12 mL) was gently heated. Firstly a solution of isoamyl nitrite (0.2 mL) in 1,2-dichloroethane (2 mL) was added and then a dropwise addition of aminoacid **119** (247 mg, 0.563 mmol) in 1,2-dichloroethane (12 mL). The mixture was heated for 30 min and after cooling evaporated to dryness. The residue was purified by column chromatography (neutral alumina; solvent: 10:3 hexanes-dichloromethane) to give a yellow solid (119 mg, 0.0843 mmol, 30%); mp > 300 °C. ¹H NMR (400 MHz, CDCl₃): δ 6.64 (d, *J* = 8 Hz, 2H), 6.75 (d, *J* = 8 Hz, 2H), 6.79-6.87 (m, 10H), 7.04-7.13 (m, 38H), 7.23-7.34 (m, 9H), 7.38 (d, *J* = 8 Hz, 2H), 8.16 (d, *J* = 8 Hz, 3H). ¹³C NMR (100 MHz, CDCl₃): δ 121.8, 122.3, 123.4, 125.0, 125.4, 126.1, 126.5, 126.9, 127.6, 127.7, 128.4, 128.7, 129.3, 129.7, 131.0, 131.5, 132.2, 133.4, 134.8, 134.9, 135.1, 135.3, 135.7, 135.8, 136.0, 136.4, 136.6, 140.4, 142.4.

2,2',5,5',8,8',19,19'-Octa-*tert*-butyl-10,10',17,17'-tetraphenyl-13,13'-

biacenaphtho[1,2-*j*]fluorantheno[8,9-*l*]fluoranthene (112). Tetraphenylacenaphthylenedione **143** (117 mg, 0.165 mmol) in 1,2-dichloroethane (7 mL) was gently heated. Firstly a solution of isoamyl nitrite (0.12 mL) in 1,2-dichloroethane (2 mL) was added, and then a suspension of aminoacid **120** (200 mg, 0.328 mmol) in 1,2-dichloroethane (9 mL) was released dropwise into the solution. The mixture was heated for 30 min, and after cooling evaporated to dryness. The residue was purified by column chromatography (neutral alumina; solvent: 10:3 hexanes-dichloromethane) to give a red-orange solid (201 mg, 0.115 mmol, 70%); mp > 300 °C. ¹H NMR (400 MHz, CDCl₃): δ 1.28 (s, 18H), 1.29 (s, 18H), 1.63 (s, 36H), 7.35-7.58 (m, 22H), 7.62-7.65 (m, 8H), 7.82 (s, 4H), 7.94 (d, *J* = 8 Hz, 4H), 7.99 (d, *J* = 8 Hz, 4H), δ 8.96 (s, 4H).

^{13}C NMR (100 MHz, CDCl_3): δ 31.8, 31.9, 35.7, 122.0, 122.1, 122.4, 122.8, 125.0, 125.3, 125.4, 125.5, 127.5, 128.4, 128.2, 128.3, 128.4, 128.9, 129.0, 129.1, 129.7, 130.0, 130.9, 132.7, 133.1, 133.2, 133.6, 133.7, 134.9, 135.8, 135.9, 136.1, 136.2, 136.3, 136.4, 136.9, 137.3, 137.5, 137.8, 140.6, 140.7, 150.4, 151.2.

10,10',13,13'-Tetra-*tert*-butyl-7,7',8,8',15,15',16,16'-octaphenyl-3,3'-

bifluorantheno[8,9-*k*]fluoranthene (113). Tetraphenylacenaphthylenedione **143** (120 mg, 0.169 mmol) and 1,2-dichloroethane (9.0 mL) were placed in a 250-mL Erlenmeyer flask, and gently heated to reflux. A solution of isoamyl nitrite (0.12 mL) in 1,2-dichloroethane (1.0 mL) was added and then aminoacid **121** (178 mg, 0.339 mmol) dissolved in 1,2-dichloroethane (9.0 mL) was dropwise transferred into the flask. The mixture was heated for 30 min, and after cooling evaporated to dryness. The residue was purified by column chromatography (neutral alumina; solvent: 10:3 hexanes-dichloromethane) to give a yellow solid (161 mg, 0.102 mmol, 30%); mp > 300 °C. ^1H NMR (400 MHz, CDCl_3): δ 1.07 (s, 36H), 5.65 (d, J = 8.0 Hz, 2H), 5.73 (d, J = 8.0 Hz, 2H), 5.81 (dd, J = 3.6, 1.2 Hz, 4H), 6.90 (t, J = 8.0 Hz, 2H), 7.04 (d, J = 8.0 Hz, 2H), 7.10-7.20 (m, 43H), 7.49 (d, J = 1.2 Hz, 3H). ^{13}C NMR (100 MHz, CDCl_3): δ 31.1, 35.2, 120.6, 121.9, 122.2, 122.7, 125.1, 126.1, 126.3, 127.5, 128.1, 128.2, 128.8, 129.3, 129.7, 130.9, 131.1, 131.8, 131.9, 132.6, 135.4, 135.6, 136.3, 136.5, 136.6, 136.9, 137.0, 137.1, 137.8, 141.8, 142.0, 150.6.

Synthesis of target compound 106. **7,7',8,8',9,9',10,10',11,11',12,12'-Dodecaphenyl-3,3'-bibenzo[*k*]fluoranthene (110)** (48.4 mg, 0.0342 mmol) and cobalt trifluoride (84.8 mg, 0.0730 mmol) in trifluoroacetic acid (10.0 mL) were refluxing for 72 h. After cooling down, methylene chloride (50 mL) was added and the resulting mixture was washed with three

portions of water (60 mL) and one portion of saturated sodium chloride solution (20 mL). The organic layer was dried over anhydrous sodium sulfate, filtered and evaporated to dryness. The product was purified by column chromatography over neutral alumina (methylene chloride/hexanes 3:10) to afford a purple solid (25 mg, 52%). The amount recovered was not suitable for NMR spectra. HRMS calcd for C₁₁₂H₁₈ 1412.5321, found 1412.5400.

References

- (1) Lawrence, D. S.; Jiang, T.; Levett, M. *Chem. Rev.* **1995**, *95*, 2229.
- (2) Cao, D. H.; Chen, K.; Fan, J.; Manna, J.; Olenyuk, B.; Whiteford, J. A.; Stang, P. J. *Pure & Appl. Chem.* **1997**, *69*, 1979.
- (3) Desiraju, G. R. *J. Mol. Struct.* **2003**, *656*, 5.
- (4) Hoskins, B. F.; Robson, R. *J. Am. Chem. Soc.* **1990**, *112*, 1546.
- (5) Venkataraman, D.; Gardner, G. B.; Lee, S.; Moore, J. S. *J. Am. Chem. Soc.* **1995**, *117*, 11600.
- (6) Aumüller, A.; Erk, P.; Klebe, G.; Hünig, S.; von Schütz, J. U.; Werner, H.-P. *Angew. Chem. Int. Ed. Engl.* **1986**, *25*, 740.
- (7) Fujita, M.; Kwon, Y. J.; Washizu, S.; Ogura, K. *J. Am. Chem. Soc.* **1994**, *116*, 1151.
- (8) Sun, D.; Yang, C.-F.; Xu, H.-R.; Zhao, H.-X.; Wei, Z.-H.; Zhang, N.; Yu, L.-J.; Huang, R.-B.; Zheng, L.-S. *Chem. Commun.* **2010**, *46*, 8168.
- (9) Fujita, M.; Yazaki, J.; Ogura, K. *Tetrahedron Lett.* **1991**, *32*, 5589.
- (10) Kondo, M.; Yoshitomi, T.; Seki, K.; Matsukada, H.; Kitagawa, S. *Angew. Chem. Int. Ed. Engl.* **1997**, *36*, 1725.
- (11) Biradha, K.; Su, C.-Y.; Vittal, J. J. *Cryst. Growth Des.* **2011**, *11*, 875.
- (12) Kitagawa, S.; Kitaura, R.; Noro, S.-I. *Angew. Chem. Int. Ed. Engl.* **2004**, *43*, 2334.
- (13) Leininger, S.; Olenyuk, B.; Stang, P. J. *Chem. Rev.* **2000**, *100*, 853.
- (14) Choi, H. J.; Suh, M. P. *Inorg. Chem.* **1999**, *38*, 6309.

- (15) Fujita, M.; Ogura, K. *Coord. Chem. Rev.* **1996**, *148*, 249.
- (16) Stang, P. J.; Olenyuk, B. *Acc. Chem. Res.* **1997**, *30*, 502.
- (17) Olenyuk, B.; Fechtenkötter, A.; Stang, P. J. *J. Chem. Soc. Dalton Trans.* **1998**, 1707.
- (18) Sun, D.; Wei, Z.-H.; Yang, C.-F.; Wang, D.-F.; Zhang, N.; Huang, R.-B.; Zheng, L.-S. *CrystEngComm.* **2011**, *13*, 1591.
- (19) Fujita, M.; Oguro, D.; Miyazawa, M.; Oka, H.; Yamaguchi, K.; Ogura, K. *Nature* **1995**, *378*, 469.
- (20) Domasevitch, K. V.; Solntsev, P. V.; Gural'skiy, I. A.; Krautscheid, H.; Rusanov, E. B.; Chernega, A. N.; Howard, A. K. *Dalton Trans.* **2007**, 3893.
- (21) Venkataraman, D.; Du, Y.; Wilson, S. R.; Hirsch, K. A.; Zhang, P.; Moore, J. *S. J. Chem. Edu.* **1997**, *74*, 915.
- (22) Venkataraman, D.; Lee, S.; Moore, J. S.; Zhang, P.; Hirsch, K. A.; Gardner, G. B.; Covey, A. C.; Prentice, C. L. *Chem. Mater.* **1996**, *8*, 2030.
- (23) Liu, F.-J.; Sun, D.; Li, Y.-H.; Hao, H.-J.; Huang, R.-B.; L.-S., *Z. J. Mol. Struct.* **2011**, *998*, 151.
- (24) Sun, D.; Zhang, N.; Xu, Q.-J.; Wei, Z.-H.; Huang, R.-B.; L.-S., *Z. Inorg. Chim. Acta* **2011**, *368*, 67.
- (25) Ni, J.; Wei, K.-J.; Liu, Y.; Huang, X.-C.; Li, D. *Cryst. Growth Des.* **2010**, *10*, 3964.
- (26) Wu, S.-T.; Long, L.-S.; Huang, R.-B.; Zheng, L.-S. *Cryst. Growth Des.* **2007**, *7*, 1746.

- (27) Yeh, C.-W.; Chen, T.-R.; Chen, J.-D.; Wang, J.-C. *Cryst. Growth Des.* **2009**, *9*, 2595.
- (28) Wei, K.-J.; Ni, J.; Gao, J.; Liu, Y.; Liu, Q.-L. *Eur. J. Inorg. Chem.* **2007**, 3868.
- (29) Campos-Fernández, C. S.; Schottel, B. L.; Chifotides, H. T.; Bera, J. K.; Bacsa, J.; Koomen, J. M.; Russell, D. H.; Dunbar, K. R. *J. Am. Chem. Soc.* **2005**, *127*, 12909.
- (30) Yilmaz, V. T.; Hamamci, S.; Gumus, S.; Büyükgüngör, O. *J. Mol. Struct.* **2006**, *794*, 142.
- (31) Pyykkö, P. *Chem. Rev.* **1997**, 597.
- (32) Bondi, A. *J. Phys. Chem.* **1964**, *68*, 441.
- (33) Uson, R.; Forniés, J.; Tomás, M.; Cotton, F. A.; Falvello, L. R. *J. Am. Chem. Soc.* **1984**, *106*, 2482.
- (34) Jansen, M. *Angew. Chem. Int. Ed. Engl.* **1987**, *26*, 1098.
- (35) Chen, C. Y.; Zeng, J. Y.; Lee, H. M. *Inorg. Chim. Acta* **2007**, *360*, 21.
- (36) Andrews, L. J.; Keefer, R. M. *J. Am. Chem. Soc.* **1949**, *71*, 3644.
- (37) Munakata, M.; Wu, L. P.; Sowa-Kuroda, T.; Maekawa, M.; Suenaga, Y.; Ning, G. L.; Kojima, T. *J. Am. Chem. Soc.* **1998**, *120*, 8610.
- (38) Zhang, J.; Bu, X. *Chem. Commun.* **2008**, 444.
- (39) Forster, P. M.; Burbank, A. R.; Livage, C.; Férey, G.; Cheetham, A. K. *Chem. Commun.* **2004**, 368.

- (40) Hennigar, T. L.; Macquarrie, D. C.; Losier, P.; Rogers, R. D.; Zaworotko, M. *J. Angew. Chem. Int. Ed. Engl.* **1997**, *36*, 972.
- (41) Withersby, M. A.; Blake, A. J.; Champness, N. R.; Cooke, P. A.; Hubberstey, P.; Li, W.-S.; Schröder, M. *Inorg. Chem.* **1999**, *38*, 2259.
- (42) Desiraju, G. R. *J. Chem. Sci.* **2010**, *122*, 667.
- (43) Hirsch, K. A.; Wilson, S. R.; Moore, J. S. *Inorg. Chem.* **1997**, *36*, 2960.
- (44) Hirsch, K. A.; Wilson, S. R.; Moore, J. S. *J. Am. Chem. Soc.* **1997**, *119*, 10401.
- (45) Kilway, K.; Deng, S.; Bowser, S.; Mudd, J.; Washington, L.; Ho, D. *Pure Appl. Chem.* **2006**, *78*, 855.
- (46) Lawrance, G. A. *Chem Rev.* **1986**, *86*, 17.
- (47) Rosenthal, M. R. *J. Chem. Educ.* **1973**, *50*, 331.
- (48) Beck, W.; Sünkel, K. *Chem Rev.* **1988**, *88*, 1405.
- (49) Corson, B. B.; Stoughton, R. W. *J. Am. Chem. Soc.* **1928**, *50*, 2825.
- (50) Antipin, M. Y.; Barr, T. A.; Cardelino, B. H.; Clark, R. D.; Moore, C. E.; Myers, T.; Penn, B.; Romero, M.; Sanghadasa, M.; Timofeeva, T. V. *J. Phys. Chem. B* **1997**, *101*, 2770.
- (51) Nesterov, V. N.; Kuleshova, L. N.; Antipin, M. Y. *Kristallografiya (Russ.) (Crystallogr. Rep.)* **2001**, *46*, 1041.
- (52) Jiang, L.; Fu, Y.; Li, H.; Hu, W. *J. Am. Chem. Soc.* **2008**, *130*, 3937.
- (53) Krukonis, A. P.; Silverman, J.; Yannoni, N. F. *Cryst. Struct. Commun.* **1974**, *3*, 233.

- (54) Allen, F. H.; Kennard, O.; Watson, D. G. *J. Chem. Soc. Perkin Trans. 2* **1987**, S1.
- (55) Turner, R. W.; Amma, E. L. *J. Am. Chem. Soc.* **1966**, 88, 3243.
- (56) Hasegawa, T.; Sekine, M.; Schaefer, W. P.; Taube, H. *Inorg. Chem.* **1991**, 30, 449.
- (57) Allen, F. H. *Acta Cryst.* **1981**, B37, 890.
- (58) Otwinowski, Z.; Minor, W. *Methods Enzymol.* **1997**, 276, 307.
- (59) Spek, A. L. *Acta Cryst.* **2009**, D65, 148.
- (60) Sheldrick, G. M. *Acta Cryst.* **2008**, A64, 112.
- (61) Oszlányi, G.; Süto, A. *Acta Cryst.* **2008**, A64, 123.
- (62) Yamashita, K.; Tanaka, T.; Hayashi, M. *Tetrahedron Lett.* **2005**, 61, 7981.
- (63) Sturz, H. G.; Noller, C. R. *J. Am. Chem. Soc.* **1949**, 71, 2949.
- (64) Weinberger, M. A.; Heggie, R. M.; Holmes, H. L. *Can. J. Chem.* **1965**, 43, 2585.
- (65) Cornélis, A.; Lambert, S.; Laszlo, P. *J. Org. Chem.* **1977**, 42, 381.
- (66) Katritzky, A. R.; Zhu, D.-W.; Schanze, K. S. *J. Phys. Chem.* **1991**, 95, 5737.
- (67) Manecke, G.; Wöhrle, D. *Die Makromolekulare Chemie* **1967**, 102.
- (68) Fetzer, J. C. *Large ($C \geq 24$) Polycyclic Aromatic Hydrocarbons: Chemistry and Analysis*; John Wiley: New York, 2000; Vol. 158.
- (69) Feng, X.; Pisula, W.; Müllen, K. *Pure Appl. Chem.* **2009**, 81, 2203.
- (70) Martin, R. H. *Angew. Chem. Int. Ed. Engl.* **1974**, 13, 649.
- (71) Shen, Y.; Chen, C.-F. *Chem Rev.* **2012**, 112, 1463.

- (72) Cahn, R. S.; Ingold, S. C.; Prelog, V. *Angew. Chem. Int. Ed. Engl.* **1966**, *5*, 385.
- (73) Janke, R. H.; Haufe, G.; Würthwein, E.-U.; Borkent, J. H. *J. Am. Chem. Soc.* **1996**, *118*, 6031.
- (74) Pascal, R. A., Jr.; McMillan, W. D.; Van Engen, D.; Eason, R. G. *J. Am. Chem. Soc.* **1987**, *109*, 4660.
- (75) Lu, J.; Ho, D. M.; Vogelaar, N. J.; Krami, C. M.; Pascal, R. A., Jr. *J. Am. Chem. Soc.* **2004**, *126*, 11168.
- (76) Barth, W. E.; Lawton, R. G. *J. Am. Chem. Soc.* **1971**, *93*, 1730.
- (77) Yamamoto, K.; Harada, T.; Nakazaki, M. *J. Am. Chem. Soc.* **1983**, *105*, 7171.
- (78) Yamamoto, K. *Pure & Appl. Chem.* **1993**, *65*, 157.
- (79) Mehta, G.; Prakash Rao, H. S. *Tetrahedron Lett.* **1998**, *54*, 13325.
- (80) Kroto, H. W.; Heath, J. R.; O'Brien, S. C.; Curl, R. F.; Smalley, R. E. *Nature* **1985**, *318*, 162.
- (81) Hirsch, A.; Brettreich, M. *Fullerenes: Chemistry and Reactions*; Wiley-VCH: Weinheim, Germany, 2005.
- (82) Hebard, A. F.; Rosseinsky, M. J.; Haddon, R. C.; Murphy, D. W.; Glarum, S. H.; Palstra, T. T. M.; Ramirez, A. P.; Kortan, A. R. *Nature* **1991**, *350*, 600.
- (83) Sijbesma, R.; Srdanov, G.; Wudl, F.; Castoro, J. A.; Wilkins, C.; Friedman, S. H.; DeCamp, D. L.; Kenyon, G. L. *J. Am. Chem. Soc.* **1993**, *115*, 6510.

- (84) Friedman, S. H.; Ganapathi, P. S.; Rubin, Y.; Kenyon, G. L. *J. Med. Chem.* **1998**, *41*, 2424.
- (85) Lin, T.; Bajpai, V.; Ji, T.; Dai, L. *Aust. J. Chem.* **2003**, *56*, 635.
- (86) Petrukhina, M. A.; Scott, L. T. E. *Fragments of Fullerenes and Carbon Nanotubes: Designed Synthesis, Unusual Reactions, and Coordination Chemistry*; John Wiley & Sons, Inc: Hoboken, New Jersey, 2012.
- (87) Yu, M.-F.; Lourie, O.; Dyer, M. J.; Moloni, K.; Kelly, T. F.; Ruoff, R. S. *Science* **2000**, *287*, 637.
- (88) Derycke, V.; Martel, R.; Appenzeller, J.; Avouris, P. *Nano Lett.* **2001**, *1*, 453.
- (89) Javey, A.; Wang, Q.; Ural, A.; Li, Y.; Dai, H. *Nano Lett.* **2002**, *2*, 929.
- (90) Terzi, G.; Melik, T. H.; Nisbet, C. *Irish J. Agr. Food Res.* **2008**, *47*, 187.
- (91) Jung, K. H.; Yan, B.; Chillrud, S. N.; Perera, F. P.; Whyatt, R.; Camann, D.; Kinney, P. L.; Miller, R. L. *Int. J. Environ. Res. Public Health* **2010**, *7*, 1889.
- (92) Sumi, K.; Konishi, G.-I. *Molecules* **2010**, *15*, 7582.
- (93) Saranya, G.; Kolandaivel, P.; Senthilkumar. *J. Phys. Chem. A* **2011**, *115*, 14647.
- (94) Ma, X.; Wu, W.; Zhang, Q.; Guo, F.; Meng, F.; Hua, J. *Dyes and Pigments* **2009**, *82*, 353.
- (95) Kagan, H. B.; Olivier, R. *Chem. Rev.* **1992**, *92*, 1007.
- (96) Nicolaou, K. C.; Snyder, S. A.; Montagnon, T.; Vassilikogiannakis, G. *Angew. Chem. Int. Ed. Engl.* **2002**, *41*, 1668.

- (97) Clar, E.; Zander, M. *J. Chem. Soc.* **1957**, 4616.
- (98) Trnka, T. M.; Grubbs, R. H. *Acc. Chem. Res.* **2001**, *34*, 18.
- (99) Grubbs, R. H.; Chang, S. *Tetrahedron* **1998**, *54*, 4413.
- (100) Scholl, M.; Ding, S.; Lee, C. W.; Grubbs, R. H. *Org. Lett.* **1999**, *1*, 953.
- (101) Fujihara, T.; Tomike, Y.; Ohtake, T.; Terao, J.; Tsuji, Y. *Chem. Commun.* **2011**, *47*, 9699.
- (102) Nicolaou, K. C.; Bulger, P. G.; Sarlah, D. *Angew. Chem. Int. Ed. Engl.* **2005**, *44*, 4490.
- (103) Hong, S. H.; Sanders, D. P.; Lee, C. W.; Grubbs, R. H. *J. Am. Chem. Soc.* **2005**, *127*, 17160.
- (104) Bonifacio, M. C.; Robertson, C. R.; Jung, J.-Y.; King, B. T. *J. Org. Chem.* **2005**, *70*, 8522.
- (105) Scott, L. T.; Necula, A. *J. Org. Chem.* **1996**, *61*, 386.
- (106) Tsefrikas, V. M.; Scott, L. T. *Chem. Rev.* **2006**, *106*, 4868.
- (107) Dötz, F.; Brand, J. D.; Ito, S.; Gherghel, L.; Müllen, K. *J. Am. Chem. Soc.* **2000**, *122*, 7707.
- (108) Tang, X.-Q.; Harvey, R. G. *J. Org. Chem.* **1995**, *60*, 3568.
- (109) Quante, H.; Müllen, K. *Angew. Chem. Int. Ed. Engl.* **1995**, *34*, 1323.
- (110) Herrmann, A.; Weil, T.; Sinigersky, V.; Wiesler, U.; Vosch, T.; Hofkens, J.; De Schryver, F.; Müllen, K. *Chem. Eur. J.* **2001**, *7*, 4844.
- (111) Müller, S.; Müllen, K. *Chem. Commun.* **2005**, 4045.

- (112) Alvino, A.; Franceschin, M.; Cefaro, C.; Borioni, S.; Ortaggi, G.; Bianco, A. *Tetrahedron Lett.* **2007**, *63*, 7858.
- (113) Huang, C.; Barlow, S.; Marder, S. R. *J. Org. Chem.* **2011**, *76*, 2386.
- (114) Hernando, J.; de Witte, P. A. J.; van Dijk, E. M. H. P.; Kortarik, J.; Nolte, R. J. M.; Rowan, A. E.; García-Parajó, M. F.; van Hulst, N. F. *Angew. Chem. Int. Ed. Engl.* **2004** *43*, 4045.
- (115) Langhals, H.; Jona, W. *Angew. Chem. Int. Ed. Engl.* **1998**, *37*, 952.
- (116) Weil, T.; Vosch, T.; Hofkens, J.; Peneva, K.; Müllen, K. *Angew. Chem. Int. Ed. Engl.* **2010**, *49*, 9068.
- (117) Zhan, X.; Tan, Z.; Domercq, B.; An, Z.; Zhang, X.; Barlow, S.; Li, Y.; Zhu, D.; Kippelen, B.; Marder, S. R. *J. Am. Chem. Soc.* **2007**, *129*, 7246.
- (118) Ahrens, M. J.; Fuller, M. J.; Wasielewski, M. R. *Chem. Mater.* **2003**, *15*, 2684.
- (119) Schmidt-Mende, L.; Fechtenkötter, A.; Müllen, K.; Moons, E.; Friend, R. H.; MacKenzie, J. D. *Science* **2001**, *293*, 1119.
- (120) Rybtchinski, B.; Sinks, L. E.; Wasielewski, M. R. *J. Chem. Soc.* **2004**, *126*, 12268.
- (121) Hippius, C.; Schlosser, F.; Vysotsky, M.; Böhmer, V.; Würther, F. *J. Am. Chem. Soc.* **2006**, *128*, 3870.
- (122) Ford, W. E.; Kamat, P. V. *J. Phys. Chem.* **1987**, *91*, 6373.
- (123) Debad, J.; Morris, J.; Lynch, V.; Magnus, P.; Bard, A. *J. Org. Chem.* **1996**, *118*, 2374.

- (124) Wehmeier, M.; Wagner, M.; Müllen, K. *Chem. Eur. J.* **2001**, *7*, , 2197.
- (125) Debad, J.; Morris, J.; Lynch, V.; Magnus, P.; Bard, A. *J. Org. Chem.* **1997**, *62*, 530.
- (126) Smyth, N.; Van Engen, D.; Pascal, R. *J. Org. Chem.* **1990**, *55*, 1937.
- (127) Seiders, T. J.; Elliott, E. L.; Grube, G. H.; Siegel, J. S. *J. Am. Chem. Soc.* **1999**, *121*, 7804.
- (128) Anderson, A. G., Jr. ; Anderson, R. G. *J. Am. Chem. Soc.* **1955**, *77*, 6610.
- (129) Walters, R.; Kraml, C.; Byrne, N.; Ho, D.; Qin, Q.; Coughlin, F.; Bernhard, S.; Pascal, R. *J. Am. Chem. Soc.* **2008**, *130*, 1635.
- (130) Miyaura, N.; Suzuki, A. *Chem. Rev.* **1995**, *95*, 2457.
- (131) Pascal, R. A., Jr. *Org. Lett.* **2003**, *5*, 369.
- (132) Takaaki, S.; Yonehara, H.; Pac, C. *J. Org. Chem.* **1997**, *62*, 3194.
- (133) Wilfried, J.; Vögtle, F. *Chem. Ber.* **1991**, *124*, 347.
- (134) Tanaka, N.; Kasai, T. *Bull. Chem. Soc. Jpn.* **1981**, *54*, 3020.
- (135) Tanaka, N.; Kasai, T. *Bull. Chem. Soc. Jpn.* **1981**, *54*, 3026.
- (136) Mitchell, R. H.; Chaudhary, M.; Williams, R. V.; Fyles, R.; Gibson, J.; Ashwood-Smith, M. J.; Fry, A. J. *Can. J. Chem.* **1992**, *70*, 1015.
- (137) Clayton, M. D.; Marcinow, Z.; Rabideau, P. W. *J. Org. Chem.* **1996**, *61*, 6052.
- (138) Neudorff, W. D.; Schulte, N.; Lentz, D.; Schlüter, A. D. *Org. Lett.* **2001**, *3*, 3115.

- (139) Müller, M.; Mauermann, V.; Müllen, K. *Angew. Chem. Int. Ed. Engl.* **1995**, *34*, 1583.
- (140) Müller, M.; Kübel, C.; K., M. *Chem. Eur. J.* **1998**, *4*, 2099.
- (141) Zhai, L.; Shukla, R.; Rathore, R. *Org. Lett.* **2009**, *11*, 3474.
- (142) Li, Y.; Wang, Z. *Org. Lett.* **2009**, *11*, 1385.
- (143) Komatsu, K. *Pure & Appl. Chem.* **1993**, *65*, 73.
- (144) Mehta, G.; Umarye, J. D.; Gagliardini, V. *Tetrahedron Lett.* **2002**, *43*, 6975.
- (145) Mehta, G.; Umarye, J. D.; Srinivas, K. *Tetrahedron Lett.* **2003**, *44*, 4233.
- (146) Jaworek, W.; Vögtle, F. *Chem. Ber.* **1991**, *124*, 347.
- (147) Sakamoto, T.; Pac, C. *J. Org. Chem.* **2001**, *66*, 94.
- (148) Holtrup, F. O.; Müller, G. R.; Uebe, J.; Müllen, K. *Tetrahedron* **1997**, *53*, 6847.
- (149) Schlichting, P.; Rohr, U.; Müllen, K. *Liebigs Ann-Recl.* **1997**, 395.
- (150) Dang, H.; Garcia-Garibay, M. A. *J. Am. Chem. Soc.* **2001**, *123*, 355.
- (151) Donovan, P. M.; Scott, L. T. *J. Am. Chem. Soc.* **2004**, *126*, 3108.
- (152) Clayton, M. D.; Marcinow, Z.; Rabideau, P. W. *Tetrahedron Lett.* **1998**, *39*, 9127.
- (153) Chang, S.-J.; Ravi Shankar, B. K.; Shechter, H. *J. Org. Chem.* **1982**, *47*, 4226.
- (154) Mulder, P. P. J.; Boerrigter, J. O.; Boere, B. B.; Zuilhof, H.; Erkelens, C. *Recl. Trav. Chim. Pays-Bas* **1993**, *112*, 287.

- (155) Qiao, X.; Padula, M. A.; Ho, D. M.; Vogelaar, N. J.; Schutt, C. E.; Pascal, R. *A. J. Am. Chem. Soc.* **1996**, *118*, 741.
- (156) Allen, C.; Ning, R. *Can. J. Chem.* **1964**, *42*, 2151.
- (157) Nürshen, H. E.; Peters, A. T. *J. Chem. Soc.* **1950**, 729.
- (158) Amick, A. W.; Griswold, K. S.; Scott, L. T. *Can. J. Chem.* **2006**, *84*, 1268.
- (159) Nakayama, J.; Ito, Y. *Sulfur Lett.* **1989**, *9*, 135.
- (160) Clapp, D. B. *J. Am. Chem. Soc.* **1939**, *61*, 2733.
- (161) Crockett, G.; Swanson, B.; D.; A.; Koch, T. *Synthetic Commun.* **1981**, *11*, 447.
- (162) Schindlbauer, H. *Monatsh. Chem.* **1973**, *104*, 848.
- (163) Wang, L.; Wang, X.; Cui, J.; Ren, W.; Meng, N.; Wang, J., Qian, X. *Tetrahedron: Asymmetry.* **2010**, *21*, 825.

VITA

Gerardo Batalla Márquez was born on October 3, 1965 in San Francisco de Yare, Venezuela. He completed his bachelor's degree in chemistry in 1993 at the Central University of Venezuela, Caracas-Venezuela, and then worked for a year teaching basic analytical chemistry at the Experimental National University, Barquisimeto-Venezuela. He moved to the United States in November 1995. He entered the University of Missouri-Kansas City (UMKC) as a Master of Science student in fall 2002 and started work under the supervision of Dr. Kilway. He was accepted as an Interdisciplinary Ph.D. student in fall 2004.

The topic of research where he spent most of his time in the program was in the synthesis of polycyclic aromatic hydrocarbons (PAHs). During his time in the program, he worked as a graduate teaching assistant for more than five years and received a Superior Graduate Teaching Assistant Award for 2006-2007. In addition, he presented at two American Chemical Society national meetings with the support of UMKC and the Department of Chemistry. One of his favorite hobbies is to participate in races, and he has completed seven marathons, which included two in Kansas City and one in New York City.

Publication:

Durig, J.R.; Zheng, C.; Marzluf, K.R.; **Márquez, G.B.**; Guirgis, G.A.; Wurrey, C.J.; Kilway, K.V., "Is 2-cyclopropylpropene really *gauche*?", *Spectrochimica Acta* **2005**, *61A*, 1357-1371.

Posters and Presentations:

1. **Márquez G.B.**; Clevenger R.G.; and Kilway K.V., “Synthesis of Polycyclic Aromatic Hydrocarbons Enclosing a Perylene Core, Second Part,” 242nd American Chemical Society Meeting, Denver, CO, August 28-31, 2011.
2. **Márquez, G.B.**; Ho, D.M.; Kilway, K.V., “Molecular Assembly of 1,2- and 1,3-bis(cyanomethyl)benzene with Silver Salts,” Poster presentation, 225th American Chemical Society Meeting, March 23-27, 2003, New Orleans, LA.